TECHNICAL UNIVERSITY OF CRETE

SCHOOL OF CHEMICAL AND ENVIRONMENTAL ENGINEERING

M.Sc. IN SUSTAINABLE ENGINEERING & CLIMATE CHANGE

MSc SPECIALIZATION AREA: SUSTAINABLE ENERGY

Climate projections for Greece: Insights from the CMIP6 multi-model ensemble.

Name: Kaza Ioanna

Examination committee:

1. Koutroulis Aristeidis (Supervisor), Associate Professor, Technical University of Crete
2. Mihalis Lazaridis, Professor, Technical University of Crete
3. Elena Floca, Professor, National and Kapodistrian of Athens

Chania, 2024

Acknowledgments

This thesis would not have been possible without the guidance and help of several people who one way or another contributed and extended their valuable assistance in the preparation and completion of this study. It is a pleasure to thank those who made it possible.

Firstly, I genuinely and sincerely thank my supervisor, Professor Aristeidis Koutroulis for his guidance, collaboration, and support throughout my study. I am grateful for our fruitful cooperation.

Moreover, I would like to thank Mr. Kostantinos Seiradakis, researcher at the atmospheric environment and climate change lab, who generously shared his time and knowledge on multiple occasions. His advice on tools and methods was very helpful and greatly appreciated.

Last but not least my deepest thanks to my family and friends for their patience, and encouragement on this journey.

Table of Contents

TABLES

FIGURES

Abstract

Global climate change is one of the most pressing issues of modern life as it significantly impacts many aspects of human life. The Coupled Model Intercomparison Project (CMIP) has been instrumental in enhancing our understanding on climate dynamics, both past and future, particularly with the progression from CMIP5 to the more advanced CMIP6 experiments. played a key role in climate study, especially with the advancement from CMIP5 to CMIP6 experiments. This progress results in new challenges for interpreting and exploiting the abundant climate data available to the scientific community. The increasing number of models that participate in climate experiments (more than 100 for the CMIP6) leads to the necessity of representative climate model selection for the needs of impact studies. The complexity of the selection among the CMIP6 multi-model ensemble is essential in the implementation of similar applications.

My thesis, entitled ¨Climate Projections for Greece. Insights from the CMIP6 multi-model ensemble¨ focuses on the region of Greece which is particularly sensitive to the impacts of climate change. The study aims to analyze temperature and precipitation trends from the pre-industrial period until the end of this century (2100) focusing on the wider region of Greece, studying historical data and future simulations according to the changes in the CMIP6 multi-model ensemble.

The basic analysis was conducted using the Climate Data Operator (CDO), following a structured methodology. First, mean global temperature and precipitation were calculated for 26 selected CMIP6 models, followed by the calculation of these parameters specifically for the region of Greece using the same models. Next, the results were compared with observation data and reanalysis from ERA5. An analysis of trends was then performed according to different SSP-RCP scenarios to present the range of expected changes in temperature and precipitation. Finally, representative models were selected based on reliability, representativeness, and independence criteria.

The study attempts to provide a comprehensive overview of the diversity of the possible climate future scenarios in the Greek region. Exploring the present trends as well as the future projections according to different SSP-RCP scenarios we aim to understand the range of the expected climate changes and limit down to a plausible and manageable and representative CMIP6 sub-ensemble.

1. Introduction

Scope and objectives of the study

Global climatic changes over the recent past have brought significant transformations to the Earth's systems, along with anticipated changes for the 21st century. Scientists have been intensively studying the impacts of climate change on terrestrial and aquatic ecosystems, as the biotic and abiotic basis for life are directly influenced by shifts in the environmental conditions, particularly climatic. The importance of investigating regional climate changes associated with global warming is increasingly being recognized. Climate change is an inter-governmental complex challenge globally with its influence over various components of the ecological, environmental, socio-political, and socio-economic disciplines (Neil Adger et al., 2005, Feliciano et al., 2022).

This study aims to evaluate the performance of 26 global climate models participating in the Coupled Model Intercomparison Project Phase 6 (CMIP6) by comparing their simulations to observed temperature and precipitation data over Greece from 1979 to 2014, coming from the hybrid GSWP3-W5E5 dataset. This assessment provides a foundation for analyzing future climate projections for the region. Using these models, the study also explores future trends under four distinct Shared Socio-economic Pathways (SSP) scenarios: SSP1-2.6, SSP2-4.5, SSP3-7.0, and SSP5-8.5. By examining the range of temperature and precipitation responses across these scenarios, the study aims to offer a comprehensive understanding of potential climate outcomes for Greece in the context of global warming.

Importance of Climate Change Studies

The Intergovernmental Panel on Climate Change (IPCC) defines “climate change” as “a change in the state of the climate that can be identified by changes in the mean and/or the variability of its properties, and that persists for an extended period, typically decades or longer (“IPCC AR4 WGI,” 2007). This definition refers to any change in climate over time, whether due to natural variability or as a result of human activity (Reay et al., 2007).

Climate change is increasingly evident I various aspects of the natural and built environment Temperature and global sea level are rising, precipitation characteristics are changing, and glaciers are melting. Climate plays a crucial role in human life, with many regions around the world exhibiting varying levels of hazard and vulnerability across different sectors. Economic, social, and human vulnerability in climate change is the origin of increased risks at coastal and inland ecosystems, as well as at water flow and food production. Warming is projected to impact human health, mostly through increased intensity, frequency, and duration of heat waves. More people are expected to be exposed to high or very high heat stress by 2050 (Rohat et al., 2019), heat-related excess mortality to be increased and human health will be at high risk of food- and water-borne diseases. Furthermore, cultural heritage sites is projected to face risks of coastal flooding and erosion. Specifically, sea level rise will increase these risks (Rizzi et al., 2017). In the Mediterranean region, beyond 2100, sea levels

are committed to rise further and represent an existential threat for the high number of coastal cultural heritage (Marzeion & Levermann, 2014).

Earth's temperature has risen by an average of 0.06° Celsius per decade since 1850, while the rate since 1982 is more than three times as fast (0.2° C per decade). The past decade (2014-2023) has been recorded as the 10 warmest years historically, and 2023 was the warmest year since global records began in 1850 by a wide margin (figure 1).

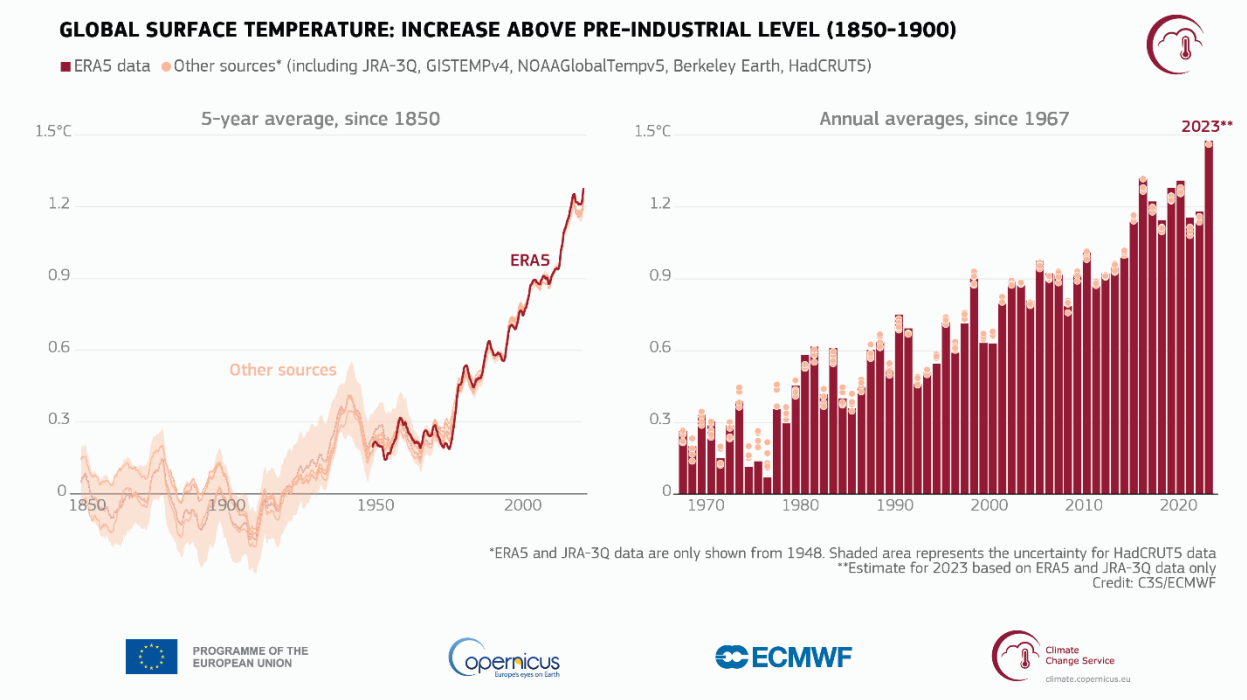

Figure 1. Global surface air temperature increase relative to the average for 1850-1900, the designated pre-industrial reference period, based on several global temperature datasets shown as 5-year averages since 1850 (left) and as annual averages since 1967 (right). Credit: C3S/ECMWF (https://climate.copernicus.eu/copernicus-2023-hottest-year-record?os=f&ref=app).

Particularly, the Mediterranean region faces new challenges due to global climate change while being exposed to several natural risks like floods, droughts, and fires. Based on global climate scenarios, the Mediterranean Sea has been classified as one of the most responsive regions to climate change (Giorgi, 2006). In the Mediterranean basin, the average annual temperatures are now 1.5°C higher than during the period 1880-1899, well above current global trends. As for the future projections, the 2 °C global mean temperature target implies 3°C warming in hot temperature extremes in the Mediterranean region (Seneviratne et al., 2016). The Mediterranean has already reached the tough target limit set out in the Paris Agreement in 2015 ((MedECC) et al., 2020) and the future annual and summer warming rates are projected to be 20% and 50% larger than the global annual average, respectively ("Mediterranean Region," 2023). However, mitigation and adaptation strategies vary from country to country due to differences in the socioeconomic, cultural, and political status.

Since 1901, global precipitation has increased at an average rate of 1mm per decade (Blunden & Boyer, 2021) (figure 2), while in the Mediterranean region analyses of long-term trends show that annual mean conditions tend to be warmer and drier (UNEP/MAP-Plan Bleu, 2009).

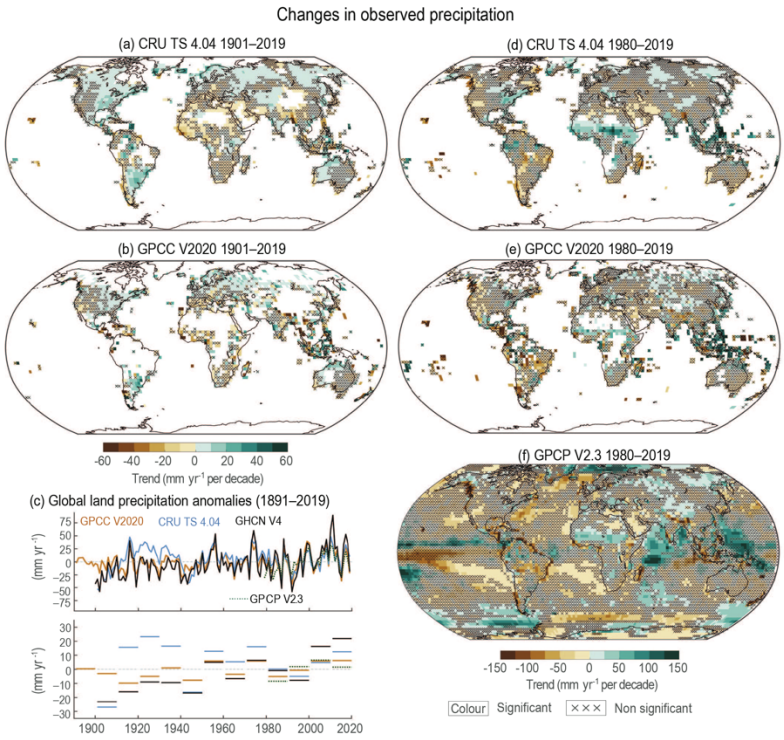

Figure 2. Changes in observed precipitation. (a, b) Spatial variability of observed precipitation trends over land for 1901–2019 for two global in-situ products. Trends are calculated using OLS regression with significance assessed following AR(1) adjustment after Santer et al. (2008) ('×' marks denote non-significant trends). (c) Annual time series and decadal means from 1891 to date relative to a 1981–2010 climatology (note that different products commence at distinct times). (d, e) as (a, b), but for the periods starting in 1980. (f) is for the same period for the globally complete merged GPCP v2.3 product, (Blunden & Boyer, 2021).

Drought conditions in the Mediterranean Basin have become both more frequent and severe over recent decades (Vicente-Serrano et al., 2014). An increase in the length of dry spell (days) is expected (Schleussner et al., 2016) and a decrease in precipitation, especially in summer and with important regional differences ("Mediterranean Region," 2023) (figure 3).

Since late 2021, southern Europe has been particularly affected by a prolonged drought, which extended through the summer of 2023 (Toreti et al., 2023). Future projections of changes in precipitation and temperature across Mediterranean regions remain uncertain, posing challenges for predicting impacts on temperature trends, water resources, and availability. Analyses using CMIP5 models indicated an expected decrease in precipitation over much of the Mediterranean (Polade et al., 2014; Mariotti et al., 2015), except for areas in the northern Mediterranean, where some models project an increase in cold-season precipitation (Polade et al., 2014). However, high levels of disagreement were observed among these models, with some suggesting precipitation increases while others indicated declines (Polade et al., 2017). Recent studies (Arias et al., 2021; Dias & Reboita, 2021; Ortega et al., 2021) suggest that CMIP6 models have made advancements over CMIP5 (Taylor et al., 2012), offering improved capabilities for projecting regional climate changes.

The widespread increase in evaporative demand and some decrease in precipitation explain the drying of the Mediterranean region during recent decades (high confidence) (WGI AR6 Chapter 11, Seneviratne et al., 2021). Droughts are projected to become more severe, more frequent, and longer under moderate emission scenarios, and strongly enhanced under severe emission scenarios (high confidence) (WGI AR6 Chapter 11, Seneviratne et al., 2021). Droughts have a direct impact on agriculture and human health, while can limit the growing season and create conditions that encourage insect and disease infestation in certain crops. Consequently, low crop yields can result in rising food prices and shortages affecting the food industry and economy. Furthermore, the soil and vegetation drought increase the likelihood of wildfires, along with the risk of high-value assets and cultural monuments being destroyed in significant areas.

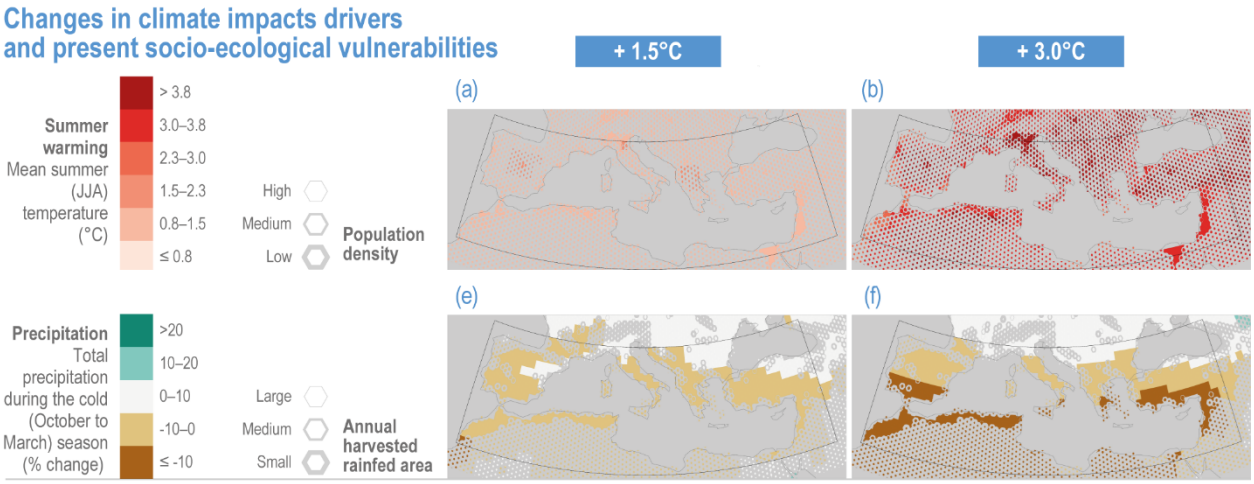

Figure 3. Changes in climate impact drivers with respect to the 1995–2014 period for 1.5°C (left column) and 3°C (right column) global warming: mean summer (June to August) temperature (°C, a, b) and, total precipitation during the cold (October to March) season (%, e, f). Values based on CMIP6 global projections and SSP5-8.5. Sea level rise concerns the long term (2081–2100) and SSP1-2.6 for (i) and SSP3-7.0 for (j) (source: figure CCP4.2, Cross-Chapter Paper 4: Mediterranean Region).

Climate Change in Greece

The Mediterranean Basin is a widely recognized climate change hot spot. Droughts in the Mediterranean Basin have increased in frequency and intensity in the last decades (Vicente-Serrano et al., 2014) and since late 2021, southern Europe has been suffering a severe drought that continued into the summer of 2023 (Toreti et al., 2023). Projections of future precipitation and air temperature changes are still highly uncertain over many Mediterranean regions, thus impeding the assessment of the overall impacts on temperature, water supply and availability. Studies using the Climate Model Intercomparison Project Phase 5 models, suggested a precipitation decrease across most parts of the Mediterranean Climate regions (Polade et al., 2014, Mariotti et al., 2015), with the exception of the northern Mediterranean Basin, where a precipitation increase during the cold season is expected (Polade et al., 2014). However, the model disagreement was found to be high over these parts of the Mediterranean Basin, with the models sometimes equally split between suggesting precipitation increase or decline (Polade et al.,2017). The studies by Arias et al. (Arias et al., 2021), Dias and Reboita (Dias & Reboita, 2021), and Ortega et al. (Ortega et al., 2021) highlight the improvements of the CMIP6 numerical models compared to the previous version CMIP5 (Taylor et al., 2012).

Areas with complex topography, like the wider area around Greece (hereafter denoted southeastern Europe) where we focus in this study, present particular interest in the response to climate variability

and the impacts of climate change. It is an area with steep orography from the mountainous regions to the coast, a long and convoluted coastline, and many small islands.

Greece, situated centrally in the Eastern Mediterranean, has faced an increasing number of extreme events in recent decades—such as wildfires, floods, and heatwaves—that are linked, directly or indirectly, to climate change. Public and political concern about climate change is also on the rise. Like many Mediterranean nations, Greece is especially vulnerable to climate impacts due to its geographic and climatic characteristics, which make it susceptible to significant environmental changes. These shifts are anticipated to affect key societal sectors, including agriculture, water management, energy, and tourism. The Mediterranean is recognized as a "hotspot" for climate change, where warming is projected to occur at a rate faster than the global average (Giorgi, 2006; Lionello et al., 2008).

The Greek scientific community has acknowledged these challenges, producing a wealth of studies on Greece's past, present, and future climate (Giannakopoulos et al., 2011; Founda et al., 2019; Nastos & Kapsomenakis, 2015). In 2011, the Climate Change Impacts Study Committee (CCISC), commissioned by the Bank of Greece, provided a comprehensive assessment of climate change effects on Greece and its implications for critical sectors such as agriculture, tourism, fisheries, transportation, and human health. They estimated that the economic cost of climate change from 2011 to 2100 could range between 578 and 701 billion euros, a figure approximately three to four times Greece's GDP in 2020 (Eurostat, 2021).

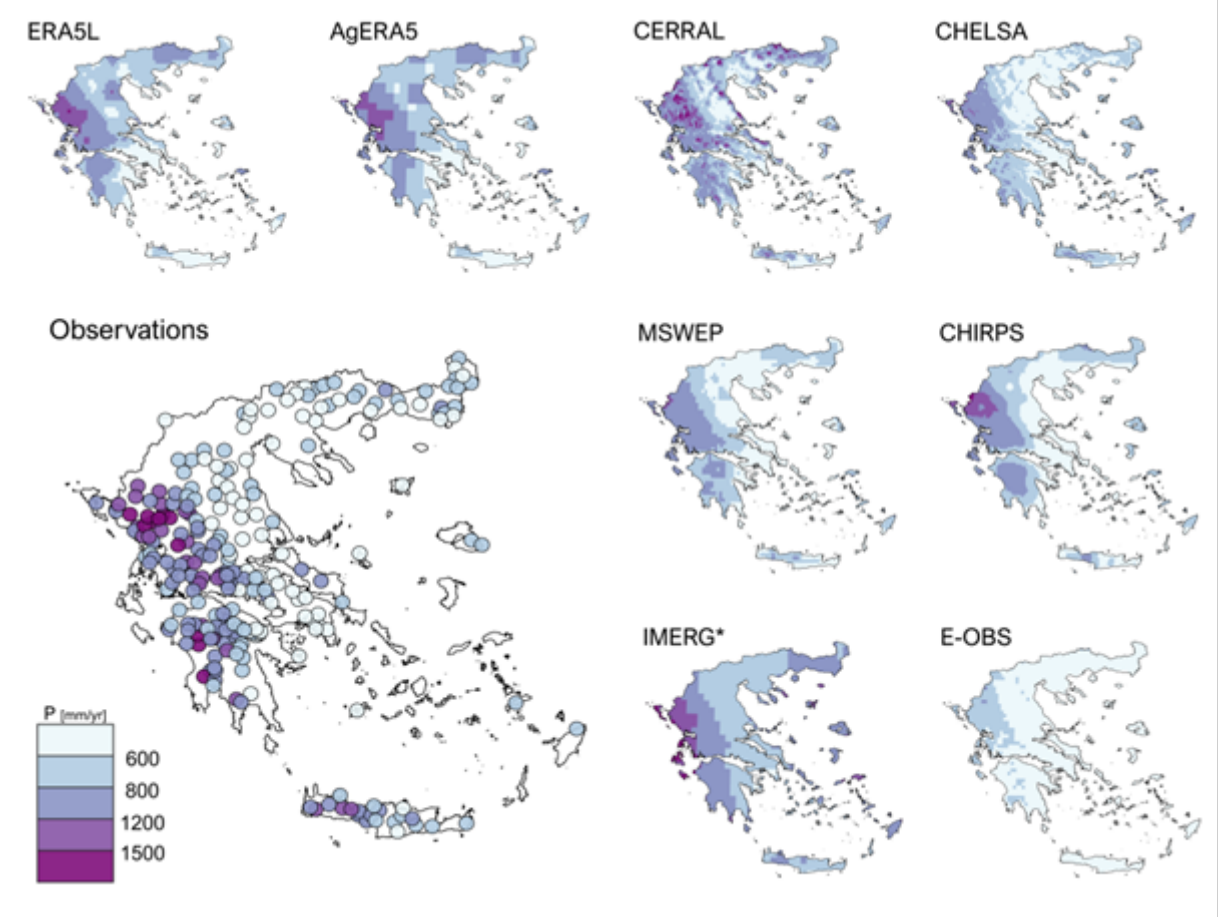

Figure 4. Mean annual rainfall distribution resulting from eight gridded datasets and point observations of the 1985 – 2016 period (Papa and Koutroulis, 2024)

Temperature Trends

Over the past decades, Greece has witnessed increasing temperatures, particularly in the summer months, with more frequent and prolonged heatwaves. This trend is expected to continue in the future, with models projecting a rise in average temperatures by 1.5 to 4°C by the end of the 21st century, depending on the emissions scenario (SSP) used (Kostopoulou & Jones, 2005; Zittis et al., 2019). Rising temperatures can lead to a variety of socio-economic challenges, such as increased energy demand for cooling, health risks due to heat stress, and negative impacts on crop yields.

Extreme Events

While the Mediterranean region as a whole exhibits shared climate characteristics, the Eastern Mediterranean and Western Mediterranean showcase distinctive climate trends. These results lead to larger summer temperature extremes, reduced precipitation, increased drought conditions, and a higher risk of wildfires. Long-term climate change suggest study that the most extremes are likely to occur over Greece and Eastern Mediterranean region (Flocas et al., 2023).

Precipitation Patterns

Alongside rising temperatures, shifts in precipitation patterns have also been observed and are expected to intensify. Greece is projected to experience reduced rainfall, particularly in the southern regions, leading to a higher frequency of droughts (Koutroulis et al., 2016; Tolika et al., 2020). The northern regions, on the other hand, may see more variability in rainfall patterns, including intense storms and extreme weather events. These changes pose risks to water availability, agriculture, and infrastructure, making water resource management a critical issue for the country.

Sea Level Rise and Coastal Erosion

As a country with an extensive coastline, Greece is particularly vulnerable to rising sea levels. Coastal areas, which are vital for tourism, urban development, and ecosystems, are at risk of erosion and flooding (Hellenic Ministry of Environment & Energy, 2016). Sea level rise, compounded by storm surges, threatens not only coastal infrastructure but also biodiversity in sensitive marine environments (Vousdoukas et al., 2017).

Impacts on Agriculture and Ecosystems

The agricultural sector, which is a cornerstone of the Greek economy, is at high risk due to climate change. Changes in precipitation, increasing temperatures, and the higher frequency of extreme weather events are expected to affect crop productivity, especially for crops like olives, grapes, and wheat (Giannakopoulos et al., 2009; Mavromatis, 2018). Ecosystems and biodiversity are also under threat, with species migration and habitat loss becoming more common as the climate continues to shift (Lazaridis et al., 2014).

Adaptation and Mitigation Efforts

Recognizing the urgency of the situation, Greece has developed national strategies for climate change adaptation and mitigation. These efforts focus on enhancing resilience in sectors like water management, agriculture, and infrastructure, while also promoting the transition to renewable energy sources (Hellenic Ministry of Environment & Energy, 2016). Greece has also committed to international climate agreements, such as the Paris Agreement, to contribute to global efforts in limiting temperature rise and reducing greenhouse gas emissions (Papadopoulos & Karamanos, 2018).

Coupled Model Intercomparison Project (CMIP)

CMIP History

The Climate Model Intercomparison Project (CMIP) plays a pivotal role in supporting the World Climate Research Program (WCRP) and advancing climate science globally. CMIP data, used by decision-makers and policy makers, aim to deepen our understanding of past, present, and future

climate changes. The project's datasets have become integral to major climate assessments, including those conducted by the Intergovernmental Panel on Climate Change (IPCC) and other national and international climate assessments.

Established in 1995 by the WCRP, CMIP seeks to harmonize efforts within the global climate modeling community by coordinating a standard set of climate simulations. This allows for a multi-model perspective on climate change, facilitating model evaluations and driving improvements in climate simulations. Through these coordinated experiments, researchers can assess model performance in reproducing historical climate trends, identify factors contributing to the variability in future projections, and conduct idealized experiments to analyze model responses to various scenarios. In addition to examining long-term climate changes, CMIP includes experiments aimed at predicting climate on multiple timescales, all from a common observed climate state.

Managed by the Working Group on Coupled Modelling (WGCM), CMIP initially focused on an idealized climate experiment with CO_2 concentrations increasing by 1% per year. Over time, CMIP has expanded to include experiments that not only use idealized forcings but also incorporate historical radiative forcings and projected future changes, broadening the scope and utility of the project's climate models. Another core goal of CMIP is to make its multi-model data output accessible in a standardized format, ensuring that these valuable resources are widely available for research and policy applications.

Coupled Model Intercomparison Project Phase 6

CMIP has grown from a modest scientific research initiative in the nineties to become a global enterprise. More than 50 modeling centers around the world are now participating in the sixth phase of CMIP, CMIP6. The Scenario Model Intercomparison Project (ScenarioMIP) within CMIP6 plays a critical role in exploring future climate scenarios. It aims to understand how different future socio-economic and environmental pathways impact climate change. ScenarioMIP's primary goal is to provide a common set of climate and socio-economic scenarios, facilitating integrated research across various fields like physical climate science, mitigation strategies, and adaptation planning. It helps in addressing uncertainties in future projections by evaluating different scenarios, including those with overshooting radiative forcing targets and different land use assumptions (O'Neill et al., 2016).

The CMIP6 dataset differs from the CMIP5 and CMIP3 datasets in terms of forcing scenarios and carbon emissions. The CMIP6 project employed updated versions of the coupled global climate models, a new start year, and a new set of Shared Socioeconomic Pathways (SSP) scenarios of concentrations (Gidden et al., 2019). The integration of Shared Socioeconomic Pathways (SSPs) with Representative Concentration Pathways (RCPs) is one of the significant advancements in ScenarioMIP, allowing researchers to combine societal futures with physical climate model simulations to analyze a broader range of outcomes, from mitigation efforts to the impacts of various socio-economic developments (O'Neill et al., 2016).

Data from the more recent phase 6 of the Coupled Model Intercomparison Project are available for analysis (Eyring et al., 2016). The present study, therefore, aims to examine the projected changes in future temperature and precipitation over Greece using the latest CMIP6 dataset.

The Coupled Model Intercomparison Project Phase Six (CMIP6) was initiated in 2014 to fill the scientific gaps remaining in CMIP5 and address new challenges emerging in climate modeling (Eyring et al., 2016). CMIP6 formed the basis of the sixth IPCC Assessment Report published in 2021 (O'Neill et al., 2016) (AR6 Climate Change 2021: The Physical Science Basis — IPCC, 2021). For climate projection, CMIP6 considers the impact of socioeconomic conditions (e.g., population, economy) on greenhouse gas emissions by linking RCPs to SSPs, which enhances the robustness of climate projections and provides better support for climate policies. Also, CMIP6 keeps four scenarios used in CMIP5 (SSP1-2.6, SSP2-4.5, SSP4-6.0, and SSP5-8.5) and adds four new scenarios (SSP1-1.9, SSP4-3.4, SSP5-3.4-OS, and SSP3-7.0) to give a wider selection of futures for scientists to simulate.

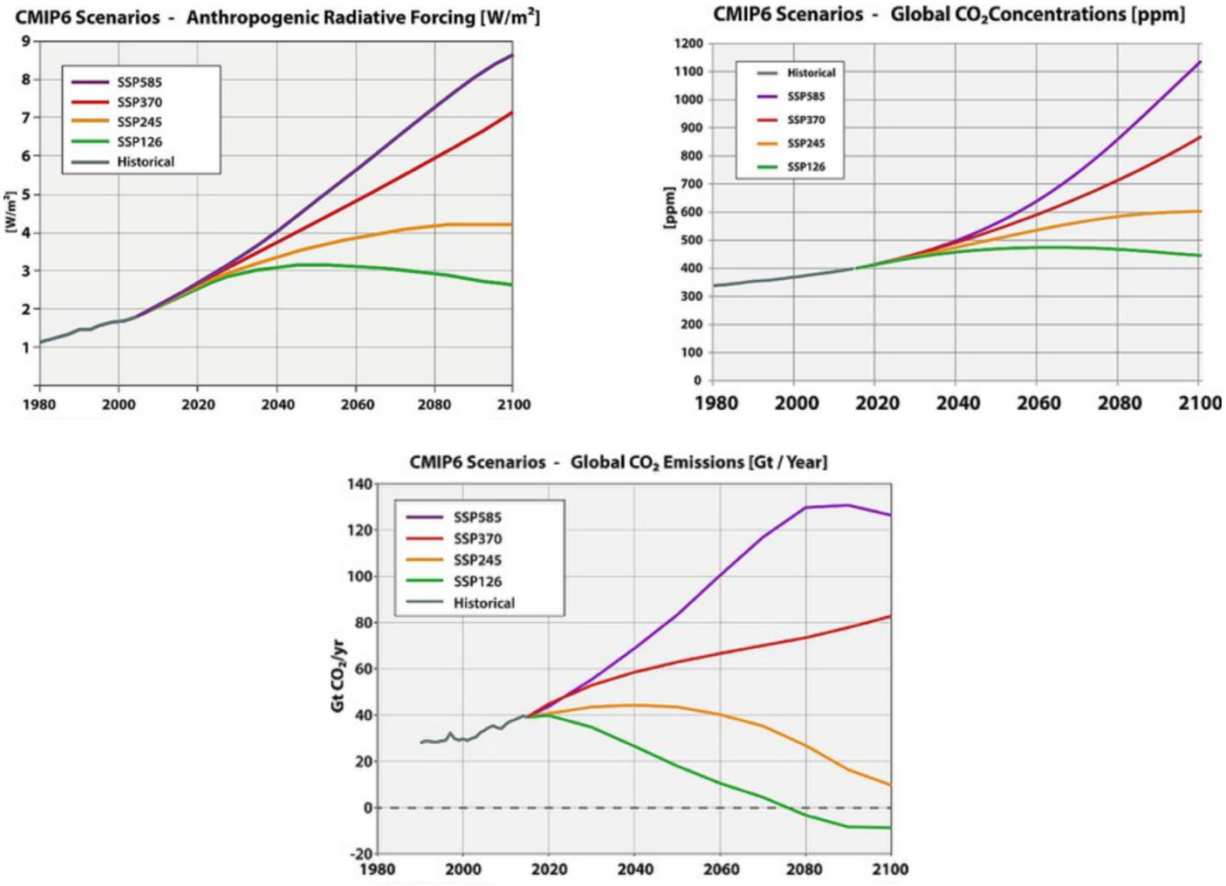

Figure 5. CO_2 emissions, concentrations, and anthropogenic radiative forcing for the 21st century under 4 different SSP-RCP scenarios (Riahi et al., 2017)

Climate Projections: Advantages and challenges of using multi-model ensembles.

Predictions and projections for weather and climate on timescales ranging from days to centuries are often generated using numerical models that represent or simulate key processes. These models contain various uncertainties, which are typically categorized as initial condition, boundary condition, parameter, and structural uncertainties. Boundary condition uncertainties arise when external datasets replace interactive components of the system. For example, sea surface temperature and sea ice cover may be prescribed in atmosphere-only models, or radiative forcing is specified over time instead of being modeled interactively. Furthermore, uncertainties related to greenhouse gas concentrations are primarily driven by assumptions about future socioeconomic developments. Different scenarios for greenhouse gas emissions reflect various possible future paths, and assigning likelihoods to these scenarios is challenging due to their dependence on unpredictable factors like policy choices and technological advancements.

The climate system's inherent complexity makes it fundamentally impossible for any model, regardless of sophistication, to capture every relevant process accurately. To address the various aspects of model uncertainty, multi-model ensembles are essential. Numerous studies across fields, including but not limited to weather and climate predictions, have demonstrated that model combinations enhance forecasting skill, reliability, and consistency, generally outperforming single-model forecasts (Cantelaube & Terres, 2005; Palmer et al., 2009). This approach has also shown improvements in accurately detecting and attributing climate influences, such as warming due to greenhouse gases and cooling from sulfate aerosols (Gillett et al., 2002). Typically, an equally weighted mean of multiple coupled climate models aligns better with observed data than any individual model (Lambert & Boer, 2001).

Multi-model ensembles consist of simulations from various structurally distinct models, where multiple initial condition ensembles may also be incorporated (creating what's known as a super-ensemble when several initial conditions are available per model) (Tebaldi & Knutti, 2007).

Although individual model performance might not outperform the best-performing single model for any specific variable, research has shown that multi-model ensembles offer significant advantages across a broad range of diagnostics. The true strength of multi-model ensembles lies in their ability to deliver consistently improved performance across different prediction aspects, as demonstrated by studies like Hagedorn et al. (2005). This approach allows for a more balanced and reliable representation of uncertainties and a better understanding of complex climate dynamics by leveraging the strengths of each individual model within the ensemble.

There are various approaches to combining climate models, and there is ongoing debate about the most effective method, especially when skill or performance is evaluated by comparing model predictions with observations. Constructing and interpreting multi-model climate projections involves several challenges, broadly categorized into four key areas:

(a) Model Validation Metrics: A model's reliability and skill are evaluated by comparing numerous independent realizations of observed climate with model predictions. This comparison uses metrics

that quantify alignment between model forecasts and real-world observations. However, for long-term climate projections, validation through direct observations isn't possible, as future boundary conditions, such as greenhouse gas emissions, might deviate from the model's assumptions. As a result, confidence in a model's skill comes not from future accuracy but from its ability to replicate historical climate patterns, variability, and known processes.

(b) Model Independence and Bias: The idea that model averaging can improve forecast accuracy is based on the assumption that independent models' errors will cancel each other out, reducing uncertainty. While models are developed independently by research groups worldwide, they share similarities, such as resolution and parameterization techniques. These shared characteristics can introduce similar errors across models, questioning the assumption of complete independence. Studies often rely on this assumption, gaining more confidence in findings consistent across multiple models than in those from single-model results.

(c) Ensemble Design and "Ensembles of Opportunity": Multi-model ensembles are often described as "ensembles of opportunity" because they include results from models based on groups' willingness and resources to contribute. This approach can lead to inconsistencies in ensemble composition, as models are not always developed to fully explore the range of possible behaviors or uncertainties. Instead, they are tuned to align as closely as possible with historical observations, often building upon previous versions without significant parameter changes unless needed.

(d) Model Tuning and Observation Matching: Models can be compared against various observations, including station data, satellite measurements, proxies, and reanalyses. While models that match observations are more likely to represent critical climate processes accurately, adjustments to parameters may sometimes improve observational alignment in ways that do not enhance the model's true representation of the system. For example, 20th-century warming trends in models may align with observations due to the combined effects of ocean heat uptake, climate sensitivity, and radiative forcing, even if biases in one factor are offset by adjustments in others (Knutti et al., 2002).

Each of these aspects highlights the complexities and trade-offs in multi-model climate projections, emphasizing the need for careful interpretation and consideration of model limitations.

Importance of selecting representative models from the CMIP6 ensemble.

Selecting representative models from the CMIP6 ensemble is crucial for producing accurate and reliable climate projections, particularly at regional scales like Greece. The CMIP6 multi-model ensemble consists of a diverse range of climate models developed by different research institutions, each with varying sensitivities, strengths, and weaknesses. Not all models perform equally well in every region or climate variable, which is why careful selection is essential (Eyring et al., 2016b).

Key reasons for selecting Representative Model:

1. Reducing Uncertainty: Climate projections inherently involve uncertainty, particularly when it comes to regional impacts. By selecting models that perform well in key statistical metrics—such as mean bias error (MBE), root mean square error (RMSE), and time correlation—researchers can reduce uncertainty and ensure that projections more accurately reflect observed climate patterns in the region of interest (Knutti & Sedláček, 2012).
2. Capturing Regional Climate Dynamics: Different models have varying abilities to simulate specific climate features, such as precipitation, temperature, and extreme events. In Greece, for example, climate models need to account for complex topographies, such as mountainous regions, as well as coastal and island climates. Selecting models that best simulate these regional features ensures that the projections are more relevant and applicable to the local context (McSweeney et al., 2012).
3. Addressing Specific Climate Variables: Different models excel in simulating different climate variables. For example, some models may be better at predicting temperature trends, while others are more accurate in simulating precipitation. Selecting a subset of models that balances these strengths ensures a more holistic understanding of future climate conditions (Knutti & Sedláček, 2012).
4. Balancing Computational Resources: Running all models in the CMIP6 ensemble can be computationally expensive and time-consuming. Selecting a representative group of models with a strong track record in simulating the region's climate allows for a more efficient use of resources while still capturing the range of potential climate outcomes (Sanderson et al., 2015).
5. Comparing Across Scenarios: By selecting representative models, researchers can better assess the impacts of different emission scenarios (SSP1-2.6, SSP2-4.5, SSP3-7.0 and SSP5-8.5). This helps in understanding how different pathways of greenhouse gas emissions will impact Greece's future climate, providing a range of outcomes that can be used for risk assessment and planning (van Vuuren et al., 2011).

In summary, selecting representative models from the CMIP6 ensemble ensures that climate projections are both accurate and regionally relevant, reducing uncertainties and improving the utility of climate information for decision-makers and researchers. This process is essential for selecting models that support the development of robust strategies to address the specific challenges posed by climate change in Greece.

2. Data

Model Data

For the scope of this research, monthly mean near surface temperature (TAS in ^{o}K) and precipitation (PR in Kg m^{-2} s^{-1}) data from 26 CMIP6 models ensemble have been analyzed, comparing the precipitation and air temperature simulations of each individual model with the observational dataset. More specifically, the simulations used in this study cover the wider domain of the region of Greece (44^{o}N –31^{o}S, 17^{o}W - 31°E).

Trends of temperature and precipitation have been analyzed for the period 1850-2100 according to 4 different SSP-RCP scenarios.

SSP (Shared Socioeconomic Pathways) scenarios refer to narratives describing different development paths of society. These basic pathways had initially not assumed any climate policies exceeding current measures or a necessity for adaptation measures to continuous climate change. Simulations with Integrated Assessment Models, simple integrated impact assessment models simulating the interplay of the economy, society and the earth system, have shown that the greenhouse gas concentration pathways described in the RCP scenarios (Representative Concentration Pathways, (van Vuuren et al., 2011)) used for CMIP5 as well as the respective climate targets such as the 2°C target are unattainable like this. This is due to the strong climate effect of the resulting greenhouse gas concentrations.

Combining the SSPs with the RCP (degree of the additional radiative forcing due to the man-made greenhouse gas effect) leads to structure the variety of possible scenarios. The denomination of individual scenarios comprises the name of the basic pathway followed by two numerals indicating the additional radiative forcing achieved by the year 2100 in units of tenths of watts:

SSP585: With an additional radiative forcing of 8.5 W/m² by the year 2100, this scenario represents the upper boundary of the range of scenarios described in the literature. It can be understood as an update of the CMIP5 scenario RCP8.5, now combined with socioeconomic reasons.

SSP370: With 7 W/m² by the year 2100, this scenario is in the upper-middle part of the full range of scenarios. It was newly introduced after the RCP scenarios, closing the gap between RCP6.0 and RCP8.5.

SSP245: As an update to scenario RCP4.5, SSP245 with an additional radiative forcing of 4.5 W/m² by the year 2100 represents the medium pathway of future greenhouse gas emissions. This scenario assumes that climate protection measures are being taken.

SSP126: This scenario with 2.6 W/m² by the year 2100 is a remake of the optimistic scenario RCP2.6 and was designed with the aim of simulating a development that is compatible with the 2°C target. This scenario, too, assumes climate protection measures being taken.

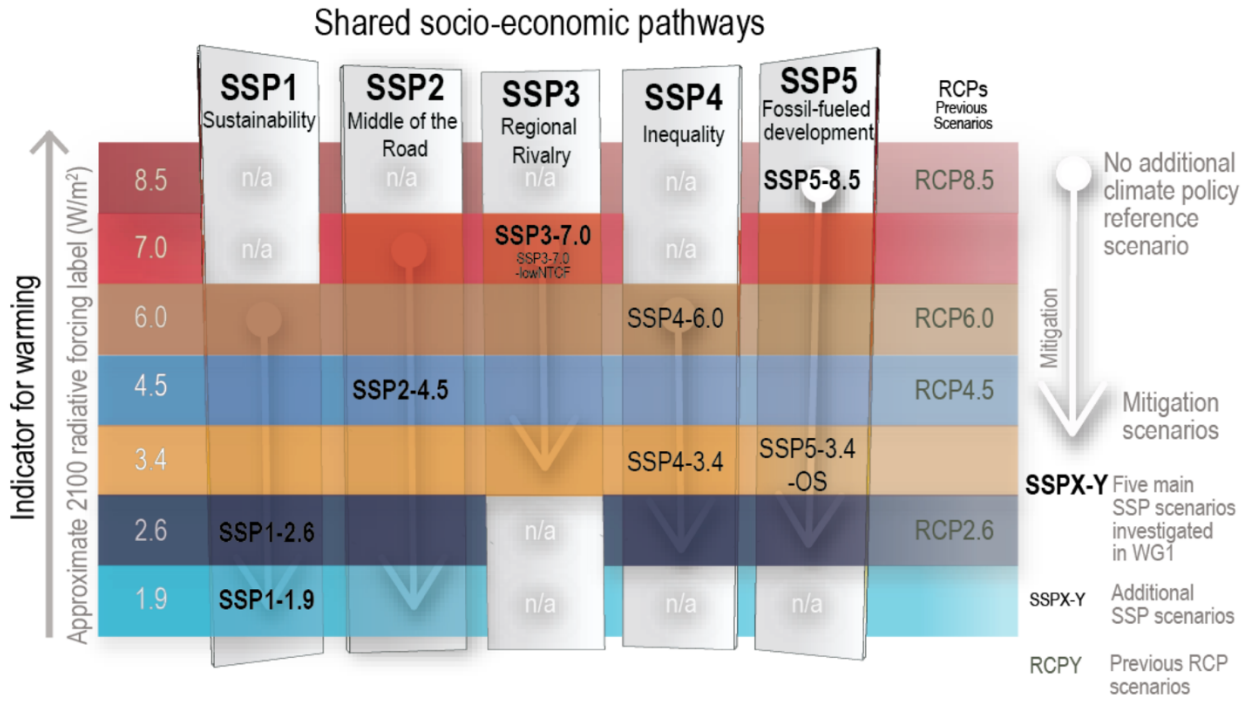

Figure 6. The SSP scenarios used in this Report, their indicative temperature evolution and radiative forcing categorization, and the five socio-economic storylines upon which they are built. The core set of scenarios used in this report – i.e., SSP1-1.9, SSP1-2.6, SSP2-4.5, SSP3-7.0 and SSP5-8.5 – is shown together with an additional four SSPs that are part of Scenario MIP, as well as previous RCP scenarios

All data used in this study derive from Climate Data Store (CDS) (https://cds.climate.copernicus.eu/) and they are available in NetCDF format, which is widely used for climate and environmental data due to its efficient storage and compatibility with many software tools.

CDS's 'CMIP6 Climate Projections' catalogue entry provides daily and monthly global climate projections data from a large number of experiments, models and time periods computed in the framework of the sixth phase of the Coupled Model Intercomparison Project (CMIP6). The term "experiments" refers to the three main categories of CMIP6 simulations:

- Historical experiments which cover the period where modern climate observations exist. These experiments show how the GCMs performs for the past climate and can be used as a reference period for comparison with scenario runs for the future. The period covered is typically 1850-2014
- Climate projection experiments following the combined pathways of Shared Socioeconomic Pathway (SSP) and Representative Concentration Pathway (RCP). The SSP scenarios provide different pathways of the future climate forcing. The period covered is typically 2015-2100.

This catalogue entry provides both two- and three-dimensional data, along with an option to apply spatial and/or temporal subsetting to data requests. The selected domain for this study is the region of Greece, thus model dataset is extracted for the subset of Greek coordinates. Latitude range of the selected domain is 31°N to 44°N and longitude ranges from 17°E to 32°E. Temporal coverage for historical experiments is 1850 to 2014, while future SSP experiments' period is 2015-2100 and the temporal resolution of selected models is monthly datasets. Surface-Air Temperature has units of Kelvin (K) and is converted to degrees Celsius (°C). Near Surface air temperature refers to the temperature of air at 2m above the surface of land, sea or inland waters and is calculated by interpolating between the lowest model level and the Earth's surface, taking account of the atmospheric conditions.

Precipitation refers to the sum of liquid and frozen water, comprising rain and snow, that falls to the Earth's surface. It is the sum of large-scale precipitation and convective precipitation and does not include fog, dew or the precipitation that evaporates in the atmosphere before it lands at the surface of the Earth. This variable represents amount of water per unit area and time (kg/ m^2 s).

Highlighted model data are dataset of high significance as are included in EURO-CORDEX (European Coordinated Regional Climate Downscaling Experiment). EURO-CORDEX is a high-resolution climate modeling initiative that provides regional climate projections for Europe. It is part of the CORDEX (Coordinated Regional Climate Downscaling Experiment) framework established by the World Climate Research Program (WCRP) to improve regional climate predictions and support impact assessments, climate adaptation, and mitigation strategies at regional and local scales.

The selection of GCMs for EURO-CORDEX project is based on their performance over Europe, especially in representing the region's climate characteristics. The models selected from CMIP6 are chosen to serve as boundary conditions for Regional Climate Models (RCMs) for Europe. The EURO-CORDEX ensemble, driven by CMIP6 models, is designed to offer a more robust framework for climate impact assessments, providing more accurate simulations with improved resolution and better physical representation of processes relevant to the European region (Sobolowski et al., 2023). The aim of this study is to provide essential insights into how the Global Climate Models (GCMs) selected by the EURO-CORDEX community are sufficiently representative for the climate characteristics of the Greek region.

Table 1. Models used in the study and the corresponding spatial resolution. EuroCORDEX driving GCMs marked in bold

#	Model	Spatial Resolution	#	Model	Spatial Resolution
1	ACCESS_CM2	1.875° x 1.25°	**14**	INM-CM4-8	2° x 1.5°
2	AWI-CM-1-1-MR	0.93° x 0.93°	**15**	INM-CM5-0	2° x 1.5°
3	BCC-CSM2-MR	1.12° x 1.12°	**16**	**IPSL-CM6A-LR**	**1.27° x 1.27°**
4	CanESM5-CanOE	2.81° x 2.79°	**17**	KACE-1-0-G	1.87° x 1.25°
5	**CESM2**	**1.25° x 0.94°**	**18**	MCM-UA-1-0	3.75° x 2.23°
6	**CMCC-CM2-SR5**	**1.25° x 0.94°**	**19**	**MIROC6**	**1.4° x 1.4°**
7	CNRM-CM6-1	1.4° x 1.4°	**20**	MIROC-ES2L	2.81° x 2.79°
8	CNRM-CM6-1-HR	0.5° x 0.49°	**21**	**MPI-ESM1-2-HR**	0.9375° x 0.9375°
9	**CNRM-ESM2-1**	**1.4 °x 1.4°**	**22**	MPI-ESM1-2-LR	1.87° x 1.86°
10	**EC-Earth3-Veg**	**0.7 °x 0.7°**	**23**	MRI-ESM2-0	1.12° x 1.12°
11	FGOALS-f3-L	1.25° x 1°	**24**	**NorESM2-MM**	1.25° x 0.94°
12	FGOALS-g3	2° x 2.02°	**25**	TaiESM1	1.25° x 0.94°
13	GFDL-ESM4	1.25° x 1°	**26**	**UKESM1-0-LL**	**1.87° x 1.25°**
			27	gswp3-w5e5	0.5° x 0.5°

Observational Data

The performance of the model has been compared and evaluated with globally reconstructed observational data. The dataset we used for the observations, GSWP3-W5E5 (ISIMIP3a), is a merged dataset combining two key datasets used in climate and hydrological research: GSWP3 (Global Soil Wetness Project Phase 3) and W5E5 (WATCH forcing data methodology applied to ERA5 reanalysis data). The combined GSWP3 and W5E5 global meteorological forcing daily data processed for ISIMIP3a, cover the periods 1801-1900 (spinclim scenario), 1851-1900 (transclim scenario) and 1901-2019 (obsclim scenario, counterclaim scenario) on a 0.5°x0.5° lat-lon grid. Observational data are available on The Inter-Sectoral Impact Model Intercomparison Project (https://www.isimip.org/) (Lange et al., 2022).

This dataset is designed to provide high-quality climate forcing data for land surface modeling and other related applications. Here's an overview of each component and the combined dataset:

GSWP3 (Global Soil Wetness Project Phase 3)

GSWP3 provides meteorological forcing data for land surface models (LSMs). It's a follow-up to the previous phases of the Global Soil Wetness Project, which aims to validate and intercompare different LSMs by providing consistent forcing data.

Data Characteristics:

- Temporal Coverage: The GSWP3 dataset typically covers multiple decades, often starting from the early 20th century to the present. The exact coverage might vary depending on the specific version or extension of the dataset.
- Spatial Resolution: GSWP3 generally provides data on a global scale with a typical resolution of 0.5° x 0.5°.
- Variables: Includes a range of atmospheric forcing variables such as precipitation, temperature, wind speed, radiation (solar and longwave), humidity, and others required to drive land surface models.

The data are extensively used for hydrological modeling, soil moisture analysis, drought monitoring, and climate impact studies.

W5E5 Dataset

W5E5 is a meteorological dataset specifically designed to provide high-resolution, bias-corrected forcing data for land surface models. It merges ERA5 reanalysis data with the WFDE5 dataset using the WATCH methodology, aiming to provide a long-term, consistent dataset for climate impact assessments.

Data Characteristics:

- Temporal Coverage: Typically, from 1979 onward, aligning with the availability of the ERA5 reanalysis data.
- Spatial Resolution: Higher resolution than GSWP3, typically at 0.5° x 0.5°, but can vary depending on the specific product.
- Variables: Similar to GSWP3, including precipitation, temperature, radiation, humidity, wind speed, and other meteorological variables.

The data are primarily used for climate impact modeling, land surface modeling, and integrated assessment models (IAMs). It is also useful for studying extremes like heatwaves, droughts, and heavy precipitation events.

GSWP3-W5E5 Combined Dataset

The GSWP3-W5E5 dataset is essentially a hybrid dataset that utilizes the strengths of both GSWP3 and W5E5 datasets. It provides a consistent and continuous set of climate forcing data that can be used for various hydrological and land surface modeling studies. The integration of GSWP3 and W5E5 aims to enhance the temporal and spatial resolution and accuracy of the data available for researchers and modelers.

Data Characteristics:

- Temporal Coverage: Merges the long-term historical coverage of GSWP3 with the recent high-resolution data of W5E5.
- Spatial Resolution: Aims to maintain the high spatial resolution of W5E5 (0.5° x 0.5°).
- Variables: A wide range of atmospheric forcing variables required for land surface modeling.

Data of GSWP3-W5E5 Combined Dataset is derived from ISIMIP Repository. ISIMIP repository is a centralized database that stores data and resources produced and used by the Inter-Sectoral Impact Model Intercomparison Project (ISIMIP). ISIMIP is a global project that aims to assess the impacts of climate change across various sectors (such as agriculture, water, health, and biodiversity) using consistent climate scenarios and impact models. Also, it provides open access to a wide range of datasets, including climate forcing data, socio-economic scenarios, and impact model outputs. Researchers, policymakers, and other stakeholders can download these datasets for their analyses.

3. Methodology

Climate Data Operator (CDO)

For the purpose of this study all data and calculation are processed in CDO (Climate Data Operator). CDO is a powerful collection of command-line tools for processing and analyzing climate and weather data. Developed primarily for use with climate and atmospheric model outputs, CDO is widely used by scientists and researchers in meteorology, climatology, and environmental sciences for handling large datasets. CDO includes a wide range of operators (over 600), which allow users to perform various data manipulation and analysis tasks, including:

⇒ Data Selection: Extracting specific variables, time steps, or spatial regions.

⇒ Data Aggregation: Averaging over time, space, or ensembles.

⇒ Mathematical Operations: Adding, subtracting, multiplying, or dividing datasets.

⇒ Statistics: Calculating means, anomalies, trends, etc.

⇒ Interpolation and Regridding: Changing the spatial resolution or projection of data.

CDO operates via a command-line interface, making it suitable for batch processing and integration into automated workflows. This feature is particularly useful for processing large datasets and performing repetitive tasks efficiently.

While CDO itself does not provide visualization capabilities, data visualization is performed with Panoply visualization tool. Panoply is a cross-platform application developed by NASA's Goddard Institute for Space Studies (GISS) for viewing and plotting geospatial data. It is specifically designed to handle multidimensional data in NetCDF (Network Common Data Form), and other file formats commonly used in climate science, meteorology, and oceanography.

Data processing

In this study observation data was upscaled to match the grid of each individual CMIP6 model. Upscaling observational data is necessary for several reasons when processing and comparing climate model outputs and observations. Grid resolution mismatch is a very common issue as observation data are provided typically on finer resolutions compared to GCMs or ESMs. The comparison of the two datasets requires aligning them on the same spatial grid. Upscaling involves adjusting finer-resolution observational data to match a coarser model grid. This process ensures consistent spatial coverage between the model and observational data, enabling a meaningful comparison. Without upscaling, directly comparing high-resolution observational data with coarser model data can introduce biases. By aligning the resolution of the observational data with the model data, upscaling helps avoid these spatial biases.

Observational data were upscaled using the command 'remapcon' in CDO. When using *remapcon* to upscale observational data to match a model grid, conservative remapping is performed. This method ensures that the total values (precipitation, temperature) are conserved during the interpolation process. It's efficiently used when dealing with large-scale variables like precipitation or temperature, where maintaining the physical consistency of data is important.

The preprocessing of the observation dataset (gswp3_w5e5) was carried out through the following steps:

⇒ First, the decadal observation datasets were merged in time in order to create consistent time series for the desired time period (1979-2014).

⇒ Then, daily data was converted to monthly data (*cdo monmean infile outfile*)

⇒ Lastly, observation data was upscaled to match the model data grid (*cdo remapcon,model.nc obs.nc upscaled_obs.nc*)

Metrics of skill evaluation

Additionally, upscaling the observation dataset is essential as climate models and observation datasets must be on the same grid to accurately compute skill metrics, such as:

- Mean differences (bias).
- Root Mean Square Error (RMSE).
- Correlation coefficients.

After selecting the desired time period of model datasets (1979-2014) using cdo command *cdo seldate,1979-01-01,2014-12-31 infile.nc outfile.nc,* statistical metrics were computed using CDO software:

1. Mean Bias Error (MBE) is used to measure the average difference between predicted values and observed values. It helps assess the accuracy and bias of a model in relation to real-world data.

$$MBE = \frac{1}{n}\sum_{i=1}^{n}(Pi - Oi)$$

Pi: Model predicted value.

Oi: Observed value.

n: Number of data points.

Positive MBE indicates that the model tends to **overestimate** the observed values, while negative MBE indicates that the model tends to **underestimate** the observed values. MBE close to 0 indicates that the model predictions are, on average, close to the observations, indicating **low bias**.

MBE is useful for understanding whether a model has a consistent tendency to over- or underestimate compared to observations. However, it does not capture the magnitude of errors (which is done by metrics like RMSE).

Mean Bias Error derives from:

- Calculation of time mean of the difference between model data and the corresponding observation dataset

  cdo timmean diff.nc diff_timemean.nc

- Calculation of mean bias error as the spatial mean of the previous step

  cdo fldmean diff_timemean.nc mbe.nc

2. Root Mean Square Error (RMSE) is commonly used to measure the difference between predicted values and observed values while indicates the magnitude of prediction errors, emphasizing larger errors due to its squaring of differences.

$$RMSE=\sqrt{\frac{1}{n}\sum_{i=1}^{n}(Pi-Oi)^2}$$

Pi: Model predicted value.

Oi: Observed value.

n: Number of data points.

RMSE measures the average magnitude of the errors between model predictions and observations. Lower RMSE indicates better model performance, as the prediction errors are smaller. Higher RMSE indicates larger discrepancies between model predictions and observed values.

Root Mean Square Error derives from:

- the computation of the difference between model data and the corresponding observation dataset.

  cdo -L sub -sellevidx,1 model.nc upscaled_obs.nc diff.nc

- Calculation of squared difference

  cdo mul diff.nc diff.nc diff_squared.nc

- Calculation of squared difference mean value

  cdo timmean diff_squared.nc diff_squared_mean.nc

- Calculation of root mean squared error (rmse)

  cdo sqrt diff_squared_mean.nc rmse.nc

3. Time correlation evaluates the strength and direction of the linear relationship between two time series (e.g., model predictions and observations) over time.

Correlation Coefficient (r) quantifies the strength and direction of the linear relationship between two variables. It ranges from -1 to 1.

- r=1: Perfect positive correlation (both time series increase/decrease together).
- r=−1: Perfect negative correlation (one increases while the other decreases).
- r=0: No correlation (no linear relationship).

$$r = \frac{\sum_{i=1}^{n}(Pi-\bar{P})(Oi-\bar{O})}{\sqrt{\sum_{i=1}^{n}(Oi-\bar{O})^2}\sqrt{\sum_{i=1}^{n}(Pi-\bar{P})^2}}$$

- Pi: Predicted values.
- Oi: Observed values.
- $\bar{P}$, $\bar{O}$: Mean of predicted and observed values, respectively.

High positive correlation means that the model accurately captures the observed temporal variations.

Low or negative correlation means that the model fails to replicate the observed temporal pattern.

Time correlation is useful in evaluating how well a model captures the timing and direction of changes over time, such as trends or seasonal cycles. Using CDO, time correlation was computed as follows:

- Calculation of monthly mean value of each month (aka mean value for all Januaries/ Februaries etc) for every model

cdo ymonmean model.nc model_ymonmean.nc

- Calculation of monthly mean value for the corresponding observation data

cdo ymonmean upscaled_obs.nc obs_ymonmean.nc

- Calculation of temporal correlation

cdo timcor obs_ymonmean.nc model_ymonmean.nc timcor.nc

- Average diff.nc over time (spatial mean)

cdo fldmean diff.nc diff_fldmean.nc

4. Standard Deviation over time measures how much a variable fluctuates around its mean value across different time steps. It quantifies the variability or dispersion of data points (e.g., temperature, precipitation) over a period (1979-2014), helping to understand how stable or volatile the variable is over time.

$$\sigma = \sqrt{\frac{1}{n}\sum_{i=1}^{n}(Xi - \bar{X})^2}$$

Xi: Value of the variable at time step iii.

$\bar{X}$: Mean value of the variable over the entire time period.

n: Number of time steps.

Low standard deviation means that the values are closely clustered around the mean, indicating little variability over time. High standard deviation means that the values fluctuate widely from the mean, indicating high variability or instability over time. In climate analysis, the standard deviation over time can help identify periods of high variability, such as extreme temperature fluctuations or variations in precipitation patterns. It provides insight into how consistent a variable is over time, which is crucial for understanding long-term trends, seasonal variability, and anomalies in time series data. Standard deviation over time was computed using the CDO command '*cdo timstd model.nc model_timstd.nc'.*

The standard deviation between the outputs of climate models and observational data should align as closely as possible. A higher degree of correspondence indicates that the model effectively captures the observations and the climatic biases for a given period.

Model selection criteria

In climate change impact assessment, it is essential to work with a manageable subset of climate model forcings to ensure the analysis remains computationally feasible while capturing the key uncertainties and variabilities. This approach enables researchers to focus on the most relevant scenarios and outputs, facilitating a more targeted and effective evaluation of climate impacts. When selecting climate models for this analysis, a range of criteria must be carefully considered to ensure that the chosen models are appropriate for the specific research objectives, region of interest, and data requirements. Below the key criteria considered when selecting models for climate analysis are presented:

- Availability of Data and Variables. It was important to ensure the model outputs were publicly available and covered the necessary variables (temperature and precipitation) and time period (1979-2100).
- Participation in Coupled Model Intercomparison Project 6 (CMIP6) and EUROCORDEX. These models have been rigorously evaluated against one another and standardized datasets.
- Multi-Model Ensembles (MME) simulation: the combination of different models to capture uncertainty and variability in model projections, improves robustness by accounting for differences in model structure and parameterization.
- Scenario Diversity: Selected models support the future scenarios that are analyzing and provide outputs for multiple greenhouse gas emission and climate forcing scenarios (e, SSP1-2.6, SSP2-4.5, SSP3-7.0, SSP5-8.5) to explore a range of possible future climates.

- Spatial Resolution: Choose models that have appropriate grid resolution for the study area (region of Greece). Ensure the spatial resolution aligns with the scale of the analyzing phenomena (temperature and precipitation).
- Temporal Resolution: Selected models were obtained at a monthly time step to evaluate them and analyze seasonal trends of the spatial phenomena.

Potential issues in data handling and model variability

When handling climate data and managing model variability, several potential issues can arise that affect the accuracy, reliability, and usability of the results. Some common data handling challenges are data quality and consistency. Missing values in data can lead to incomplete analyses and inconsistent formats resulting in incompatibility across datasets. Data resolution, coverage, and temporal alignment are also common issues. Mismatched resolutions between datasets (e.g., observations vs. model outputs) and regional coverage may impact the accuracy of comparisons. Datasets with different time steps, interpolation, or aggregation may be needed to align them for analysis.

4. Results

Comparison with observation data

Observed total annual precipitation and mean annual air temperature for the period 1979-2014 are analyzed and illustrated at the following Figures (7,8). There is a robust trend of increase of the near-surface temperature (more than 1 °C) (fig.7b), while precipitation is mostly dominated by multi-annual variability with no clear trend over the 1979-2014 time period (fig.7a).

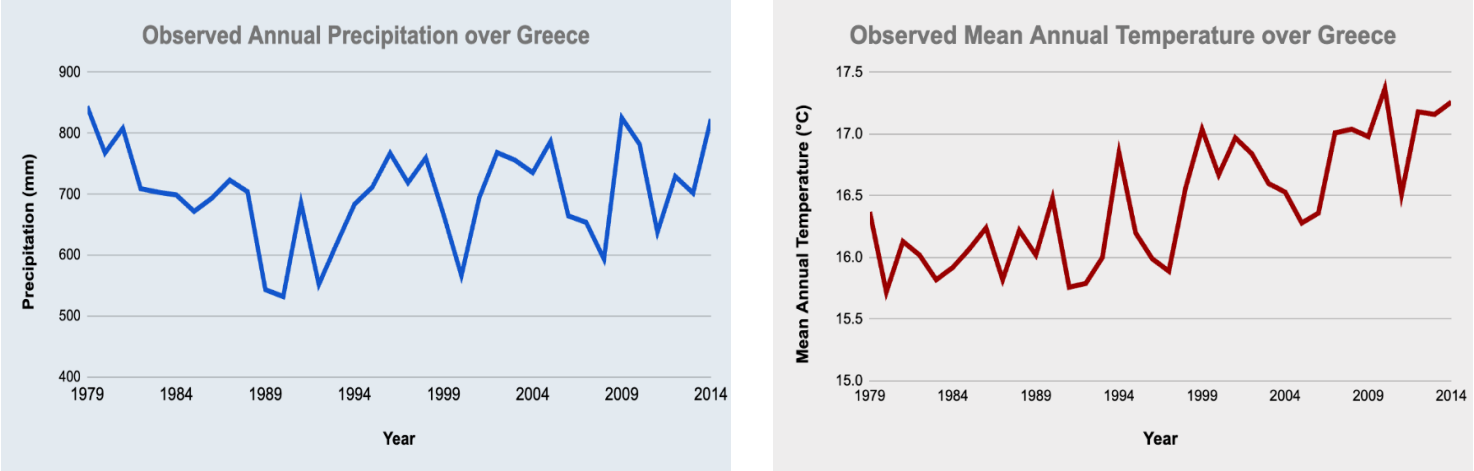

(a) (b)

Figure 7. Observed annual mean air temperature (a) and total annual precipitation(b) for the period 1979-2014.

The mean annual temperature is found increased in southern and coastal parts of the country, while lower mean temperature is observed in the mainland. The spatial pattern seems to be linked to the orography of central Greece as the temperature is lower in the inland, mountainous region (fig.8b). Precipitation patterns vary across the Greek region with lower accumulations especially in the eastern mainland and the Aegean Sea. In contrast, the western region, which contains the majority of Greece's mountainous terrain, experiences higher levels of precipitation (fig. 8a). According to figure 8a, typical precipitation over western mountainous region in Greece range between 1000-2000mm/year, while coastal and island region in Greece experience drier climatologies with precipitation range from 400 to 1000 mm/year based on GSWP3-W5E5 dataset.

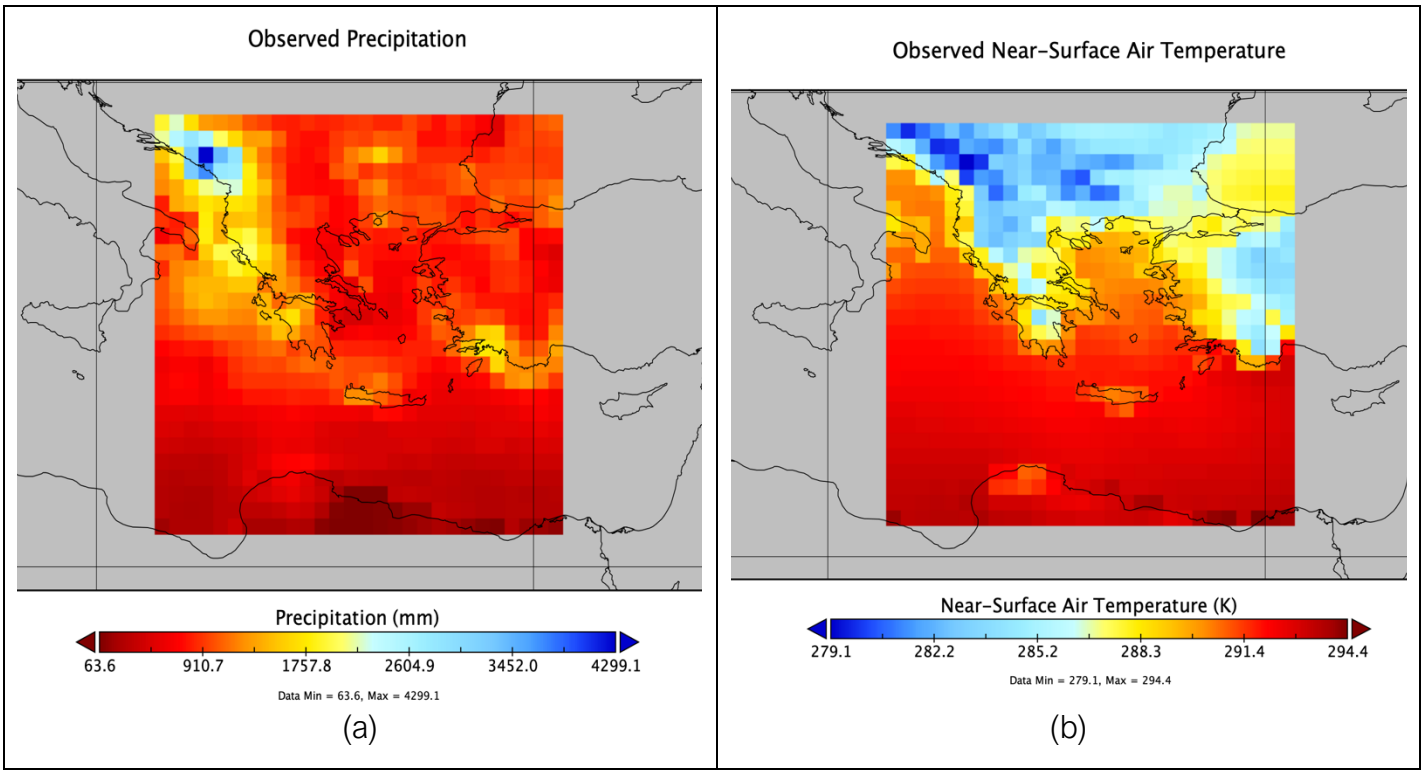

Figure 8. Observed annual mean air temperature (a) and total annual precipitation(b) over the region of Greece for the period 1979-2014.

Precipitation Mean Bias Error

Mean Bias Error (MBE) and Root Mean Square error (RMSE) between model outputs and observations are analyzed and compared over the Greek region for the period 1979-2014. Temperature and precipitation results are visualized using Panoply software and presented in figures 9,10,11 and 12).

Figure 9 shows the spatial distribution of the precipitation mean bias error across the Greek region. Areas with positive bias indicate that the model overestimates precipitation compared to observations and the opposite for areas with negative bias, while color shading represents the magnitude of the bias. Darker shades represent larger deviations (higher bias) from observations, while lighter shades represent areas where the model closely matches observed precipitation.

Selected models exhibit variation in mean bias error outputs with a trend to underestimate precipitation. The models capture precipitation well over flat terrains, but high biases are noted over mountainous regions (MBE $_{\text{CNRM-CM6-1}}$= -0.1mm/month, MBE $_{\text{CNRM-CM6-1-HR}}$= 5.5 mm/month, MBE $_{\text{CNRM-ESM2-1}}$= 0.3 mm/month).

Spatial visualization of the mean bias error contributes to identifying whether the model performs well across different regions (e.g. mountainous or coastal areas). The Mean Bias Error (MBE) results for 26 different climate models range from -16 mm/month (INM-CM4-8) to 9.5 mm/month (MIROC-ES2L), showing a significant spread in how different models simulate precipitation (figure 9). This indicates variability in model structure, parameterization, and regional resolution, which all affect the accuracy of precipitation simulation. The majority of the models show a negative bias (underestimation of precipitation), with 20 out of the 26 models having MBE values below zero. This suggests that most models tend to simulate less precipitation than observed in the region. Only a few models show positive bias (overestimation), including values such as CNRM-CM6-1-HR (MBE=5.5 mm/month), MIROC-ES2L (MBE=9.5 mm/month), GFDL-ESM4(MBE=0.4) and CNRM-ESM2-1 (MBE=0.3 mm/month). Several models display large negative biases, especially INM-CM4-8 (-16.0 mm/month), CanESM5-CanOE (-14.0 mm/month), MCM-UA-1-0 (-13.9 mm/month), NorESM2-MM (-13.6 mm/month), TaiESM1(-13.1 mm/month), AWI-CM-1-1-MR (-12.4 mm/month), FGOALS-f3-L (-12.2 mm/month), and CMCC-CM2-SR5 (-11.2 mm/month). These substantial underestimations could indicate that these models have difficulty capturing regional precipitation dynamics, possibly due to limitations in how they represent physical processes. A negative bias greater than 10 mm is seen in many models, suggesting that the tendency to underestimate precipitation is widespread across different models. There are a few models that perform well in terms of bias, with values close to zero, including MIROC6 (0.0 mm/month), CNRM-CM6-1(0.1 mm/month), CNRM-ESM2-1 (0.3 mm/month), and GFDL-ESM4(0.4 mm/month). These models are better at capturing the actual precipitation patterns in the region and could be considered more reliable for precipitation projections.

Precipitation Root Mean Square Error

By visualizing the precipitation root mean square error (RMSE) between model outputs and observations in Panoply, the overall accuracy of the model's precipitation predictions is effectively illustrated. Figure 10 presents the extent the model's predictions deviate from observations, emphasizing areas with larger errors. Unlike the mean bias error (which shows the average difference), RMSE focuses on the magnitude of the error, regardless of whether the model over- or underestimates precipitation. Larger errors have a greater influence because RMSE squares the differences before averaging them. Thus, regions with significant model inaccuracies are highlighted.

RMSE, likely to MBE, reveals patterns of error across different terrain types. Over the Greek mountain range Pindos, some models struggle to simulate precipitation (CNRM-CM6-1, CNRM-CM6-1-HR, CNRM-ESM2-1). Low RMSE is observed over Mediterranean Sea (south of Crete Island), while on the mainland of Greece RMSE has moderate values indicating the model's uncertainties across diverse spatial patterns. These patterns align with the results of table 2 where CNRM-CM6-1, CNRM-CM6-1-HR, CNRM-ESM2-1 present high RMSE values (above 49 mm/month) (Table 2).

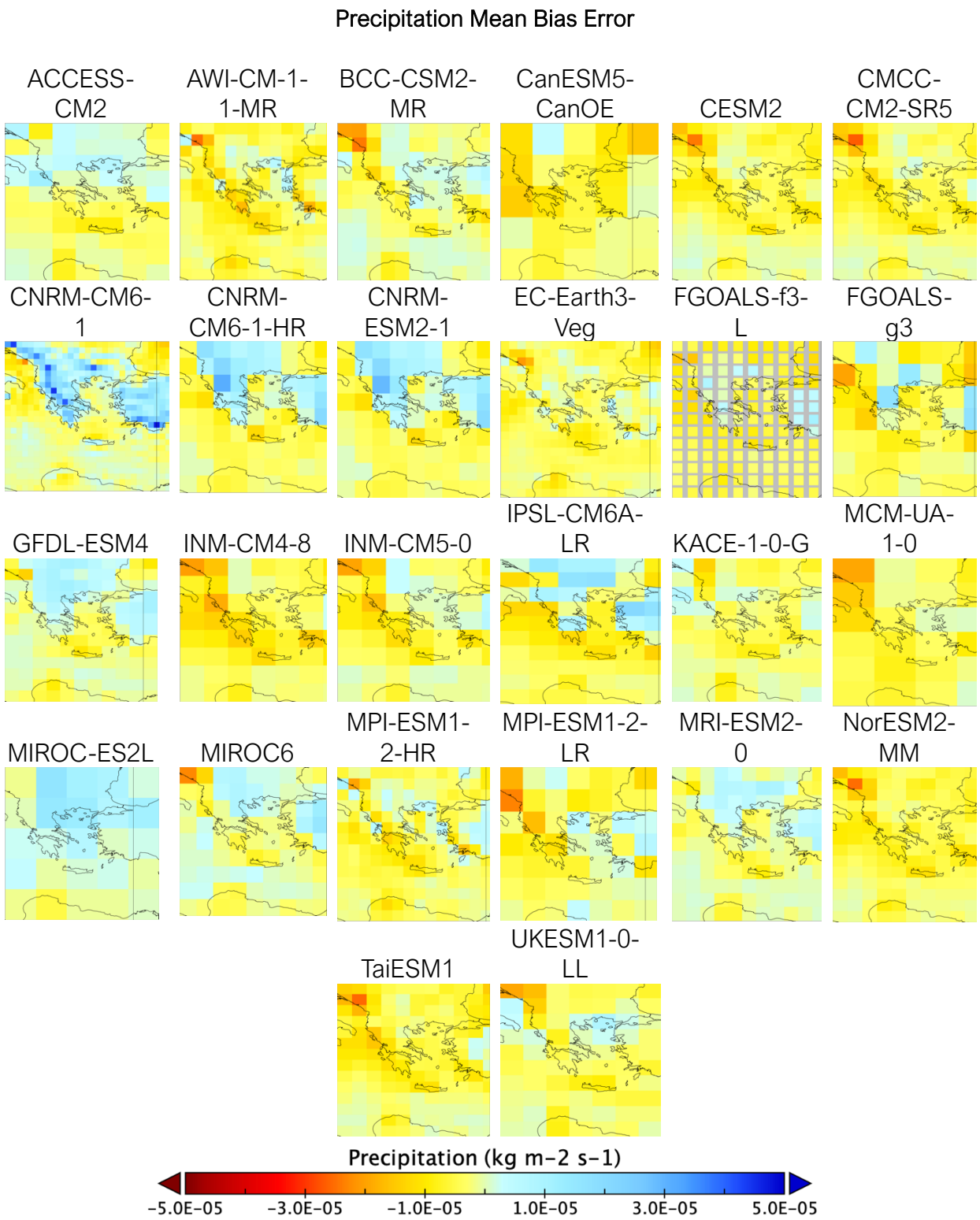

Figure 9. Precipitation Mean Bias Error of the selected climate models. Annual average calculated for a 35-year climatology (1979–2014)

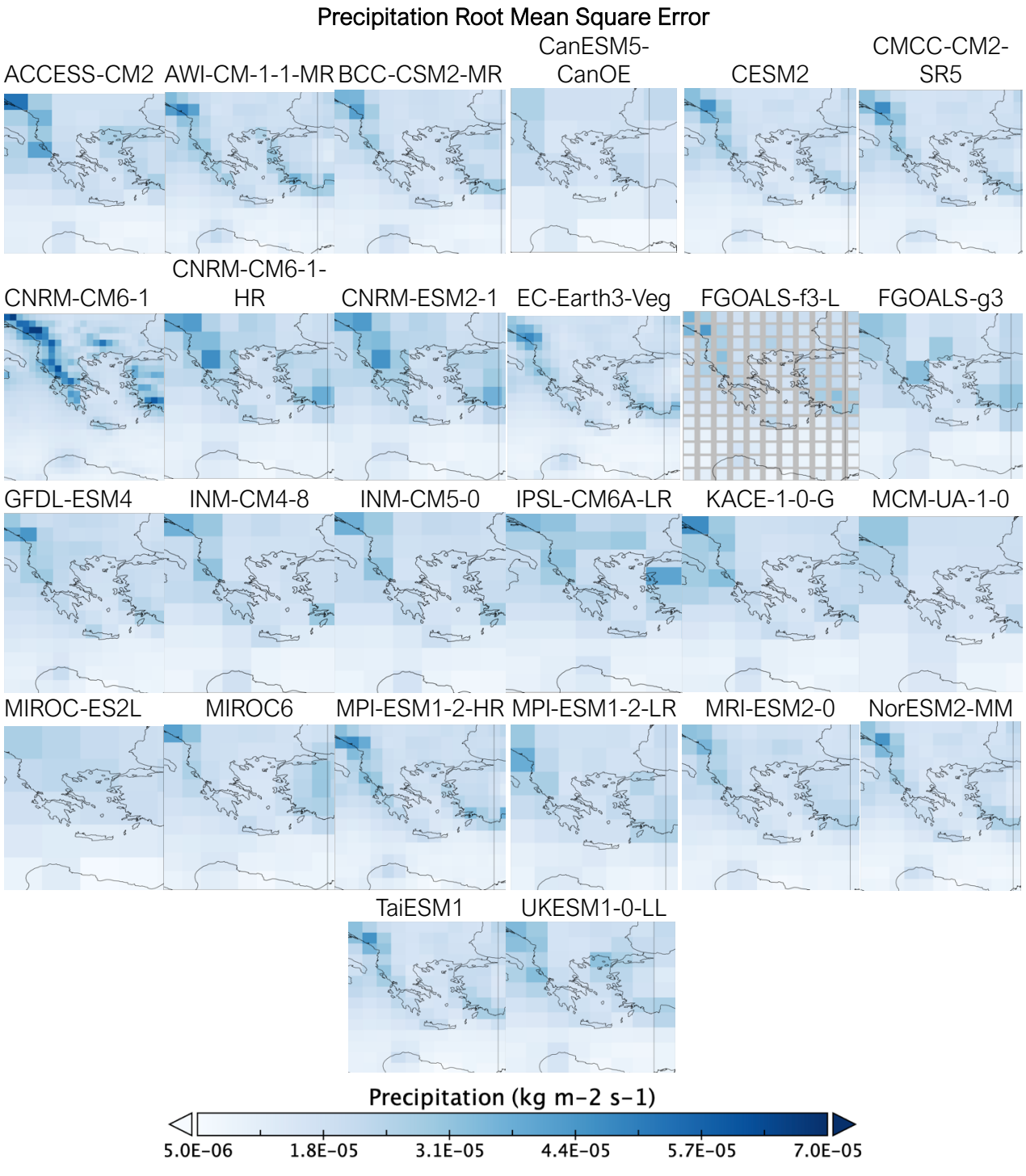

Figure 10 . Precipitation Root Mean Square Error of the selected climate models. Annual average calculated for a 35-year climatology (1979–2014)

Near-Surface Air Temperature Mean Bias Error

Figure 11 shows the spatial distribution of the temperature mean bias error across the Greek region. The figure demonstrates a common tendency of the models to overestimate temperature compared with observations across the mainland of Greece, especially over central and north Greece. High MBE values are observed also over Peloponnesus (MIROC6, MIROC-ES2L, CESM2, CMCC-CM2-SR5), while the majority of the models seems to perform well across island regions, Aegean and Ionian Sea. However, some models present high biases across all over the Greek domain (MBE $_{MIROC6}$ =2.54°K, $MBE_{MIROC\text{-}ES2L}$=1.39 °K, $MBE_{INM\text{-}CM4\text{-}8}$=1.27 °K, $MBE_{CNRM\text{-}CM6\text{-}1\text{-}HR}$= -1.09 °K)

High positive bias values such as MIROC6, MIROC-ES2L, and INM-CM4-8 suggest that the respective models tend to overestimate the temperature compared to observed values. The highest MBE value here is MIROC6=2.54 °K (table 2), indicating a significant overestimation by that model. Negative MBE values (such as ACCESS-CM2=-0.92 °K, CNRM-CM6-1-HR= -1.09, and GFDL-ESM4 = -0.87 °K) are suggesting this model's temperature predictions are lower than the observed values. According to table 2, the best MBE values among 26 models are 0.01°K (MCM-UA-1-0), 0.10 °K (CNRM-CM6-1 and EC-Earth3-Veg), suggesting that these models align more closely with the observed data, indicating higher accuracy for those models in simulating the temperature.

The variability in MBE across models highlights the challenges in accurately simulating temperature, as different models may use different assumptions and parameterizations. Overall, this range of MBEs demonstrates the importance of using multiple models in climate projections to capture the full range of potential biases and uncertainties.

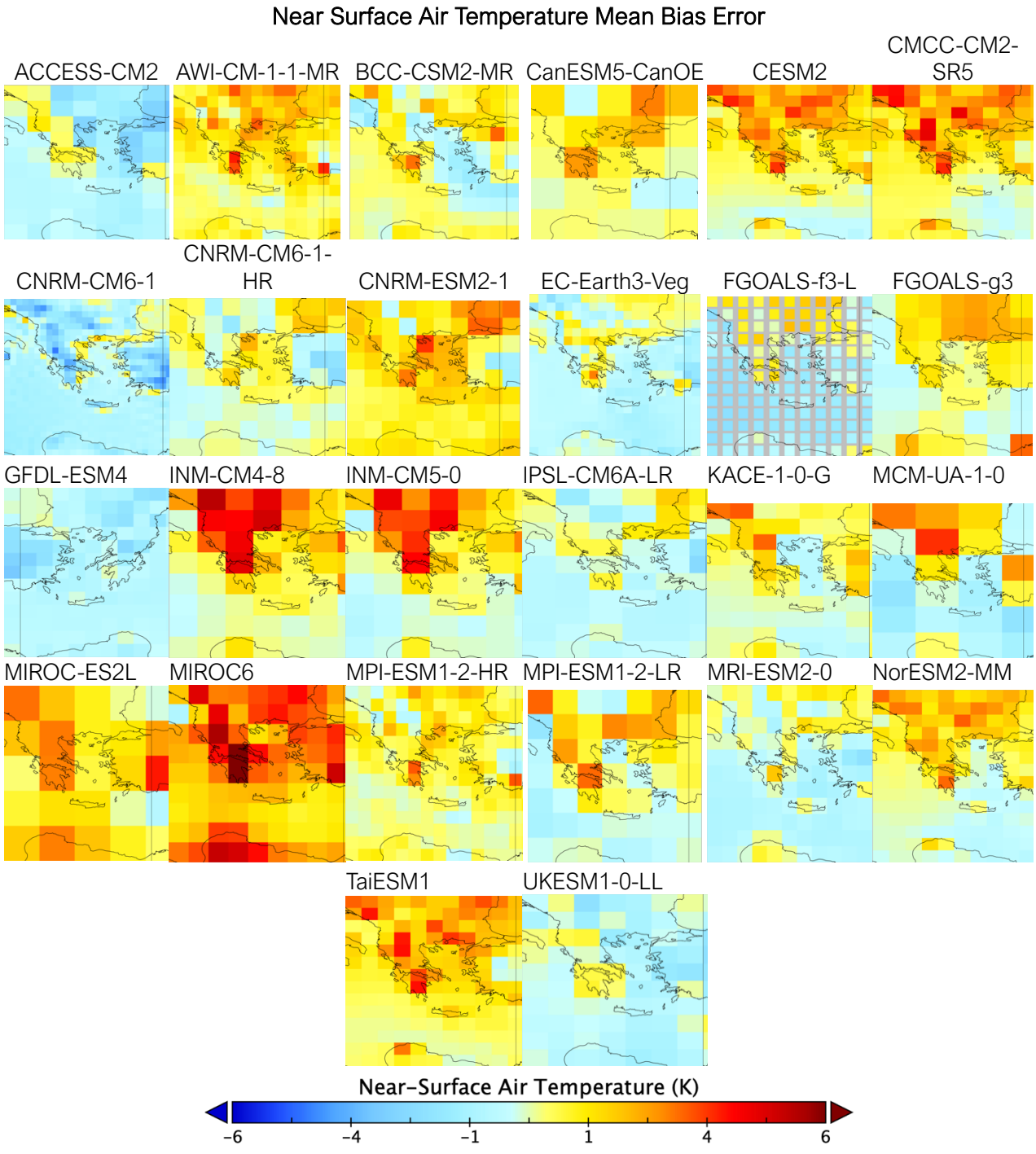

Figure 11. Near-surface air temperature Mean Bias Error of the selected climate models. Annual average calculated for a 35-year climatology (1979–2014)

Near Surface Air Temperature Root Mean Square Error

Figure 12 presents the Root Mean Square Error (RMSE) results for 26 climate models, ranging from 1.78 to 3.52 °K (table 2). These values provide insight into the accuracy of each model's temperature simulations compared to observational data. Higher RMSE values indicate regions with greater uncertainty in the temperature predictions of the models. This uncertainty arises from various sources, such as inaccurate representation of atmospheric processes, surface characteristics, and boundary conditions (greenhouse gas concentration, ozone levels, and solar radiation). In regions with low RMSE values, the model's temperature projections are more reliable, indicating greater confidence in its ability to simulate future temperature trends in those areas. Conversely, high RMSE values suggest lower confidence in the model's temperature projections for that region.

The results of this study show that the selected models demonstrate considerable reliability over the region of Greece. Most of the RMSE values fall between 1.78 and 2.53 ° K, indicating that the ensemble of models generally captures temperature patterns, though some variation exists. MCM-UA-1-0 and MIROC6 present higher RMSE values (3.52 and 3.48 ° K respectively) denoting that these models have errors over 3 ° K, which is significantly higher than the rest of the ensemble (table 2). Such high RMSE values suggest that these models struggle more with simulating temperature accurately.

The models with the lowest RMSE values (indicating better performance) are CNRM-CM6-1 (1.78 ° K), IPSL-CM6A-LR (1.81 ° K), RI-ESM2-0 (1.87 ° K), CNRM-ESM2-1 (1.88 ° K), and CanESM5-CanOE (1.89 ° K) (table 2). These models have a RMSE below 1.9, making them the most accurate at simulating temperature compared to the observations. These top-performing models can be prioritized in climate impact studies where temperature accuracy is critical, as they consistently provide more reliable temperature simulations.

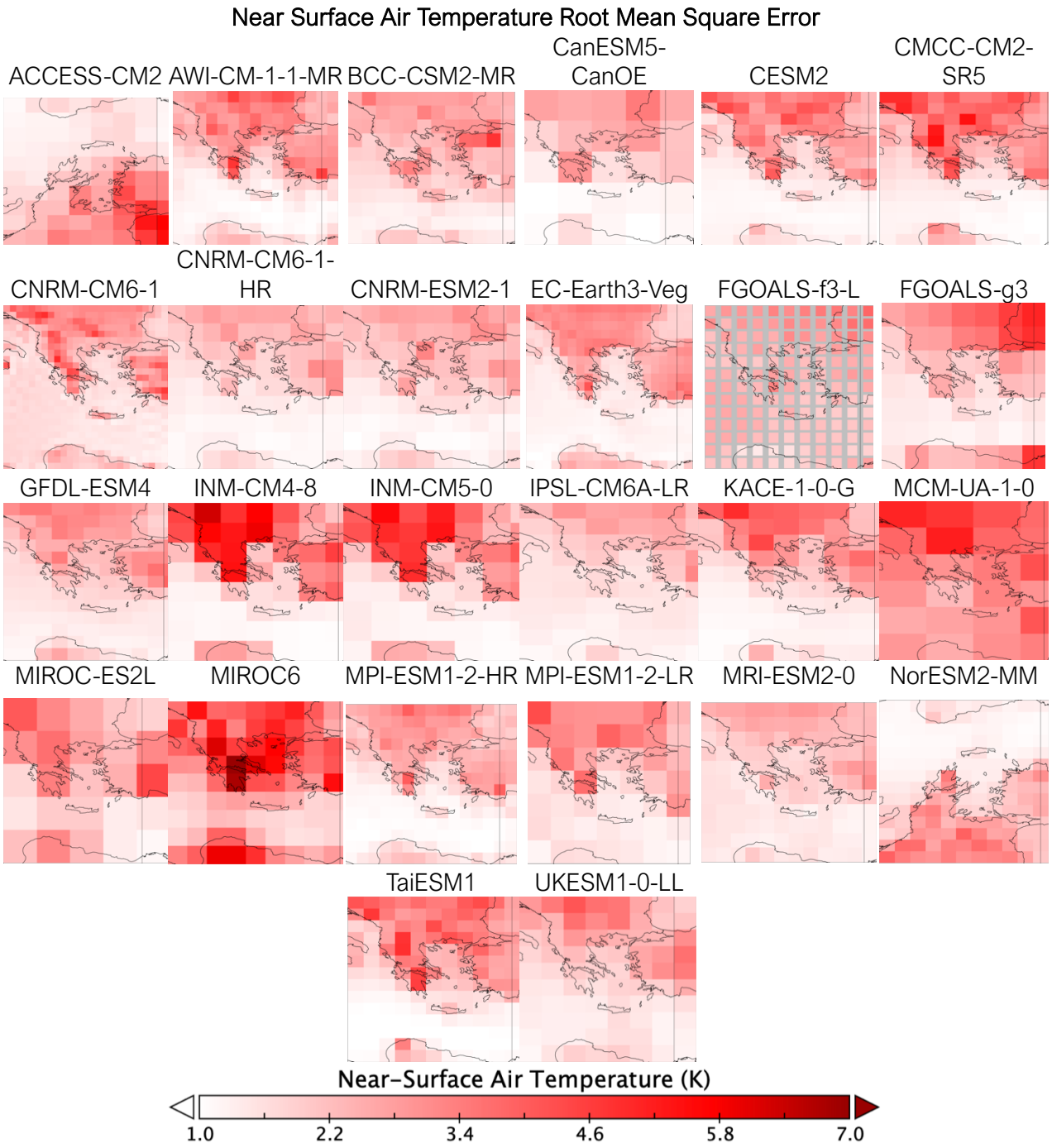

Figure 12. Near-surface air temperature Root Mean Square Error of the selected climate models. Annual average calculated for a 35-year climatology (1979–2014)

Table 2. Selected models' evaluation metrics results for temperature and precipitation over the period 1979-2014. Euro-CORDEX models marked in bold.

		Temperature				Precipitation			
#	MODEL	MBE (K)	RMSE (K)	STD (K)	Corr.	MBE (mm/month)	RMSE (mm/month)	STD (mm/month)	Corr.
obs	GSWP3-W5E5			5.7				41.7	
1	ACCESS-CM2	-0.92	2.31	6.28	0.993	-2.3	47.6	43.2	0.875
2	AWI-CM-1-1-MR	1.01	2.19	6.39	0.995	-12.4	46.1	37.5	0.852
3	BCC-CSM2-MR	0.25	2.14	5.34	0.972	-5.1	44.1	34.4	0.782
4	CanESM5-CanOE	0.69	1.89	5.84	0.995	-14.0	40.8	28.6	0.917
5	**CESM2**	**0.95**	**2.08**	**5.82**	**0.997**	**-11.1**	**42.4**	**34.1**	0.859
6	**CMCC-CM2-SR5**	**1.17**	**2.37**	**6.44**	0.993	**-11.2**	**42.4**	**33.3**	**0.923**
7	CNRM-CM6-1	0.10	1.78	5.75	**0.997**	-0.1	49.0	39.2	**0.886**
8	CNRM-CM6-1-HR	-1.09	2.15	5.72	**0.997**	5.5	52.7	43.4	0.854
9	**CNRM-ESM2-1**	**0.57**	**1.88**	**5.94**	**0.997**	**0.3**	**49.7**	**40.3**	0.878
10	**EC-Earth3-Veg**	0.10	1.99	6.48	**0.996**	-9.6	42.7	36.3	0.874
11	FGOALS-f3-L	-0.75	2.45	5.40	0.990	-12.2	44.7	35.7	0.845
12	FGOALS-g3	0.65	2.39	5.92	0.988	-9.3	46.2	30.5	0.704
13	GFDL-ESM4	-0.87	2.08	6.07	0.995	0.4	45.7	37.8	0.871
14	INM-CM4-8	1.27	2.71	6.44	0.981	-16.0	44.2	31.1	0.851
15	INM-CM5-0	0.85	2.53	6.32	0.983	-9.7	44.4	36.5	0.851
16	**IPSL-CM6A-LR**	**-0.32**	**1.81**	**5.75**	0.996	**-4.8**	**49.5**	**38.1**	0.761
17	KACE-1-0-G	0.30	2.15	6.43	**0.996**	-7.1	45.8	45.1	0.877
18	MCM-UA-1-0	0.01	3.52	8.20	0.984	-13.9	42.8	32.1	0.703
19	**MIROC6**	**2.54**	**3.48**	**6.97**	0.994	**0.0**	**44.1**	**39.6**	0.887
20	MIROC-ES2L	1.39	2.46	6.58	0.994	9.5	43.0	40.5	0.889
21	**MPI-ESM1-2-HR**	**0.53**	**1.91**	**6.12**	0.995	**-8.9**	**45.0**	**38.8**	0.871
22	MPI-ESM1-2-LR	0.34	2.22	6.28	0.995	-10.1	46.5	40.2	0.826
23	MRI-ESM2-0	-0.39	1.87	5.09	**0.997**	-0.8	43.7	39.9	**0.911**
24	**NorESM2-MM**	0.55	1.93	5.71	0.995	-13.6	41.4	32.2	0.869
25	TaiESM1	1.20	2.26	6.25	0.994	-13.1	43.8	34.1	0.892
26	**UKESM1-0-LL**	**-0.61**	**2.06**	**6.24**	**0.997**	**-8.0**	**45.8**	**43.1**	**0.913**

Annual cycle of modelled temperature and precipitation against gswp3-w5g5

Annual cycle comparison plots of temperature and precipitation between climate models and observations provide valuable insight into the model's ability to capture real-world data variability across different times of the year. In the following plots (fig13,14), the model outputs are compared to observed temperature and precipitation data every month, highlighting the extent to which the model can replicate seasonal patterns such as summer heatwaves and droughts or winter cold spells. These plots reveal important seasonal dynamics, such as how accurately the model simulates temperature extremes or transitions between seasons, like the onset of winter or summer. Such comparisons are key to validating the model's performance and building confidence in its ability to project future climate seasonality. This is particularly crucial for climate-sensitive regions, like Greece, where seasonal temperature variations are significant for sectors like agriculture, water management, and public health.

In order to sort the models into categories, the Mean Bias Error and correlation were used as a guide (Fig. 13,14b). It is observed that the models simulate the annual cycle of temperature and precipitation with variable accuracy. However, several models display large negative biases. Models with low MBEs and high time correlation coefficients and correlations closer to 1 demonstrate a high ability to capture the temporal variability in observed temperature and precipitation accurately.

The time correlation coefficients of seasonal temperature range from 0.972 to 0.997, indicating a very strong correlation between the model outputs and observed temperatures across all models, while the MBE values vary from -1.09 K to 2.54 K, indicating that they lag in capturing certain temperature fluctuations over time compared to observations (fig.13).

The correlation coefficients for precipitation range from 0.703 to 0.923, showing how well each model captures the seasonal pattern of precipitation compared to observations. Models with correlation values above 0.900 (e.g., 0.923, 0.917, 0.913) suggest they are highly effective at simulating seasonal variations in precipitation. Models with correlations closer to 0.700, such as 0.703 and 0.704, indicate that these models have difficulty simulating the correct timing of precipitation. These models may fail to accurately capture the climatology of precipitation seasonality. The MBE values of precipitation range from -16.0 mm/month to 9.5 mm/month, indicating significant variability in how well different models simulate precipitation, however some models, such as MIROC6 (0.0 mm/month) or CNRM-ESM2-1 (0.3 mm/month), demonstrate the best accuracy in terms of MBE, indicating a close alignment with observed precipitation data. MIROC6 demonstrate low MBE (0.0 mm/month) while also show strong correlations (0.887), indicating good overall performance (Fig.14).

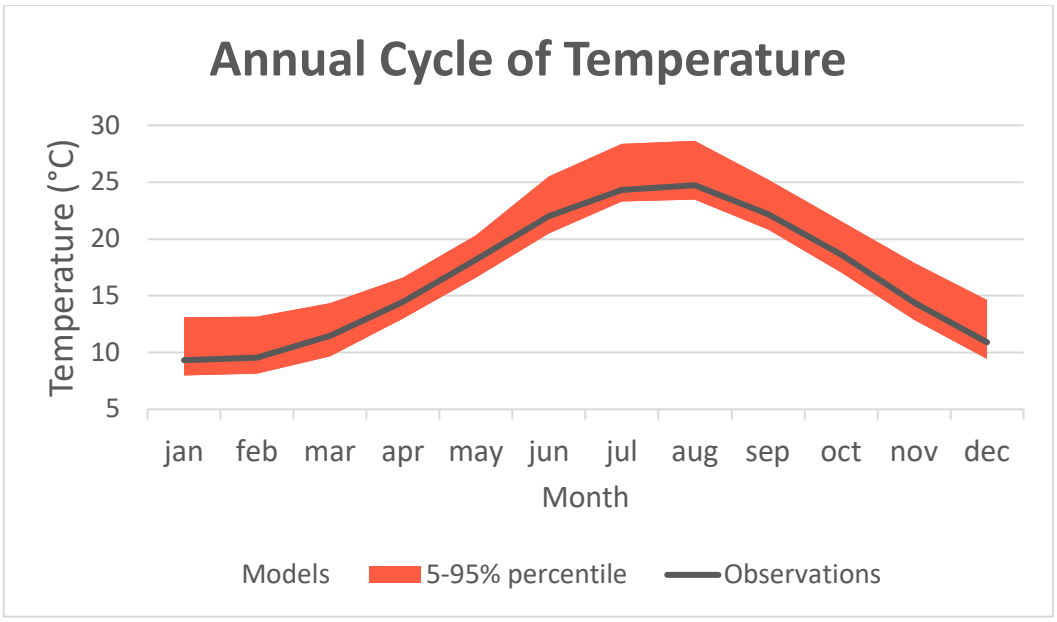

(a)

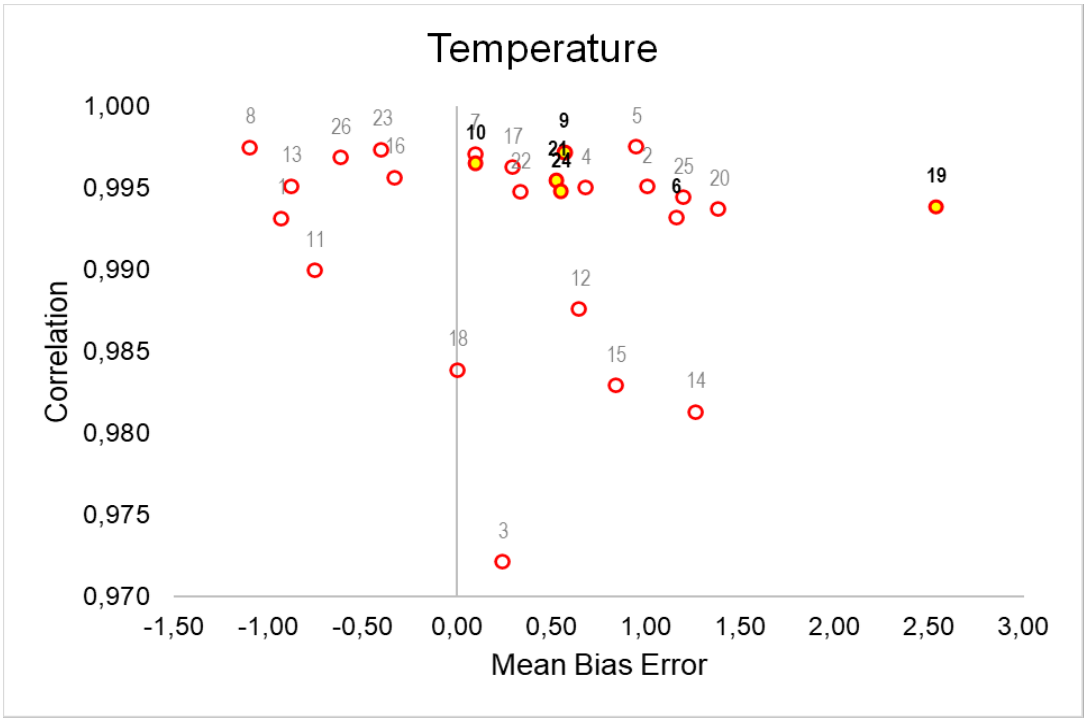

(b)

1:ACCESS-CM2 2:AWI-CM-1-1-MR 3:BCC-CSM2-MR 4:CanESM5-CanOE **5:CESM2** **6:CMCC-CM2-SR5** 7:CNRM-CM6-1
8:CNRM-CM6-1-HR **9:CNRM-ESM2-1** **10:EC-Earth3-Veg** 11:FGOALS-f3-L 12:FGOALS-g3 13:GFDL-ESM4 14:INM-CM4-8
15:INM-CM5-0 **16:IPSL-CM6A-LR** 17:KACE-1-0-G 18:MCM-UA-1-0 **19:MIROC6** 20:MIROC-ES2L **21:MPI-ESM1-2-HR**
22:MPI-ESM1-2-LR 23:MRI-ESM2-0 **24:NorESM2-MM** 25:TaiESM1 **UKESM1-0-LL**

Figure 13. Temperature annual cycle); model comparison with observations (shown as solid black line). Time Correlation and MBEs for each model. Monthly averages are taken over a 35-year climatology (1979–2014).

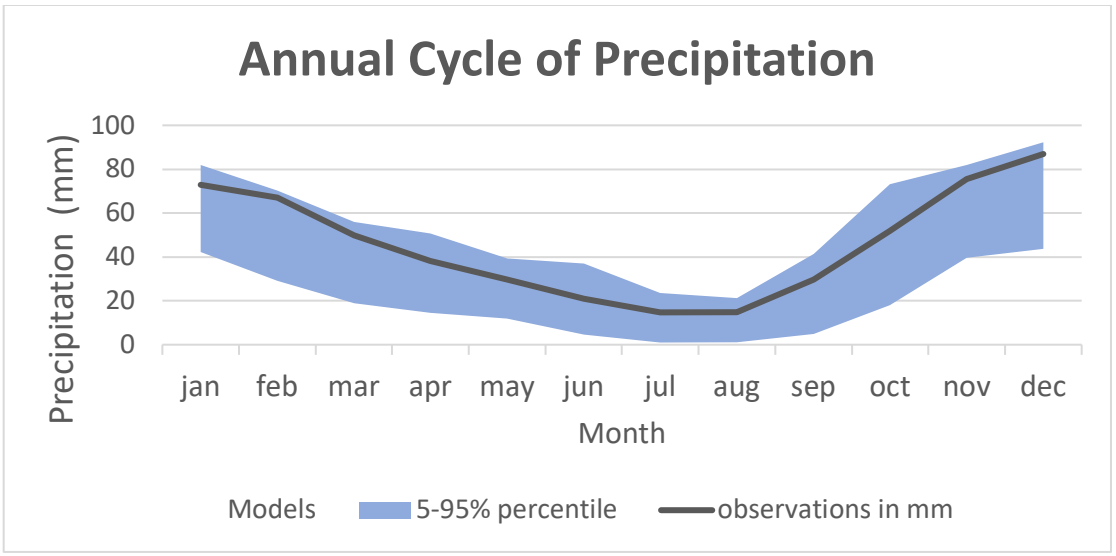

(a)

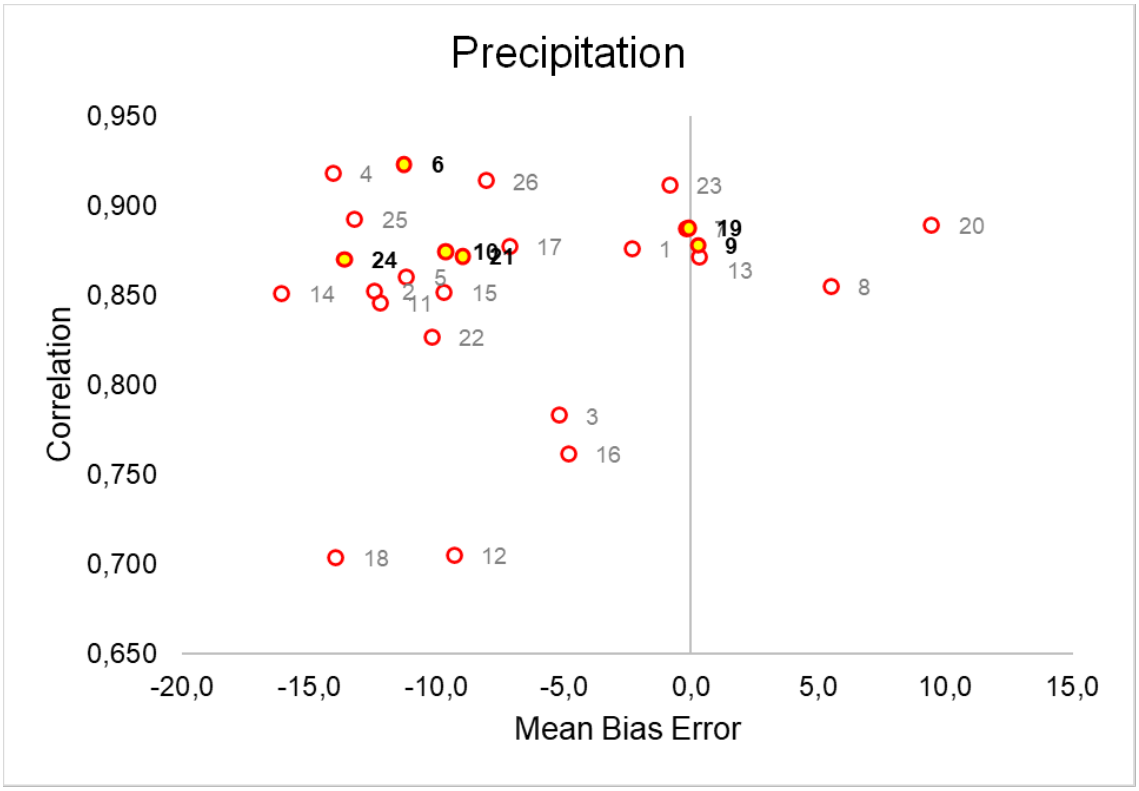

(b)

1:ACCESS-CM2 2:AWI-CM-1-1-MR 3:BCC-CSM2-MR 4:CanESM5-CanOE **5:CESM2** **6:CMCC-CM2-SR5** 7:CNRM-CM6-1
8:CNRM-CM6-1-HR **9:CNRM-ESM2-1** **10:EC-Earth3-Veg** 11:FGOALS-f3-L 12:FGOALS-g3 13:GFDL-ESM4 14:INM-CM4-8
15:INM-CM5-0 **16:IPSL-CM6A-LR** 17:KACE-1-0-G 18:MCM-UA-1-0 **19:MIROC6** 20:MIROC-ES2L **21:MPI-ESM1-2-HR**
22:MPI-ESM1-2-LR 23:MRI-ESM2-0 **24:NorESM2-MM** 25:TaiESM1 **UKESM1-0-LL**

Figure 14. Precipitation annual cycle); model comparison with observations (shown as solid black line). Time Correlation and MBEs for each model. Monthly averages are taken over a 35-year climatology (1979–2014).

General Score (GS) was calculated for Mean Bias Error, Root Mean Square Error and Standard Deviation (table 4) in order to systematically evaluate how well models capture observed temperature and precipitation and rank models based on their performance. The general score provides a quantitative measure of how well each model replicates observed data, combining statistical metrics into one comprehensive evaluation. Best-performing models of temperature are CNRM-CM6-1 (GS= 0.98), IPSL-CM6A-LR (GS= 0.95), CNRM-ESM2-1 (GS= 0.9), and NorESM2-MM (GS=0.896), indicating that they have the best alignment with observed temperature data. Respectively, the models capture best observed data of precipitation are MRI-ESM2-0 (GS=0.88), MIROC6 (GS=0.852), GFDL-ESM4 (GS=0.757), MIROC-ES2L (GS=0.744), and ACCESS-CM2 (GS=0.739).

To combine MBE, RMSE, STDV, and Time Correlation into a general score, first each metric was normalized. Normalization involves transforming each metric so they're comparable on the same scale.

MBE normalization:

$$\text{Normalized MBE} = 1 - |\text{MBE}| / \text{maxMBE}$$

RMSE normalization:

$$\text{Normalized RMSE} = 1 - (\text{RMSE} - \text{MIN}_{\text{RMSE}}) / (\text{MAX}_{\text{RMSE}} - \text{MIN}_{\text{RMSE}})$$

STDV normalization:

$$\text{Normalized STDV} = 1 - |\text{STDVmodel} - \text{STDVobs}| / \text{MAX}_{|\text{STDV}|}$$

Correlation normalization:

$$\text{Normalized Time correlation} = \text{TimCor} - \text{MIN}_{\text{timcor}} / \text{MAXtimcor} - \text{MIN}_{\text{timcor}}$$

GENERAL SCORE = (Normalized MBE + Normalized RMSE + Normalized STDV + Normalized Time correlation/4

Table 3. Model ranking based on General Score. Euro-CORDEX models marked in bold. Top 5 ranked models marked in color.

	Temperature		**Precipitation**		**Overall**	
model	General Score	rank	General Score	rank	General Score	Rank
ACCESS-CM2	0.732	16	0.739	5	0.735	9
AWI-CM-1-1-MR	0.748	15	0.535	19	0.642	18
BCC-CSM2-MR	0.638	22	0.553	16	0.595	23
CanESM5-CanOE	0.878	6	0.526	21	0.702	13
CESM2	**0.85**	**9**	**0.576**	**15**	**0.713**	**12**
CMCC-CM2-SR5	**0.684**	**20**	**0.631**	**12**	**0.658**	**17**
CNRM-CM6-1	0.981	1	0.738	6	0.86	2
CNRM-CM6-1-HR	0.838	11	0.553	16	0.695	15
CNRM-ESM2-1	**0.901**	**3**	**0.732**	**7**	**0.817**	**3**
EC-Earth3-Veg	**0.872**	**7**	**0.653**	**11**	**0.762**	**6**
FGOALS-f3-L	0.726	19	0.526	21	0.626	20
FGOALS-g3	0.728	17	0.28	26	0.504	24
GFDL-ESM4	0.81	14	0.757	3	0.783	5
INM-CM4-8	0.508	24	0.394	24	0.451	25
INM-CM5-0	0.603	23	0.593	13	0.598	21
IPSL-CM6A-LR	**0.94**	**2**	**0.491**	**23**	**0.715**	**11**
KACE-1-0-G	0.832	12	0.668	9	0.75	8
MCM-UA-1-0	0.365	25	0.307	25	0.336	26
MIROC6	**0.343**	**26**	**0.852**	**2**	**0.597**	**22**
MIROC-ES2L	0.64	21	0.744	4	0.692	16
MPI-ESM1-2-HR	**0.866**	**8**	**0.658**	**10**	**0.762**	**6**
MPI-ESM1-2-LR	0.818	13	0.585	14	0.702	13
MRI-ESM2-0	0.886	5	0.879	1	0.883	1
NorESM2-MM	**0.896**	**4**	**0.535**	**19**	**0.716**	**10**
TaiESM1	0.727	18	0.553	16	0.64	19
UKESM1-0-LL	**0.839**	**10**	**0.732**	**7**	**0.786**	**4**

Table 4. Normalized Statistical Metrics of Temperature and Precipitation

model	Norm_MBE_Temperature	Norm_RMSE_Temperature	Norm_STD_Temperature	Norm_Corr_Temperature	Norm_MBE_Precipitation	Norm_RMSE_Precipitation	Norm_STD_Precipitation	Norm_Corr_Precipitation	Combined_Temperature_Skill	Combined_Precipitation_Skill	Overall_Skill
MRI-ESM2-0	0.845	0.950	0.755	0.994	0.951	0.760	0.861	0.947	0.886	0.879	**0.883**
CNRM-CM6-1	0.959	1.000	0.982	0.983	0.993	0.315	0.809	0.836	0.981	0.738	**0.860**
CNRM-ESM2-1	0.775	0.939	0.903	0.989	0.981	0.256	0.894	0.796	0.901	0.732	**0.817**
UKESM1-0-LL	0.759	0.839	0.785	0.975	0.500	0.580	0.890	0.958	0.839	0.732	**0.786**
GFDL-ESM4	0.656	0.826	0.851	0.906	0.975	0.585	0.704	0.764	0.810	0.757	**0.783**
EC-Earth3-Veg	0.961	0.875	0.690	0.961	0.402	0.841	0.588	0.780	0.872	0.653	**0.762**
MPI-ESM1-2-HR	0.790	0.921	0.832	0.921	0.443	0.643	0.779	0.768	0.866	0.658	**0.762**
KACE-1-0-G	0.883	0.785	0.708	0.952	0.558	0.581	0.740	0.792	0.832	0.668	**0.750**
ACCESS-CM2	0.637	0.696	0.768	0.828	0.859	0.426	0.884	0.786	0.732	0.739	**0.735**
NorESM2-MM	0.782	0.914	0.996	0.894	0.154	0.952	0.275	0.758	0.896	0.535	**0.716**
IPSL-CM6A-LR	0.872	0.982	0.979	0.926	0.703	0.270	0.726	0.264	0.940	0.491	**0.715**
CESM2	0.624	0.824	0.950	1.000	0.306	0.862	0.423	0.713	0.850	0.576	**0.713**
CanESM5-CanOE	0.730	0.935	0.946	0.901	0.127	1.000	0.000	0.976	0.878	0.526	**0.702**
MPI-ESM1-2-LR	0.866	0.748	0.769	0.891	0.368	0.520	0.889	0.562	0.818	0.585	**0.702**
CNRM-CM6-1-HR	0.571	0.788	0.992	0.999	0.655	0.000	0.868	0.689	0.838	0.553	**0.695**
MIROC-ES2L	0.453	0.609	0.649	0.850	0.407	0.815	0.908	0.845	0.640	0.744	**0.692**
CMCC-CM2-SR5	0.541	0.661	0.705	0.830	0.300	0.867	0.358	1.000	0.684	0.631	**0.658**
AWI-CM-1-1-MR	0.601	0.765	0.723	0.905	0.228	0.558	0.678	0.678	0.748	0.535	**0.642**
TaiESM1	0.526	0.723	0.781	0.878	0.180	0.750	0.420	0.861	0.727	0.553	**0.640**
FGOALS-f3-L	0.706	0.614	0.881	0.702	0.242	0.675	0.538	0.647	0.726	0.526	**0.626**
INM-CM5-0	0.667	0.567	0.752	0.425	0.398	0.697	0.602	0.674	0.603	0.593	**0.598**
MIROC6	0.000	0.023	0.494	0.856	0.998	0.726	0.843	0.839	0.343	0.852	**0.597**
BCC-CSM2-MR	0.903	0.792	0.856	0.000	0.680	0.725	0.444	0.362	0.638	0.553	**0.595**
FGOALS-g3	0.743	0.650	0.910	0.609	0.422	0.544	0.146	0.008	0.728	0.280	**0.504**
INM-CM4-8	0.502	0.462	0.706	0.362	0.000	0.715	0.187	0.673	0.508	0.394	**0.451**
MCM-UA-1-0	0.997	0.000	0.000	0.463	0.133	0.832	0.263	0.000	0.365	0.307	**0.336**

Effect of resolution on model skill

The following figures (fig. 15 a, b,c) show the spatial resolution of climate models versus their performance metrics (MBE, RMSE, and Correlation) in order to evaluate how model resolution influences model accuracy and reliability.

It is observed that there is no significant correlation between spatial resolution and the performance metrics of temperature, which suggest that resolution isn't the sole determinant of the selected model quality for this variable. Satisfactory MBE and RMSE values are observed among models with a variety in spatial resolution. The majority of the models have spatial resolution under 4°, however some models, such as MCM-UA-1-0 and CanESM5-CanOE present low biases despite the coarse resolution. Fine resolution models, overall, show high correlation, while two low resolution models (MIROC-ES2L and CanESM5-CanOE) present satisfactory correlation as well.

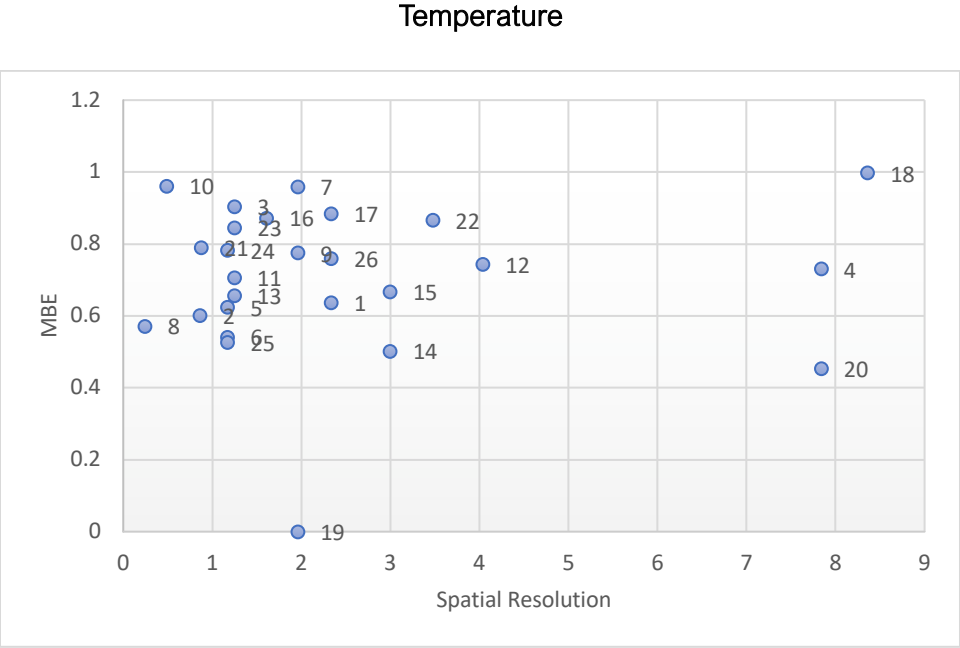

(a)

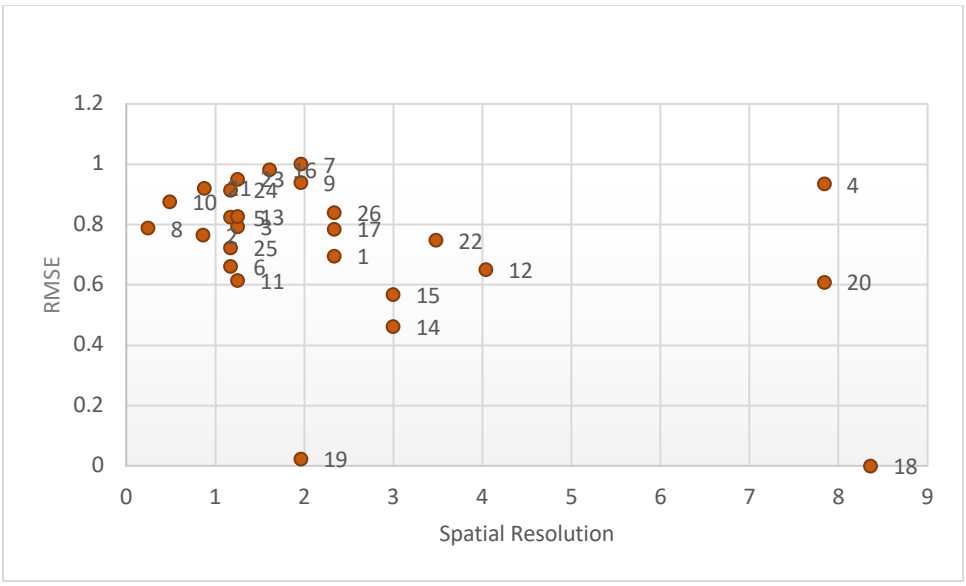

(b)

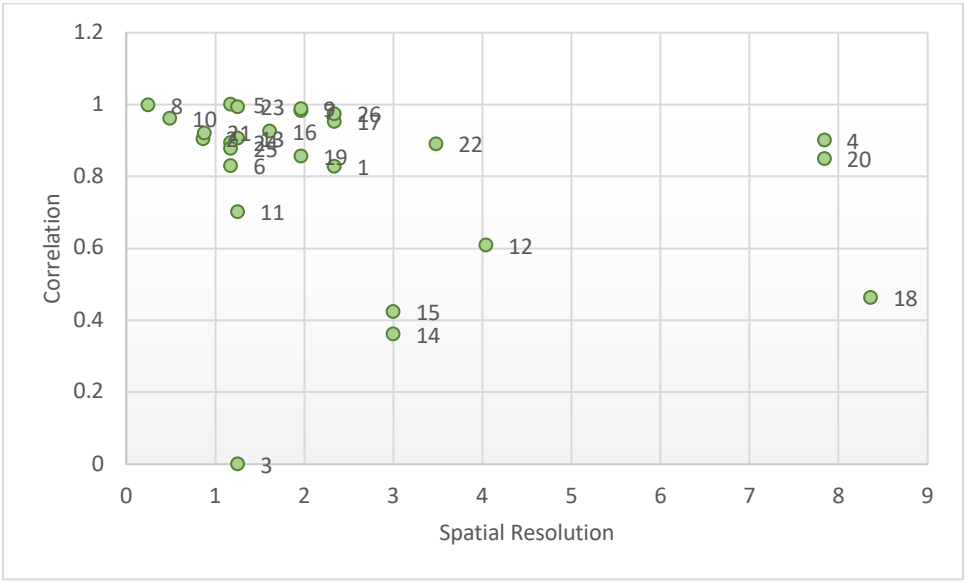

(c)

1:ACCESS-CM2 2:AWI-CM-1-1-MR 3:BCC-CSM2-MR 4:CanESM5-CanOE **5:CESM2** **6:CMCC-CM2-SR5** 7:CNRM-CM6-1
8:CNRM-CM6-1-HR **9:CNRM-ESM2-1** **10:EC-Earth3-Veg** 11:FGOALS-f3-L 12:FGOALS-g3 13:GFDL-ESM4 14:INM-CM4-8
15:INM-CM5-0 **16:IPSL-CM6A-LR** 17:KACE-1-0-G 18:MCM-UA-1-0 **19:MIROC6** 20:MIROC-ES2L **21:MPI-ESM1-2-HR**
22:MPI-ESM1-2-LR 23:MRI-ESM2-0 **24:NorESM2-MM** 25:TaiESM1 **UKESM1-0-LL**

Precipitation

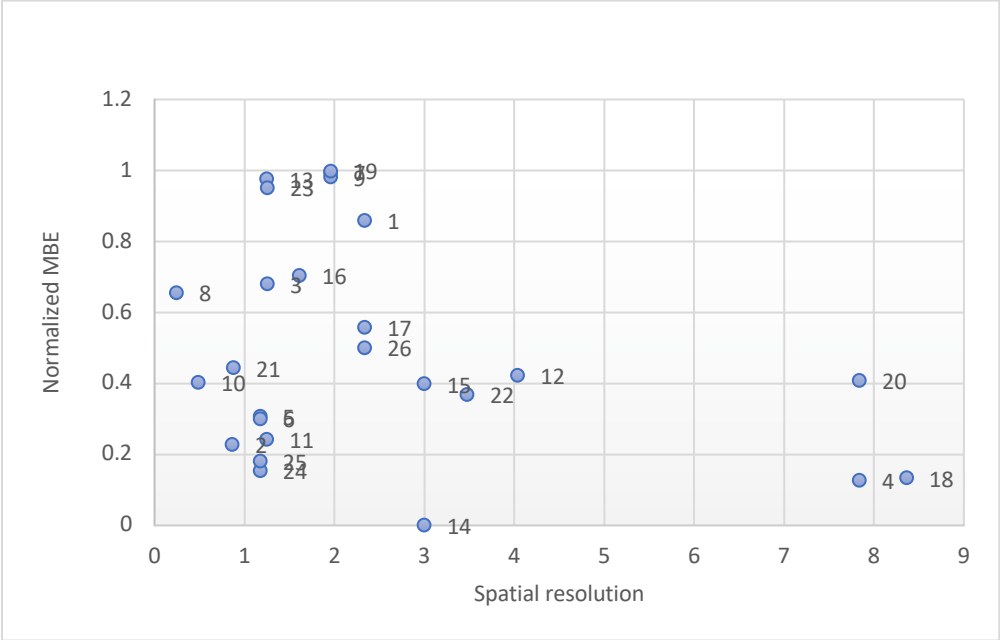

(d)

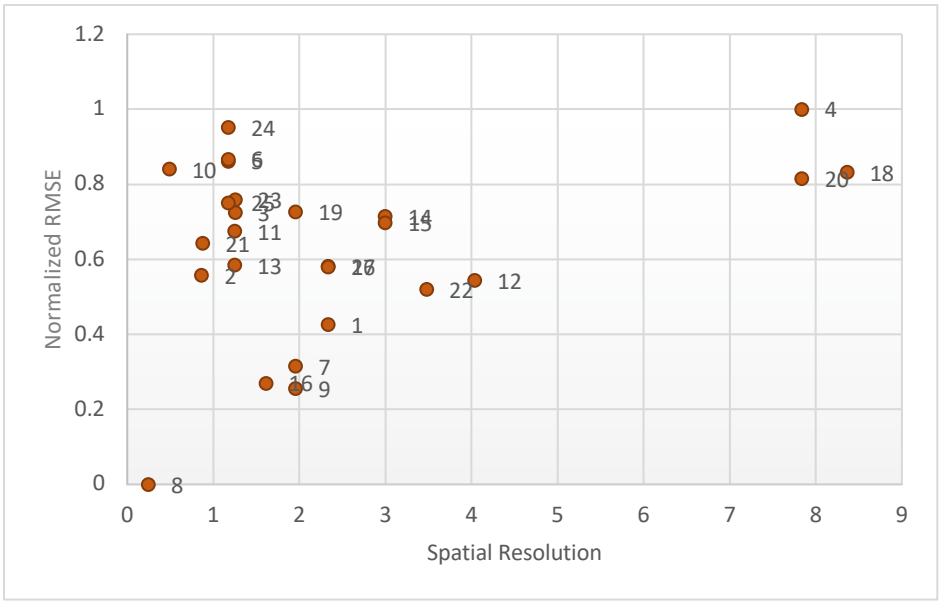

(e)

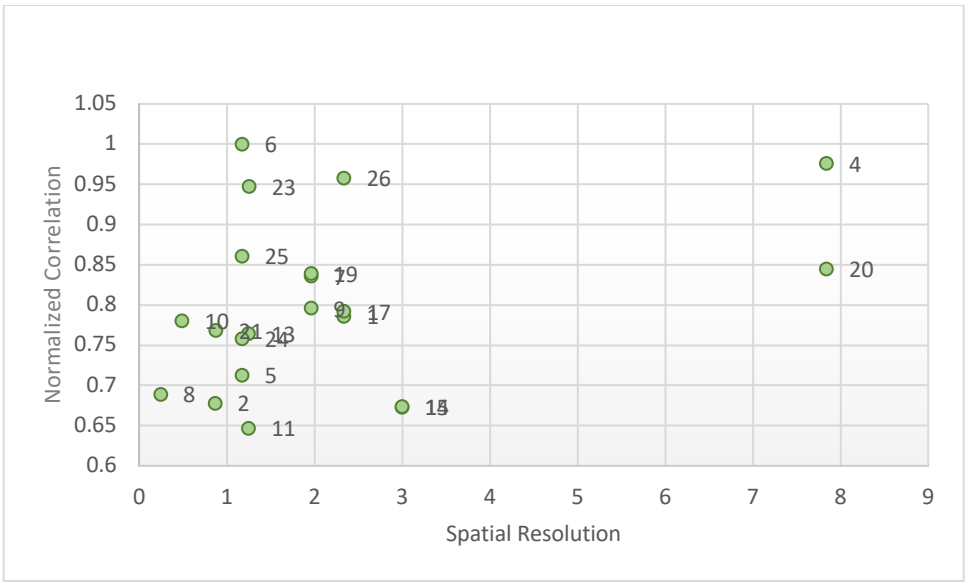

(f)

1:ACCESS-CM2 2:AWI-CM-1-1-MR 3:BCC-CSM2-MR 4:CanESM5-CanOE **5:CESM2** **6:CMCC-CM2-SR5** 7:CNRM-CM6-1
8:CNRM-CM6-1-HR **9:CNRM-ESM2-1** **10:EC-Earth3-Veg** 11:FGOALS-f3-L 12:FGOALS-g3 13:GFDL-ESM4 14:INM-CM4-8
15:INM-CM5-0 **16:IPSL-CM6A-LR** 17:KACE-1-0-G 18:MCM-UA-1-0 **19:MIROC6** 20:MIROC-ES2L **21:MPI-ESM1-2-HR**
22:MPI-ESM1-2-LR 23:MRI-ESM2-0 **24:NorESM2-MM** 25:TaiESM1 **UKESM1-0-LL**

Figure 15. Spatial resolution of climate models vs the performance metrics (MBE (a,d), RMSE(b,e), and Correlation(c,f)) of air temperature and precipitation.

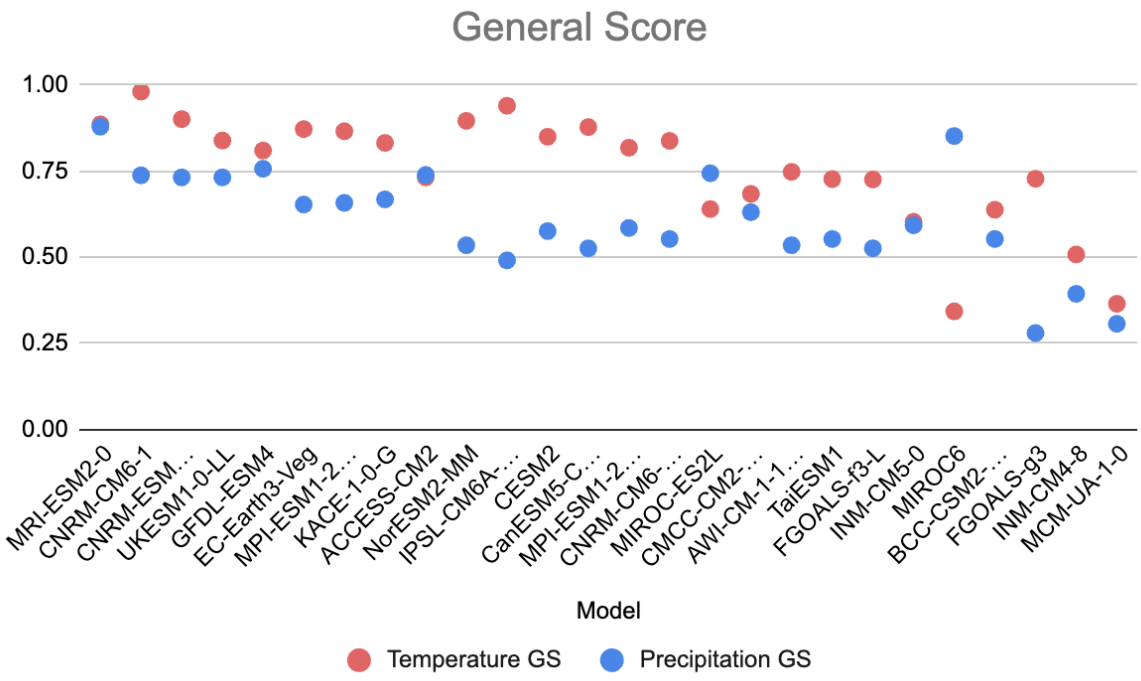

Figure 16. General Score for temperature and precipitation

Insights of CMIP6 projections

The projection spread of each model under the scenario SSP585 is carried out and demonstrated at the following figure (fig.17). Scenario SSP 585 is selected as it presents the higher response in temperature increase. The spread of points across the DT-DP space indicates the variability among different climate models. A wide spread suggests a high degree of uncertainty in future projections for temperature and precipitation. The majority of the models present a relative tight cluster (DT range: 4-6 °C and DP range: -200 to -100 mm), indicating overall agreement among the models. Points far from the main cluster, such as FGOALS-g3, CanESM5-CanOE, and IPSL-CM6A-LR, indicate models that project significantly different futures, highlighting potential outliers or models that may be sensitive to certain boundary conditions.

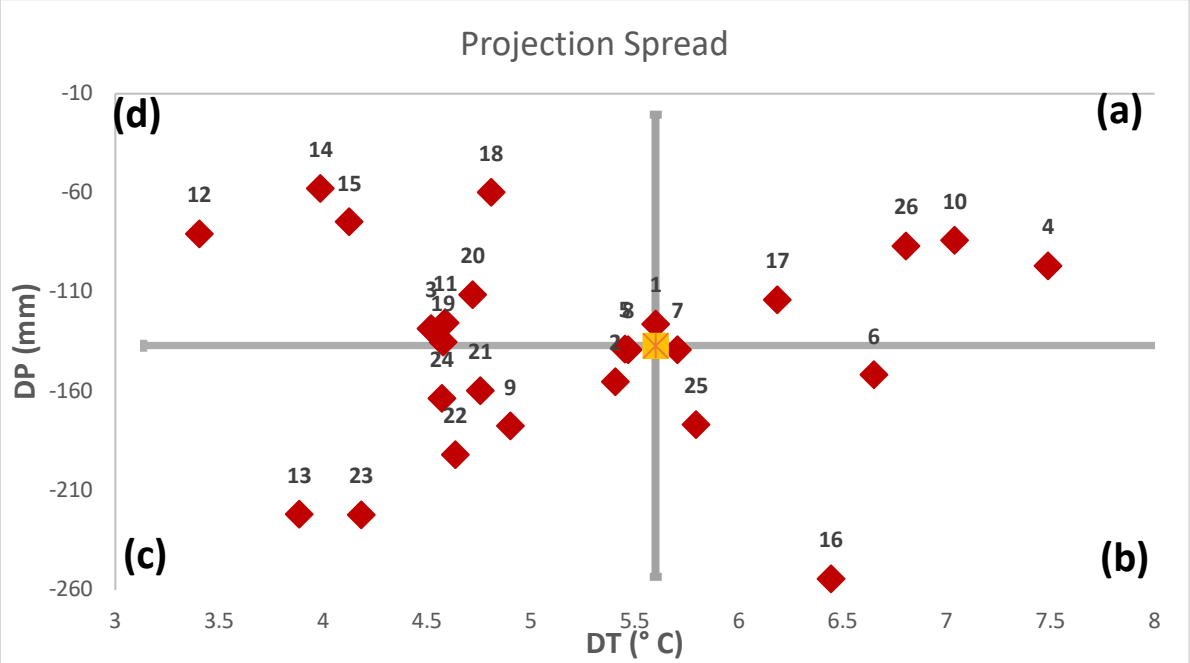

(a): warmer-wetter (b)warmer-drier (c)cooler-drier (d)cooler-wetter

1:ACCESS-CM2 2:AWI-CM-1-1-MR 3:BCC-CSM2-MR 4:CanESM5-CanOE **5:CESM2** **6:CMCC-CM2-SR5** 7:CNRM-CM6-1
8:CNRM-CM6-1-HR **9:CNRM-ESM2-1** **10:EC-Earth3-Veg** 11:FGOALS-f3-L 12:FGOALS-g3 13:GFDL-ESM4 14:INM-CM4-8
15:INM-CM5-0 **16:IPSL-CM6A-LR** 17:KACE-1-0-G 18:MCM-UA-1-0 **19:MIROC6** 20:MIROC-ES2L **21:MPI-ESM1-2-HR**
22:MPI-ESM1-2-LR 23:MRI-ESM2-0 **24:NorESM2-MM** 25:TaiESM1 **UKESM1-0-LL**

Model Classification	Model
(a) Warmer-wetter	1: ACCESS-CM2, 4: CanESM5-CanOE, **10:EC-Earth3-Veg,** 17: KACE-1-0-G, **26: UKESM1-0-LL**
(b) Warmer-drier	**6: CMCC-CM2-SR5,** 7: CNRM-CM6-1, **16: IPSL-CM6A-LR**, 25: TaiESM1
(c) Cooler-drier	2: AWI-CM-1-1-MR, **5: CESM2**, 8: CNRM-CM6-1-HR, **9: CNRM-ESM2-1**, 13: GFDL-ESM4, **21: MPI-ESM1-2-HR**, 22: MPI-ESM1-2-LR, 23: MRI-ESM2-0, **24: NorESM2-MM**
(d) Cooler-wetter	3: BCC-CSM2-MR, 11: FGOALS-f3-L, 12: FGOALS-g3, 14: INM-CM4-8, 15: INM-CM5-0, 18: MCM-UA-1-0, **19: MIROC6**, 20: MIROC-ES2L

*Figure 16 Temperature and precipitation projection range (SSP585; 2018–2100 relative to 1850–1900) for CMIP6 multi-model ensemble. Model classification based on temperature and precipitation response. *Highlighted models represent the best performing models of each category based on the general score.*

Projected temperature and precipitation are analyzed based on different ssp scenarios (fig.18&19). Projected precipitation under SSP1-2.6, SSP2-4.5, SSP3-7.0, and SSP5-8.5 presents a range of potential future precipitation changes, driven by varying greenhouse gas emission scenarios. In the SSP1-2.6 scenario, which assumes strong mitigation efforts, the changes in precipitation are modest with a slight decrease followed by stabilization until 2100. The SSP2-4.5 scenario, representing moderate mitigation, reflects a similar trend, though with more pronounced changes in decreasing precipitation patterns. Under SSP3-7.0 and SSP5-8.5, which reflect higher emissions and limited mitigation, the plot reveals more substantial declines in precipitation (more than 100mm/year) by the end of the century.

Projected temperature under SSP1-2.6, SSP2-4.5, SSP3-7.0, and SSP5-8.5 reveals distinct future warming pathways based on different greenhouse gas emission scenarios. SSP1-2.6, the most optimistic scenario, reflects stringent mitigation strategies and results in the least warming, with temperature increases until 2050 and then stabilizing below 2°C by the end of the century. In contrast, SSP5-8.5 represents a "business-as-usual" trajectory, leading to the most extreme temperature rise, reaching up to 4°C. SSP2-4.5 and SSP3-7.0 represent intermediate pathways, with moderate levels of warming, particularly under SSP2-4.5, which assumes some mitigation efforts.

The spread in the projections among these scenarios highlights the critical impact of policy decisions and emission pathways on future climate outcomes.

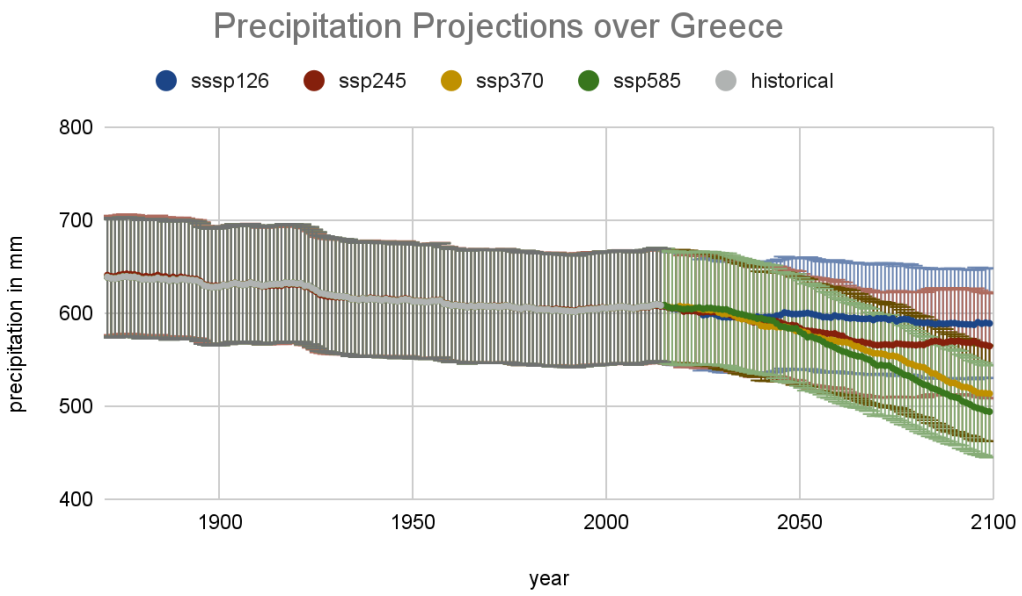

Figure 17 Precipitation changes under 4 different SSP scenarios, relative to 2014.

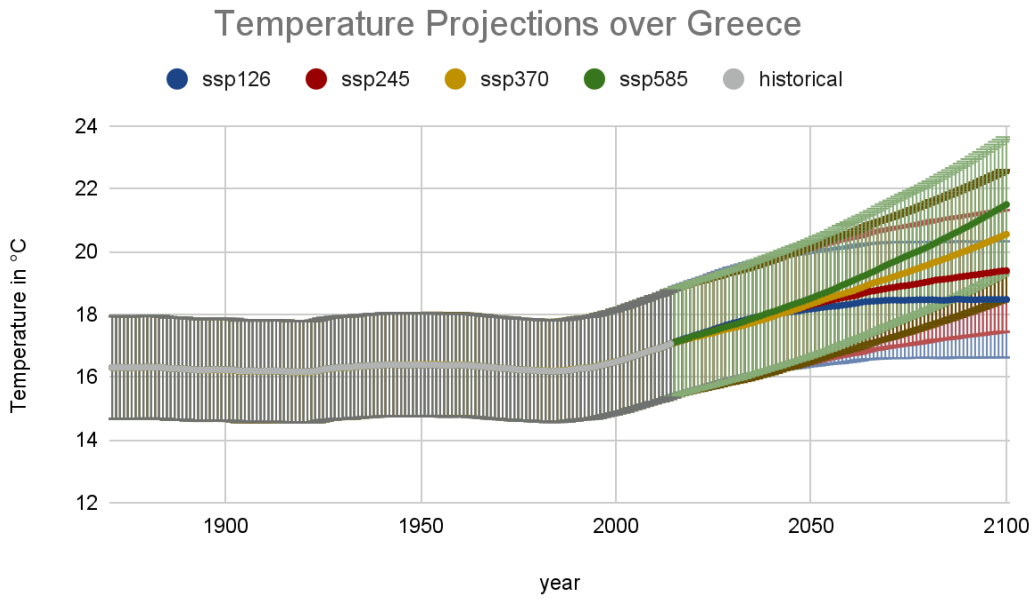

Figure 18 Temperature change under 4 different SSP scenarios, relative to 2014.

Model Selection

Based on the findings of this study, a subset of climate models demonstrates strong accuracy and reliable results when compared with observational data. However, the selection of climate models for further analysis hinges on a robust combined performance across multiple statistical metrics. As shown in Table 3 and 4, and Figure 13, models CNRM-CM6-1, CNRM-ESM2-1, and IPSL-CM6A-LR are top ranked models based on the performance metrics of temperature and the general score. However, both the BCC-CSM2-MR and MCM-UA-1-0 models exhibit commendable performance in temperature metrics, with their results showing a strong balance between time correlation and mean bias error (MBE). Notably, the MCM-UA-1-0 model achieves a mean bias error value near zero, indicating minimal deviation from observed temperature data. In terms of precipitation, BCC-CSM2-MR and IPSL-CM6A-LR perform well, particularly in time correlation and MBE. Best overall performed models based on the general score of precipitation are MRI-ESM2-0, and MIROC6. However, the most accurate MBE results are observed at CNRM-CM6-1, MIROC6, CNRM-ESM2-1, GFDL-ESM4, and MRI-ESM2-0 models. An overview of the aggregated performance across these models and metrics is presented in the accompanying table (table 5), offering a clearer comparative analysis of their suitability for future projections and assessments.

The selection of representative models is based on established criteria ensuring that the model selection process is systematic and not arbitrary. One of the key criteria is how well a model performs when compared to real-world observations. This involves accuracy, precision, and the model's ability to reproduce historical data and how well a model predicts temperatures and precipitation in comparison with the actual observational data. Another key criterion is how well the model captures the diversity of patterns across particular region.

All models have been classified into the four categories (warmer-wetter, warmer-drier, cooler-drier, cooler-wetter) based on DT (temperature change) and DP (precipitation change) spread. Combining the results of table 3 of overall model skill (table 3) and figure 17, the best performed model among warmer-wetter models' category is the UKESM1-0-LL (General Score=0.786). The highest general score of warmer-drier and cooler-wetter categories are CNRM-CM6-1(GS=0.860) and MIROC-ES2L (GS=0.692) respectively, while the model with the highest general score over all belong to cooler-wetter model (GS=0.883).

Table 5. Aggregated performance across selected climate models

Metric	Temperature	Precipitation
MBE	CNRM-CM6-1, EC-Earth3-Veg, MCM-UA-1-0 >0.9	CNRM-CM6-1, MIROC6, CNRM-ESM2-1, GFDL-ESM4, MRI-ESM2-0 >0.9
Time Correlation	CESM2, CNRM-CM6-1-HR, CNRM-ESM2-1, CNRM-CM6-1, MRI-ESM2-0 >0.98	CMCC-CM2-SR5, CanESM5-CanOE, UKESM1-0-LL, MRI-ESM2-0 >0.9
RMSE	CNRM-CM6-1, MRI-ESM2-0, CNRM-ESM2-1, IPSL-CM6A-LR, CanESM5-CanOE, NorESM2-MM, MPI-ESM1-2-HR >0.9	CanESM5-CanOE, NorESM2-MM >0.9
Time correlation-MBE	BCC-CSM2-MR, CNRM-CM6-1-HR	BCC-CSM2-MR, IPSL-CM6A-LR
General Score	CNRM-CM6-1, CNRM-ESM2-1, IPSL-CM6A-LR >0.9	MRI-ESM2-0, MIROC6 >0.8

Comparison with Other Regional Studies

Several climate studies focus on Greece and the broader Mediterranean region due to its vulnerability to climate change and its unique geographical and climatic conditions. The Mediterranean is a transition zone between temperate and subtropical climates, making it sensitive to shifts in climate patterns. Euro-Mediterranean Center on Climate Change (CMCC) provide insights into Greece's future climate scenarios, predicting hotter summers, reduced rainfall, and an increase in extreme weather events (Ruti et al., 2016).

The Mediterranean Climate Change and Impact Study (CIRCE) provides a foundation for understanding climate risks for Greece indicating a projected temperature increase of 2 to 4°C by the end of the 21st century and a decline in annual precipitation by up to 20% in the Mediterranean basin, with more pronounced drying in Greece (Mariotti et al., 2015).

A study published in 2022 suggest that according to the RCP4.5, the largest warming is obtained over the eastern part of the country (some northeastern inland parts and eastern coasts) reaching up to 2 °C in the period 2025–2049 and extends more towards southeastern areas up to 2.5 °C in the period 2075–2099. On the other hand, in the case of the RCP8.5 scenario, the difference between the two future periods is remarkably more pronounced and the mean daily temperature is found to increase up to 4.5 °C in the far future, particularly in some eastern and coastal parts. It is also observed that the pattern of changes is clearly linked to the orography of central Greece and the island of Crete (Politi et al., 2022). Moreover, an analysis based on an ensemble of 11 high-resolution EURO-CORDEX regional climate model (RCM) simulations, point towards decrease of precipitation under RCP8.5 by − 16%, and increase of the number of consecutive dry days per year by 15.4 days (30%) at the end of the century over the region of Greece (Georgoulias et al., 2022).

More recent climate studies for Greece and the Mediterranean region have also highlighted increasing vulnerability to extreme weather events and climate change impacts. Greece and the broader Mediterranean region are warming significantly, with Greece experiencing a rise of about 1.5°C from 1991 to 2020, with some areas exceeding 2°C. This has led to fewer frost days and more extreme heatwaves, such as those in 2023 when temperatures reached 48°C in parts of southern Europe. Studies indicate that the Mediterranean, including Greece, will experience warming at a rate faster than the global average (Tarín-Carrasco, 2024). Projections suggest a temperature increase of 3-5°C by the end of the 21st century under high-emission scenarios and heatwaves are expected to become more frequent and intense, while the intensity of rainfall is expected to increase in winter, leading to a higher likelihood of flooding events (Tarín-Carrasco, 2024).

Challenges and Limitations

Climate change impact assessment studies, especially those focusing on projections, face several challenges and limitations. One of the primary challenges faced in this study was dealing with model

uncertainties inherent in climate projections. The Coupled Model Intercomparison Project 6(CMIP6) ensembles are widely used to project future climate scenarios. However, different models produce varying results due to differences in model architecture, parameterizations, and assumptions. The challenge lies in balancing the output from these diverse models to provide robust predictions (Tarín-Carrasco, 2024). Also, global climate models (GCMs) operate at coarse spatial resolutions, which makes it difficult to capture local climate variations, especially in geographically complex regions like Greece and the Mediterranean. Downscaling techniques were used to address this, but they added another layer of uncertainty (Pantavou et al., 2024).

Regional complexity is a significant challenge for this research. Greece and the Mediterranean are geographically diverse, with mountainous terrain, coastal areas, and islands that all experience varying microclimates. Climate models often struggle to account for these fine-scale variations, particularly when studying regional impacts like localized extreme weather events or coastal flooding.

Data limitations were another significant hurdle. In some parts of Greece, especially remote and island areas, there was a lack of reliable, long-term observational data to validate the model outputs, which added uncertainty to the projections. Reliable climate records are critical for validating models. However, in regions like the Mediterranean, long-term observational data, especially for temperature and precipitation may be sparse or incomplete. Data gaps limit the accuracy of model calibration and make it harder to discern long-term trends.

Furthermore, scenario and policy uncertainties impact the reliability of the outputs. Climate projections depend on assumptions about future greenhouse gas emissions (Socio-economic Pathways, SSPs). These scenarios are inherently uncertain, as they rely on socio-economic, technological, and policy developments that are difficult to predict. This leads to a range of possible future climate outcomes, making long-term planning difficult (Pantavou et al., 2024). The effectiveness of mitigation and adaptation strategies is particularly uncertain. While some models include scenarios for future policy actions, there is uncertainty in how these will be implemented and whether they will effectively limit warming. This adds complexity when evaluating the effectiveness of different adaptation strategies in regional studies. While physical climate models have improved, integrating socio-economic variables (e.g., impacts on agriculture, water resources, infrastructure) into projections remains limited. This reduces the ability to provide holistic assessments of climate risks at the regional level, particularly in regions like Greece, where sectors like tourism and agriculture are highly climate-sensitive.

Finally, predicting the frequency and intensity of extreme events (e.g., heatwaves, storms, floods) is challenging because these events often result from complex, non-linear interactions within the climate system. Models may underestimate or overestimate the likelihood of extreme events due to their inherent limitations. Climate systems may exhibit thresholds or tipping points, beyond which changes become abrupt and irreversible. Capturing these phenomena in models remains challenging, as the exact points at which they occur still need to be better understood. In Greece, the complexity of modeling these tipping points introduces a significant limitation in projecting long-term climate outcomes. This limitation arises primarily from uncertainties in identifying where such tipping points

may occur in systems like regional ecosystems, water resources, or marine environments. For instance, the Mediterranean Sea's thermohaline circulation, temperature threshold of wildfire risk, and agriculture sector are some of the tipping point limitations on climate analysis of Mediterranean regions.

5. Discussion and Conclusions

Summary of Findings

The selected climate models of this study exhibit moderate performance in terms of mean bias error (MBE), with a tendency to underestimate precipitation, particularly in mountainous regions such as the Greek Pindos range (CNRM-CM6-1, CNRM-CM6-1-HR, CNRM-ESM2-1). While precipitation is captured well over flat terrains, the models show higher biases over complex topographies. Geographical visualizations of MBE and root mean square error (RMSE) help identify the spatial variation of errors, revealing that models generally perform well in coastal and island regions but struggle in more diverse terrains like central and northern Greece. Over the mainland, temperature overestimation is common, especially in regions such as the northern Greece and Peloponnese, while models perform well in the Aegean and Ionian islands. However, some models demonstrate sufficient performance overall. CNRM-CM6-1, CNRM-ESM2-1, IPSL-CM6A-LR capture well the temperature changes with general score over 0.9 and MRI-ESM2-0, MIROC6 (general score over 0.8) exhibit adequate results over precipitation patterns.

Temperature and precipitation comparisons on a monthly basis demonstrate that the models can replicate seasonal patterns reasonably well, particularly in capturing extremes like summer heatwaves and winter cold spells. However, performance varies across models, with BCC-CSM2-MR and MCM-UA-1-0 excelling in temperature metrics, combining good time correlation and low MBE values. For precipitation, BCC-CSM2-MR and IPSL-CM6A-LR show strong performance, though CNRM-CM6-1 and MIROC6 produce the most accurate MBE results.

Projections for the 21st century show a significant temperature increase and precipitation decline. Under the high-emission SSP5-8.5 scenario, models predict that temperatures could rise by up to 5°C compared to pre-industrial levels, reaching a mean annual temperature of 23°C by 2100. Precipitation is expected to decline from 700 mm to 400 mm, raising concerns over increased drought risk. In contrast, the SSP1-2.6 scenario predicts temperature stabilization after 2050. These projections emphasize the need for effective climate adaptation and mitigation strategies, especially in vulnerable regions.

How this thesis advances understanding of climate projections for Greece

This thesis significantly advances the understanding of climate projections for Greece by offering a detailed analysis of temperature and precipitation trends using the CMIP6 multi-model ensemble. By evaluating historical data and future climate simulations, the study provides a comprehensive picture of how climate patterns in Greece are likely to evolve throughout the 21st century. The assessment

of multiple models, including their biases and error patterns across different terrains, enhances the understanding of regional climate dynamics, especially in complex geographic areas like mountainous regions and coastal zones.

Moreover, this thesis emphasizes the importance of using statistical metrics, such as mean bias error (MBE) and root mean square error (RMSE), for model evaluation, offering a refined method for selecting models that perform reliably in capturing seasonal and regional variations in climate. The identification of models that overestimate or underestimate climate variables, such as precipitation and temperature, contributes to more accurate and localized projections.

By comparing model outputs under different emission scenarios, such as SSP1-2.6, SSP2-4.5, SSP3-7.0 and SSP5-8.5, the thesis provides critical insights into potential future climate outcomes for Greece, including the risks of increased temperature, heatwaves, and droughts. These projections are crucial for informing national and local climate adaptation strategies, enabling policymakers to address climate risks more effectively.

Ultimately, this work not only enhances scientific understanding of how global climate models perform in a Greek context but also provides a foundation for more targeted and regionally specific climate policy and adaptation planning.

Contributions to Climate Science

This study makes a significant contribution to climate science by improving our understanding of regional climate dynamics projections in Greece. By employing high-resolution models (CMIP6) and comparing multiple scenarios (ssp1-2.6, ssp2-4.5, ssp3-7.0, and ssp5-8.5) this research addresses the challenge of downscaling global climate models to better capture local phenomena such changes in temperature and precipitation patterns. This is particularly important in a geographically complex region like Greece, where topographical features and coastal interactions heavily influence local climate behavior. Furthermore, my study contributes to the growing body of literature on climate projections by providing new insights into the annual and seasonal patterns of future climate events, under different greenhouse gas emission pathways. By filling critical data gaps in regional climate projections, this research provides valuable information for policymakers and stakeholders to develop effective adaptation strategies in key sectors such as agriculture, water management, and disaster preparedness. Additionally, the study highlights limitations in current models regarding model uncertainties, data limitation, and regional complexity, offering a foundation for future research into these critical climate thresholds in the Mediterranean region.

Implications for Climate Change Policies in Greece. How this study informs local and national climate strategies

This study provides valuable insights into how climate change could impact Greece, a region known for its sensitivity to climate variability. The findings of the research provide information for policymakers and stakeholders and inform local and national climate strategies. Temperature and precipitation future projections can help local governments develop targeted adaptation strategies. Local plans might include measures for water conservation, crop adaptation strategies, or heatwave response plans to deal with impacts on water resources, agriculture, and health.

The outcomes of the study can guide infrastructure improvements by identifying potential changes in future weather events. Adaptation strategies, including water resource management, energy infrastructure, and energy demand management may need to be enhanced.

Deploying information on shifting precipitation patterns and temperature trends, agricultural policies can be tailored to support crop varieties more resilient to new climatic conditions. Identifying regions vulnerable to climate change may lead to the cultivation of more suitable, drought-resilient types of crops and the development of soil moisture conservation techniques.

Changes in temperature and precipitation affect energy demand and supply. The study's projections can assist in planning for energy infrastructure that can handle future climate conditions, and in optimizing energy production, especially from renewable sources. Energy-efficient buildings, passive cooling techniques, resilient power grids, smart urban design, and energy demand reduction programs are some of the high-energy demand adaptation strategies and measures that can be taken from local or national governments.

Understanding how climate change will impact health, such as through increased heatwaves or changes in vector-borne diseases, local and national health strategies can be adjusted. This might include developing early warning systems and improving healthcare infrastructure.

At a national level, climate policies and commitments can be informed. The analysis using the CMIP6 models will offer a more robust understanding of future scenarios, which is crucial for making proactive decisions and adaptation plans. It can provide a scientific basis for Greece's climate action plans, helping to set more specific targets and measures that align with the projected climate impacts.

Future Research

Climate analysis studies are critical for understanding future risks and guiding adaptation strategies, but they face several challenges due to model uncertainties, data limitations, regional complexities, and scenario uncertainties. Despite these challenges, ongoing advancements in regional climate modeling and data collection are helping improve the reliability of projections. However, careful interpretation of results and continuous updates are essential to better inform policy and planning efforts.

Building on the insights from this study, there are numerous future research directions that could be pursued using CMIP6 and other emerging datasets. These future studies can deepen understanding of climate impacts in Greece and more broadly in southern Europe and Mediterranean basin, while also advancing the methodologies used for climate modeling. There are several key areas that future studies may take under consideration.

Regional downscaling and high-resolution climate projections for the selected region may result in better accuracy. While this thesis uses CMIP6 models, future studies could apply regional climate models (RCMs) or statistical downscaling techniques to provide higher-resolution projections for specific areas in Greece. This would offer more localized insights into climate impacts on small-scale regions such as islands, coastal cities, and mountainous areas.

Extreme events analysis is also suggested for future research. They can explore how climate change might intensify the occurrence and frequency of extreme weather events like heatwaves, droughts, wildfires, and floods in Greece and examine how multiple hazards (e.g., heatwaves followed by wildfires) might interact, compounding their impacts on ecosystems, agriculture, and human health. They may focus on climate change attribution for specific extreme weather events in Greece (e.g., recent droughts or heatwaves) by using CMIP6 models and methodologies to quantify the role of anthropogenic forcing in increasing the likelihood or intensity of these events.

Impact studies on sectors and ecosystems would be an interesting idea to extent this research. For instance, exploring the potential impact of climate change on agricultural sector based on different CMIP6 future emission scenarios could provide significant information about adaptation strategies such as changes on crop yields, water resources management, and implementation of alternative agricultural practices in Greece. Insights on water resources and hydrology impacts would help address concerns about droughts, water security, and transboundary water management. Additionally, investigation on how changes in temperature, precipitation, and extreme events will affect ecosystems and biodiversity in Greece, including marine and coastal ecosystems, could assess shifts in habitat ranges, species vulnerabilities, and impacts on ecosystem services such as carbon storage, tourism, and fisheries. Moreover, health sector is inevitably linked with climate conditions, particularly heatwaves. Rise of temperature and extended heatwave events impact on public health, including heat-related mortality and the spread of vector-borne diseases (e.g., malaria, West Nile virus). Focusing on the social and economic consequences, CMIP6 projections could also inform risk assessments related to displacement and future resource needs provoked by internal migration or immigration to Greece due to climate-driven impacts (e.g., extreme heat, droughts, or sea-level rise). Future research could model how various sectors of the Greek economy will be affected under different CMIP6 scenarios by performing an integrated assessment of the economic implications of climate change, focusing on public health, infrastructure, agriculture, and energy demand sector.

Besides climate change impacts under different greenhouse emission scenarios, future studies can dive into climate change adaptation strategies in Greece based on projected model outputs for future climate conditions. Investigating the potential of nature-based solutions (e.g., reforestation, wetland

restoration, and urban green spaces) to mitigate climate impacts like heatwaves, flooding, and biodiversity loss, further research could evaluate the effectiveness of these strategies under different CMIP6 climate scenarios. Furthermore, they can assess the role of climate-resilient infrastructure, including renewable energy, water management, and transport systems, in adapting to climate impacts projected, focusing on urban and industrial environments. Long-term planning and investment in sustainable infrastructure in Greece would be crucial for the future multi-sector sustainability of the country and the surrounding region.

Ultimately, as the CMIP7 model ensemble becomes available, conducting comparative studies between CMIP6 and CMIP7 could highlight advancements in climate projections and their implications for Greece. This would also provide updated insights into model uncertainties and confidence levels. Future research could focus on quantifying uncertainties within CMIP6 projections, particularly with regard to model parameterizations and internal variability. This would provide more robust conclusions and help stakeholders make informed decisions under uncertainty. There are ongoing efforts to improve climate models, particularly in the representation of cloud feedbacks, aerosols, and regional climate dynamics and atmospheric processes. Further study could explore the role of these uncertainties in shaping future climate projections for Greece, contributing to the refinement of future models.

These research directions, leveraging CMIP6 and beyond, would not only deepen understanding of climate change in Greece but also inform policy, improve resilience, and provide more localized and actionable insights for decision-makers.

6. References

1. AR6 climate change 2021: The physical science basis — IPCC. (2021). IPCC. https://www.ipcc.ch/report/sixth-assessment-report-working-group-i/
2. Arias et al., P. A. (2021). In Climate Change 2021 – The Physical Science Basis (pp. 35–144). Cambridge University Press. http://dx.doi.org/10.1017/9781009157896.002
3. Blunden, J., & Boyer, T. (2021). State of the climate in 2020. Bulletin of the American Meteorological Society, 102(8), S1–S475. https://doi.org/10.1175/2021bamsstateoftheclimate.1
4. Cantelaube, P., & Terres, J.-M. (2005). Seasonal weather forecasts for crop yield modelling in Europe. Tellus A: Dynamic Meteorology and Oceanography, 57(3), 476. https://doi.org/10.3402/tellusa.v57i3.14669
5. CCISC. (2011). The environmental, economic and social impacts of climate change in Greece.
6. Dias, C. G., & Reboita, M. S. (2021). Assessment of CMIP6 simulations over Tropical South America. Revista Brasileira de Geografia Física, 14(3), 1282–1295. https://doi.org/10.26848/rbgf.v14.3.p1282-1295
7. Eurostat. (2021, September 13). Key figures on Europe. Publications Office of the EU. https://op.europa.eu/publication/manifestation_identifier/PUB_KSEI21001ENN
8. Eyring, V., Bony, S., Meehl, G. A., Senior, C. A., Stevens, B., Stouffer, R. J., & Taylor, K. E. (2016a). Overview of the Coupled Model Intercomparison Project Phase 6 (CMIP6) experimental design and organization. Geoscientific Model Development, 9(5), 1937–1958. https://doi.org/10.5194/gmd-9-1937-2016
9. Eyring, V., Bony, S., Meehl, G. A., Senior, C. A., Stevens, B., Stouffer, R. J., & Taylor, K. E. (2016b). Overview of the Coupled Model Intercomparison Project Phase 6 (CMIP6) experimental design and organization. Geoscientific Model Development, 9(5), 1937–1958. https://doi.org/10.5194/gmd-9-1937-2016
10. Feliciano, D., Recha, J., Ambaw, G., MacSween, K., Solomon, D., & Wollenberg, E. (2022). Assessment of agricultural emissions, climate change mitigation and adaptation practices in Ethiopia. Climate Policy, 22(4), 427–444. https://doi.org/10.1080/14693062.2022.2028597
11. Flocas, H., Kourtesiotis, C., Quan, L., Philippopoulos, K., Tzanis, C., & Matei, D. (2023, August 25). Internal climate variability and extreme temperatures over the Mediterranean. 16th International Conference on Meteorology, Climatology and Atmospheric Physics&Mdash;COMECAP 2023. http://dx.doi.org/10.3390/environsciproc2023026057

12. Founda, D., Varotsos, K. V., Pierros, F., & Giannakopoulos, C. (2019). Observed and projected shifts in hot extremes' season in the Eastern Mediterranean. Global and Planetary Change, 175, 190–200. https://doi.org/10.1016/j.gloplacha.2019.02.012

13. Georgoulias, A. K., Akritidis, D., Kalisoras, A., Kapsomenakis, J., Melas, D., Zerefos, C. S., & Zanis, P. (2022). Climate change projections for Greece in the 21st century from high-resolution EURO-CORDEX RCM simulations. *Atmospheric Research*, *271*, 106049. https://doi.org/10.1016/j.atmosres.2022.106049

14. Giannakopoulos, C., Kostopoulou, E., Varotsos, K. V., Tziotziou, K., & Plitharas, A. (2011). An integrated assessment of climate change impacts for Greece in the near future. Regional Environmental Change, 11(4), 829–843. https://doi.org/10.1007/s10113-011-0219-8

15. Giannakopoulos, C., Le Sager, P., Bindi, M., Moriondo, M., Kostopoulou, E., & Goodess, C. M. (2009). Climatic changes and associated impacts in the Mediterranean resulting from a 2 °C global warming. Global and Planetary Change, 68(3), 209–224. https://doi.org/10.1016/j.gloplacha.2009.06.001

16. Gidden, M. J., Riahi, K., Smith, S. J., Fujimori, S., Luderer, G., Kriegler, E., van Vuuren, D. P., van den Berg, M., Feng, L., Klein, D., Calvin, K., Doelman, J. C., Frank, S., Fricko, O., Harmsen, M., Hasegawa, T., Havlik, P., Hilaire, J., Hoesly, R., … Takahashi, K. (2019). Global emissions pathways under different socioeconomic scenarios for use in CMIP6: A dataset of harmonized emissions trajectories through the end of the century. Geoscientific Model Development, 12(4), 1443–1475. https://doi.org/10.5194/gmd-12-1443-2019

17. Gillett, N. P., Hegerl, G. C., Allen, M. R., Stott, P. A., & Schnur, R. (2002). Reconciling two approaches to the detection of anthropogenic influence on climate. Journal of Climate, 15(3), 326–329. https://doi.org/10.1175/1520-0442(2002)015<0326:RTATTD>2.0.CO;2

18. Giorgi, F. (2006). Climate change hot-spots. Geophysical Research Letters, 33(8). https://doi.org/10.1029/2006gl025734

19. Hagedorn, R., Doblas-Reyes, F. J., & Palmer, T. N. (2005). The rationale behind the success of multi-model ensembles in seasonal forecasting – I. Basic concept. Tellus A: Dynamic Meteorology and Oceanography, 57(3), 219. https://doi.org/10.3402/tellusa.v57i3.14657

20. Hellenic Ministry of Environment & Energy. (2016). National Climate Change Adaptation Strategy for Greece. https://ypen.gr

21. Hellenic National Meteorological Service. (2021). "Climate Change Projections and Trends for Greece." HNMS Reports. http://www.hnms.gr

22. IPCC AR4 WGI. (2007). https://archive.ipcc.ch/publications_and_data/ar4/wg1/en/annexessglossary-a-d.html

23. Knutti, R., & Sedláček, J. (2012). Robustness and uncertainties in the new CMIP5 climate model projections. Nature Climate Change, 3(4), 369–373. https://doi.org/10.1038/nclimate1716

24. Knutti, R., Stocker, T. F., Joos, F., & Plattner, G.-K. (2002). Constraints on radiative forcing and future climate change from observations and climate model ensembles. Nature, 416(6882), 719–723. https://doi.org/10.1038/416719a

25. Kostopoulou, E., & Jones, P. D. (2005). Assessment of climate extremes in the Eastern Mediterranean. Meteorology and Atmospheric Physics, 89(1–4), 69–85. https://doi.org/10.1007/s00703-005-0122-2

26. Koutroulis, A. G., Grillakis, M. G., Daliakopoulos, I. N., Tsanis, I. K., & Jacob, D. (2016). Cross sectoral impacts on water availability at +2 °C and +3 °C for east Mediterranean island states: The case of Crete. Journal of Hydrology, 532, 16–28. https://doi.org/10.1016/j.jhydrol.2015.11.015

27. Lange, S., Mengel, M., Treu, S., & Büchner, M. (2022, October 24). *ISIMIP3a atmospheric climate input data*. ISIMIP Repository. https://data.isimip.org/10.48364/ISIMIP.982724.1

28. Lambert, S. J., & Boer, G. J. (2001). CMIP1 evaluation and intercomparison of coupled climate models. Climate Dynamics, 17(2–3), 83–106. https://doi.org/10.1007/pl00013736

29. Lazaridis, M., Symeonidis, P., Tzortziou, M., & Lazaridou, D. (2014). Impacts of climate change on biodiversity and ecosystems. Global NEST Journal, 16(1), 170-184.

30. Lionello, P., Malanotte-Rizzoli, P., & Boscolo, R. (2006). Mediterranean Climate variability. Elsevier.

31. Lionello, P., Özsoy, E., Planton, S., & Zanchetta, G. (2017). Climate variability and change in the Mediterranean Region. Global and Planetary Change, 151, 1–3. https://doi.org/10.1016/j.gloplacha.2017.04.005

32. Mariotti, A., Pan, Y., Zeng, N., & Alessandri, A. (2015). Long-term climate change in the Mediterranean region in the midst of decadal variability. Climate Dynamics, 44(5–6), 1437–1456. https://doi.org/10.1007/s00382-015-2487-3

33. Marzeion, B., & Levermann, A. (2014). Loss of cultural world heritage and currently inhabited places to sea-level rise. Environmental Research Letters, 9(3), 034001. https://doi.org/10.1088/1748-9326/9/3/034001

34. Mavromatis, T. (2018). Climate change and olive growing: Impacts and mitigation measures. Olive Oil Times. https://oliveoiltimes.com/

35. McSweeney, C. F., Jones, R. G., & Booth, B. B. B. (2012). Selecting ensemble members to provide regional climate change information. Journal of Climate, 25(20), 7100–7121. https://doi.org/10.1175/jcli-d-11-00526.1

36. (MedECC), M. E. on C. and environmental C., Azzopardi, B., Balzan, M. V., Cherif, S., Doblas-Miranda, E., Santos, M. dos, Dobrinski, P., Falder, M., Hassoun, A. E. R., Giupponi, C., Koubi, V. (Vassiliki), Lange, M. A., Lionello, P., Llasat, M. C., Moncada, S., Mrabet, R., Paz, S., Savé, R., Snoussi, M., … Xoplaki, E. (2020). Climate and environmental change in the Mediterranean Basin – current situation and risks for the future. First Mediterranean Assessment report. MedECC.

37. Mediterranean Region. (2023). In Climate Change 2022 – Impacts, Adaptation and Vulnerability (pp. 2233–2272). Cambridge University Press. http://dx.doi.org/10.1017/9781009325844.021

38. Nastos, P. T., & Kapsomenakis, J. (2015). Regional climate model simulations of extreme air temperature in Greece. Abnormal or common records in the future climate? Atmospheric Research, 152, 43–60. https://doi.org/10.1016/j.atmosres.2014.02.005

39. Neil Adger, W., Arnell, N. W., & Tompkins, E. L. (2005). Successful adaptation to climate change across scales. Global Environmental Change, 15(2), 77–86. https://doi.org/10.1016/j.gloenvcha.2004.12.005

40. O'Neill, B. C., Tebaldi, C., van Vuuren, D. P., Eyring, V., Friedlingstein, P., Hurtt, G., Knutti, R., Kriegler, E., Lamarque, J.-F., Lowe, J., Meehl, G. A., Moss, R., Riahi, K., & Sanderson, B. M. (2016). The scenario model intercomparison project (scenariomip) for CMIP6. Geoscientific Model Development, 9(9), 3461–3482. https://doi.org/10.5194/gmd-9-3461-2016

41. Ortega, G., Arias, P. A., Villegas, J. C., Marquet, P. A., & Nobre, P. (2021). Present-day and future climate over central and South America according to CMIP5/CMIP6 models. International Journal of Climatology, 41(15), 6713–6735. https://doi.org/10.1002/joc.7221

42. Palmer, M. A., Lettenmaier, D. P., Poff, N. L., Postel, S. L., Richter, B., & Warner, R. (2009). Climate change and river ecosystems: Protection and adaptation options. Environmental Management, 44(6), 1053–1068. https://doi.org/10.1007/s00267-009-9329-1

43. Pantavou, K., Kotroni, V., Kyros, G., & Lagouvardos, K. (2024). Thermal bioclimate in Greece based on the Universal Thermal Climate Index (UTCI) and insights into 2021 and 2023 heatwaves. Theoretical and Applied Climatology, 155(7), 6661–6675. https://doi.org/10.1007/s00704-024-04989-5

44. Papa, M., & Koutroulis, A. G. (2024). Evaluation of precipitation datasets over greece. Insights from comparing multiple gridded products with observations. Elsevier BV. http://dx.doi.org/10.2139/ssrn.4780965

45. Papadopoulos, A. M., & Karamanos, A. (n.d.). Climate change and energy poverty in Greece: A challenge for social justice . Energy Policy, 124, 544-556. https://doi.org/https://doi.org/10.1016/j.enpol.2018.10.017

46. Polade, S. D., Pierce, D. W., Cayan, D. R., Gershunov, A., & Dettinger, M. D. (2014). The key role of dry days in changing regional climate and precipitation regimes. Scientific Reports, 4(1). https://doi.org/10.1038/srep04364

47. Politi, N., Vlachogiannis, D., Sfetsos, A., & Nastos, P. T. (2022). High resolution projections for extreme temperatures and precipitation over Greece. *Climate Dynamics*, *61*(1–2), 633–667. https://doi.org/10.1007/s00382-022-06590-w

48. Reay, D., Sabine, C., Smith, P., & Hymus, G. (2007). Spring-time for sinks. Nature, 446(7137), 727–728. https://doi.org/10.1038/446727a

49. Riahi, K., van Vuuren, D. P., Kriegler, E., Edmonds, J., O'Neill, B. C., Fujimori, S., Bauer, N., Calvin, K., Dellink, R., Fricko, O., Lutz, W., Popp, A., Cuaresma, J. C., Kc, S., Leimbach, M., Jiang, L., Kram, T., Rao, S., Emmerling, J., … Tavoni, M. (2017). The Shared Socioeconomic Pathways and their energy, land use, and greenhouse gas emissions implications: An overview. Global Environmental Change, 42, 153–168. https://doi.org/10.1016/j.gloenvcha.2016.05.009

50. Rizzi, J., Torresan, S., Zabeo, A., Critto, A., Tosoni, A., Tomasin, A., & Marcomini, A. (2017). Assessing storm surge risk under future sea-level rise scenarios: A case study in the North Adriatic coast. Journal of Coastal Conservation, 21(4), 453–471. https://doi.org/10.1007/s11852-017-0517-5

51. Ruti, P. M., Somot, S., Giorgi, F., Dubois, C., Flaounas, E., Obermann, A., Dell'Aquila, A., Pisacane, G., Harzallah, A., Lombardi, E., Ahrens, B., Akhtar, N., Alias, A., Arsouze, T., Aznar, R., Bastin, S., Bartholy, J., Béranger, K., Beuvier, J., … Vervatis, V. (2016). Med-CORDEX Initiative for Mediterranean Climate Studies. Bulletin of the American Meteorological Society, 97(7), 1187–1208. https://doi.org/10.1175/bams-d-14-00176.1

52. Sanderson, B. M., Knutti, R., & Caldwell, P. (2015). A representative democracy to reduce interdependency in a multimodel ensemble. Journal of Climate, 28(13), 5171–5194. https://doi.org/10.1175/jcli-d-14-00362.1

53. Schleussner, C.-F., Lissner, T. K., Fischer, E. M., Wohland, J., Perrette, M., Golly, A., Rogelj, J., Childers, K., Schewe, J., Frieler, K., Mengel, M., Hare, W., & Schaeffer, M. (2016). Differential climate impacts for policy-relevant limits to global warming: The case of 1.5 °C and 2 °C. Earth System Dynamics, 7(2), 327–351. https://doi.org/10.5194/esd-7-327-2016

54. Seneviratne, S. I., Donat, M. G., Pitman, A. J., Knutti, R., & Wilby, R. L. (2016). Allowable CO2 emissions based on regional and impact-related climate targets. Nature, 529(7587), 477–483. https://doi.org/10.1038/nature16542

55. Sobolowski, S., Somot, S., Fernandez, J., Evin, G., Maraun, D., Kotlarski, S., Jury, M., Benestad, R. E., Teichmann, C., Christensen, O. B., Katharina, B., Buonomo, E., Katragkou, E., Steger, C., Sørland, S., Nikulin, G., McSweeney, C., Dobler, A., Palmer, T., … Brands, S.

(2023, February 24). *EURO-CORDEX CMIP6 GCM selection & ensemble design: Best practices and recommendations*. Zenodo. https://zenodo.org/record/7673399

56. Tarín-Carrasco, P. (2024). Assessment of Future Precipitation Changes in Mediterranean Climate Regions from CMIP6 ensemble. EGUsphere. https://doi.org/10.5194/egusphere-2023-3057-rc1

57. Taylor, K. E., Stouffer, R. J., & Meehl, G. A. (2012). An overview of CMIP5 and the experiment design. Bulletin of the American Meteorological Society, 93(4), 485–498. https://doi.org/10.1175/bams-d-11-00094.1

58. Tebaldi, C., & Knutti, R. (2007). The use of the multi-model ensemble in probabilistic climate projections. Philosophical Transactions of the Royal Society A: Mathematical, Physical and Engineering Sciences, 365(1857), 2053–2075. https://doi.org/10.1098/rsta.2007.2076

59. Tolika, K., Vagena, S., Anagnostopoulou, C., & Maheras, P. (2020). Evaluating future climate change in the Mediterranean region and the anticipated shifts in the Köppen-Geiger zones. https://doi.org/ https://doi.org/10.3390/cli8020029

60. Toreti et al. (2023, June 13). Drought in western Mediterranean. Publications Office of the EU. https://op.europa.eu/publication/manifestation_identifier/PUB_KJNA31555ENN

61. UNEP/MAP-Plan Bleu. (2009). UNEP/MAP-Plan Bleu: State of the Environment and Development in the Mediterranean.

62. van Vuuren, D. P., Edmonds, J., Kainuma, M., Riahi, K., Thomson, A., Hibbard, K., Hurtt, G. C., Kram, T., Krey, V., Lamarque, J.-F., Masui, T., Meinshausen, M., Nakicenovic, N., Smith, S. J., & Rose, S. K. (2011). The representative concentration pathways: An overview. Climatic Change, 109(1–2), 5–31. https://doi.org/10.1007/s10584-011-0148-z

63. Vicente-Serrano, S. M., Lopez-Moreno, J.-I., Beguería, S., Lorenzo-Lacruz, J., Sanchez-Lorenzo, A., García-Ruiz, J. M., Azorin-Molina, C., Morán-Tejeda, E., Revuelto, J., Trigo, R., Coelho, F., & Espejo, F. (2014). Evidence of increasing drought severity caused by temperature rise in southern Europe. Environmental Research Letters, 9(4), 044001. https://doi.org/10.1088/1748-9326/9/4/044001

64. Vousdoukas, M. I., Mentaschi, L., Voukouvalas, E., Verlaan, M., & Feyen, L. (2017). Extreme sea levels on the rise along Europe's coasts. Earth's Future, 5(3), 304–323. https://doi.org/10.1002/2016ef000505

65. WGI AR6 Chapter 11, Seneviratne et al. (2021). Weather and climate extreme events in a changing climate. In Climate Change 2021 – The Physical Science Basis (pp. 1513–1766). Cambridge University Press. http://dx.doi.org/10.1017/9781009157896.013

66. Zachariah, M., & Kotroni, Kotroni. (2023). Interplay of climate change-exacerbated rainfall, exposure and vulnerability led to widespread impacts in the Mediterranean region (pp. 1–30). Imperial College Press.

https://spiral.imperial.ac.uk/bitstream/10044/1/106501/14/scientific%20report%20-%20Mediterranean%20floods.pdf (2023)

67. Zittis, G., Hadjinicolaou, P., Fnais, M., & Lelieveld, J. (2019). Projected changes in heat wave characteristics in the eastern Mediterranean and the Middle East. Regional Environmental Change, 19(1), 123-137. https://doi.org/https://doi.org/10.1007/s10113-019-01476-9

Appendix

Annual Cycle of Temperature

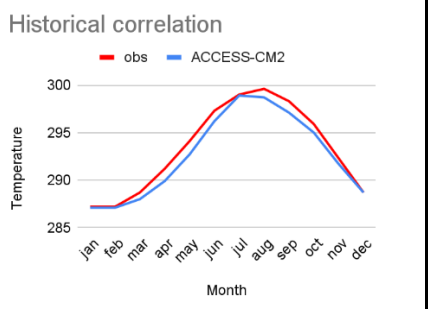

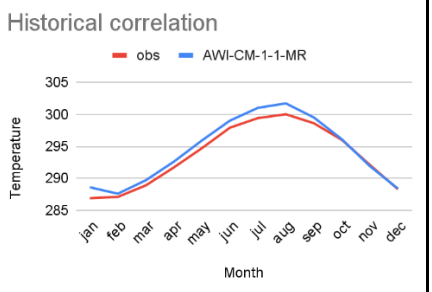

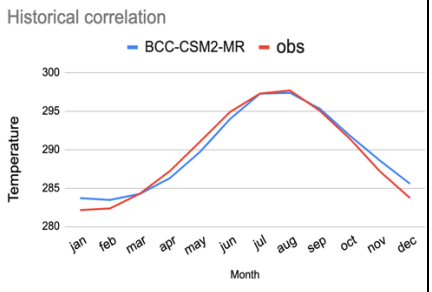

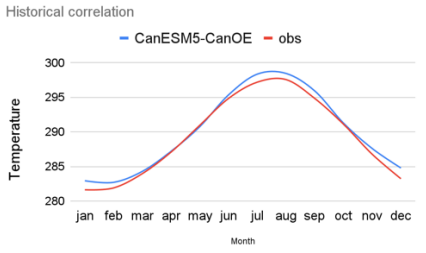

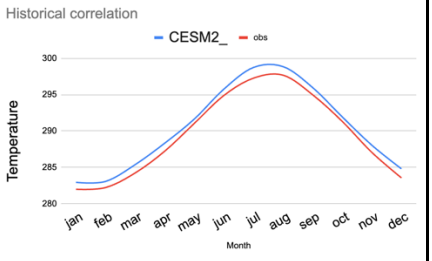

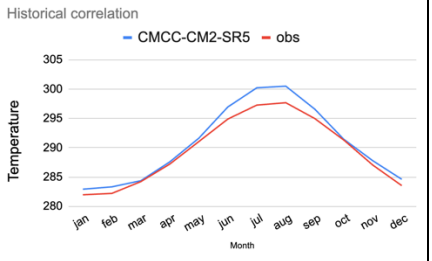

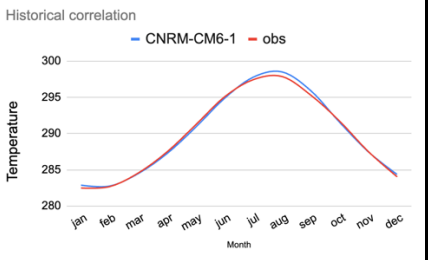

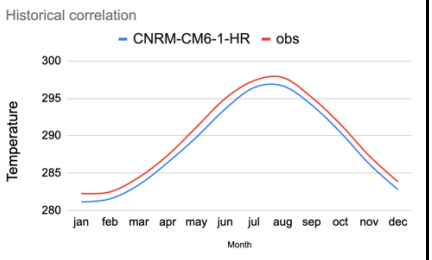

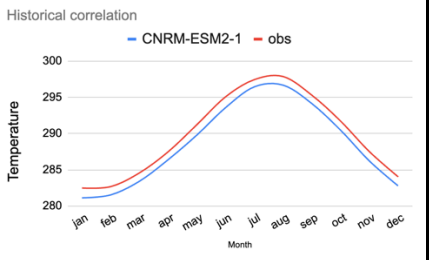

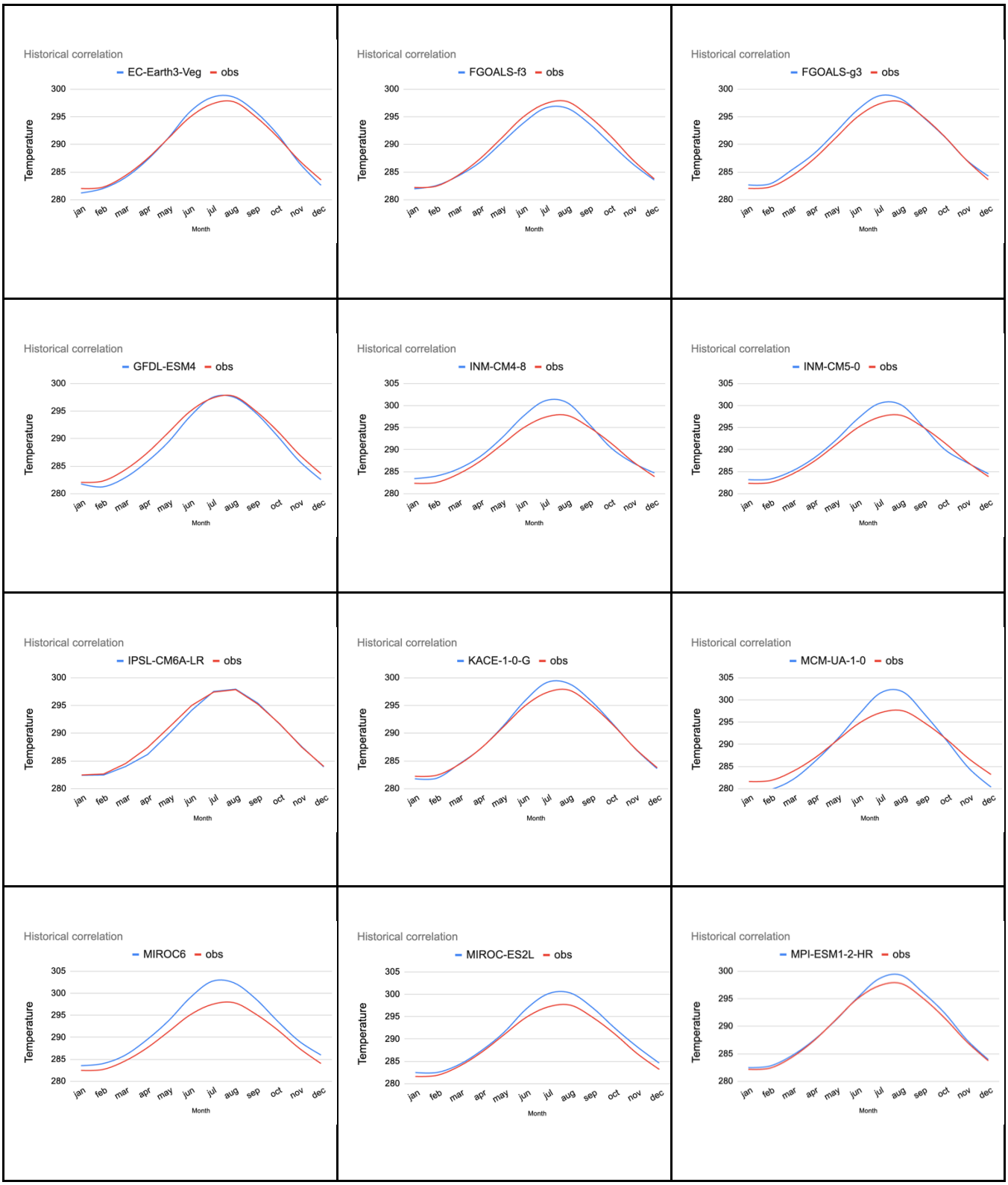
Historical correlation
EC-Earth3-Veg obs
FGOALS-f3 obs
FGOALS-g3 obs
GFDL-ESM4 obs
INM-CM4-8 obs
INM-CM5-0 obs
IPSL-CM6A-LR obs
KACE-1-0-G obs
MCM-UA-1-0 obs
MIROC6 obs
MIROC-ES2L obs
MPI-ESM1-2-HR obs
Temperature
Month
jan feb mar apr may jun jul aug sep oct nov dec

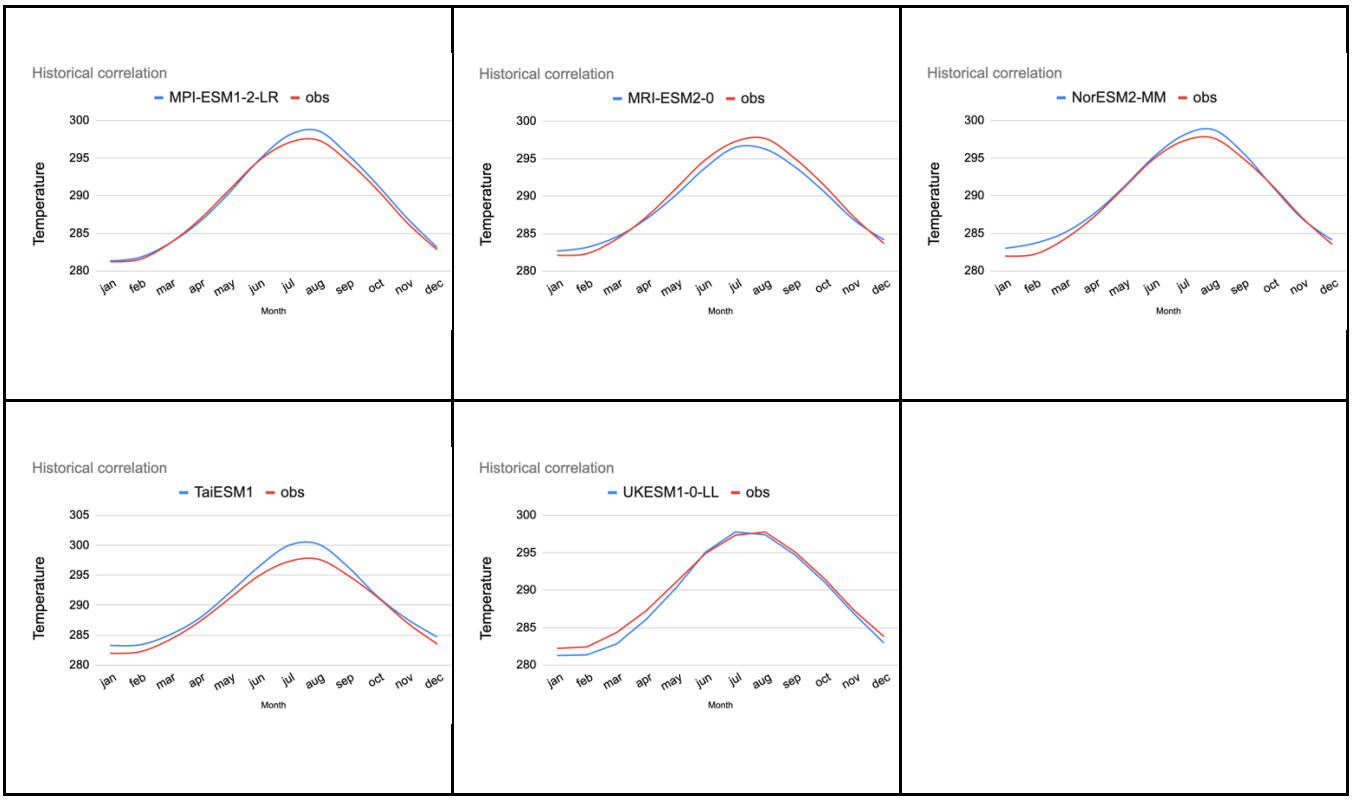

Annual Cycle of Precipitation

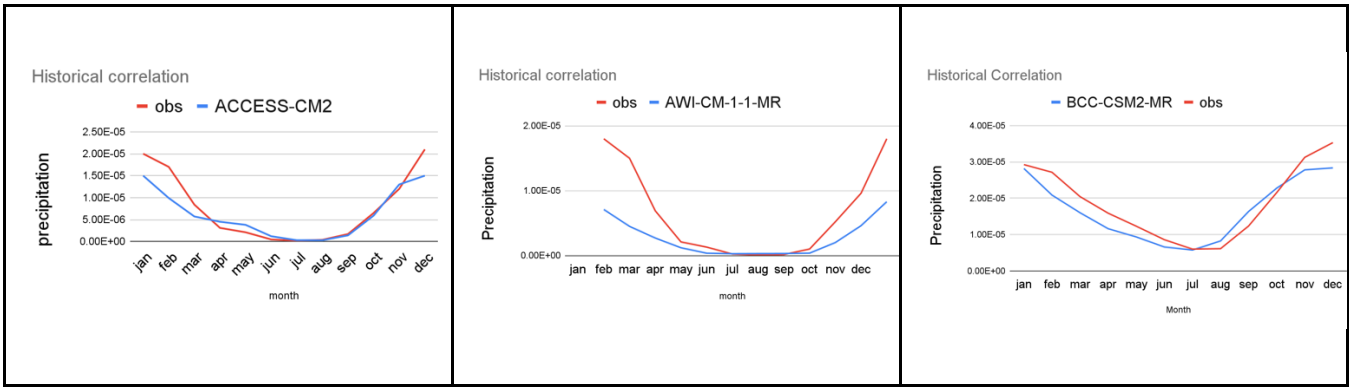

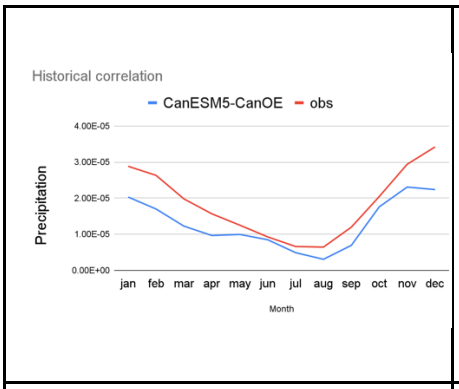
Historical correlation
CanESM5-CanOE
obs
Precipitation
4.00E-05
3.00E-05
2.00E-05
1.00E-05
0.00E+00
jan feb mar apr may jun jul aug sep oct nov dec
Month

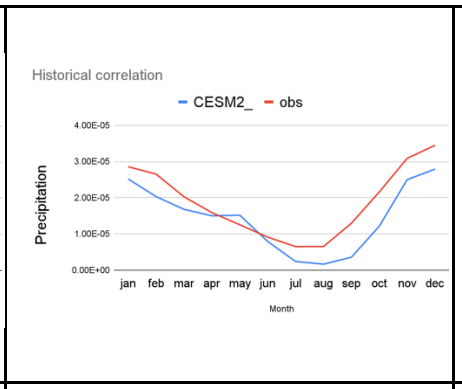
Historical correlation
CESM2_
obs
Precipitation
4.00E-05
3.00E-05
2.00E-05
1.00E-05
0.00E+00
jan feb mar apr may jun jul aug sep oct nov dec
Month

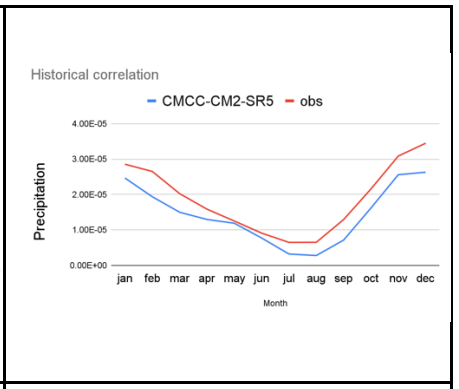
Historical correlation
CMCC-CM2-SR5
obs
Precipitation
4.00E-05
3.00E-05
2.00E-05
1.00E-05
0.00E+00
jan feb mar apr may jun jul aug sep oct nov dec
Month

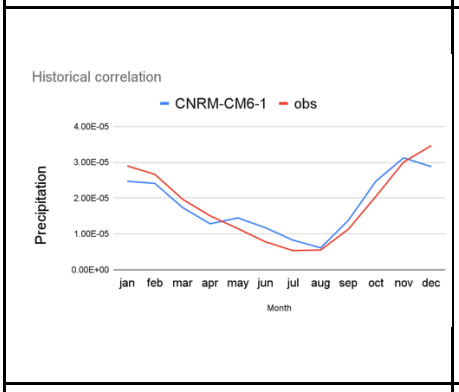
Historical correlation
CNRM-CM6-1
obs
Precipitation
4.00E-05
3.00E-05
2.00E-05
1.00E-05
0.00E+00
jan feb mar apr may jun jul aug sep oct nov dec
Month

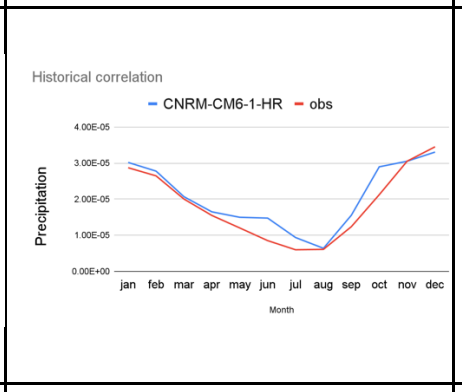
Historical correlation
CNRM-CM6-1-HR
obs
Precipitation
4.00E-05
3.00E-05
2.00E-05
1.00E-05
0.00E+00
jan feb mar apr may jun jul aug sep oct nov dec
Month

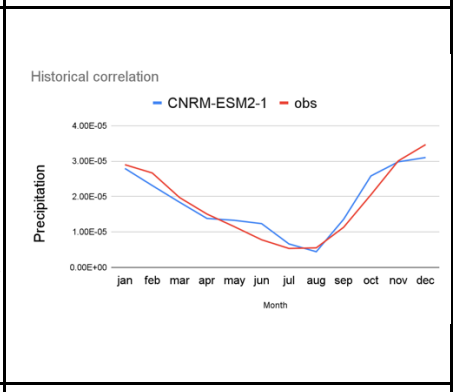
Historical correlation
CNRM-ESM2-1
obs
Precipitation
4.00E-05
3.00E-05
2.00E-05
1.00E-05
0.00E+00
jan feb mar apr may jun jul aug sep oct nov dec
Month

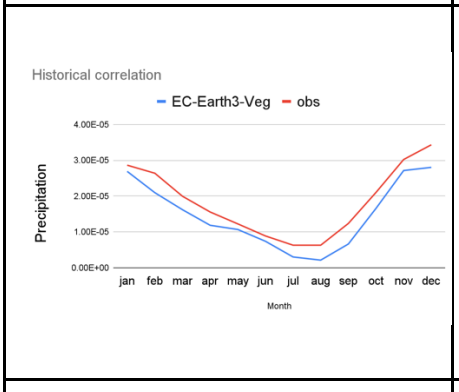
Historical correlation
EC-Earth3-Veg
obs
Precipitation
4.00E-05
3.00E-05
2.00E-05
1.00E-05
0.00E+00
jan feb mar apr may jun jul aug sep oct nov dec
Month

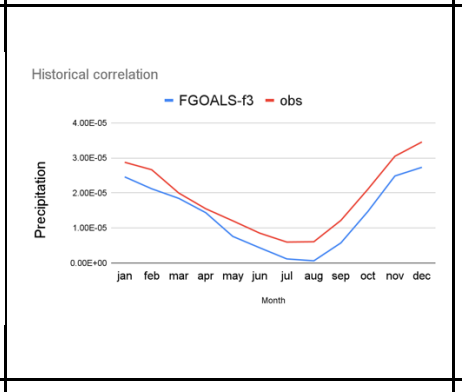
Historical correlation
FGOALS-f3
obs
Precipitation
4.00E-05
3.00E-05
2.00E-05
1.00E-05
0.00E+00
jan feb mar apr may jun jul aug sep oct nov dec
Month

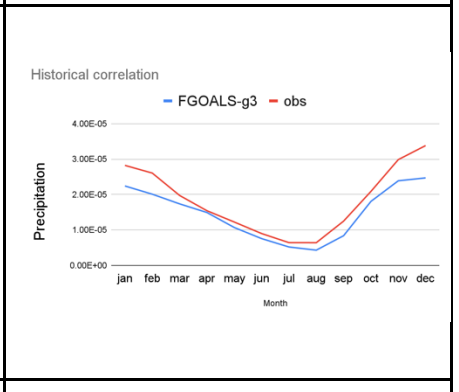
Historical correlation
FGOALS-g3
obs
Precipitation
4.00E-05
3.00E-05
2.00E-05
1.00E-05
0.00E+00
jan feb mar apr may jun jul aug sep oct nov dec
Month

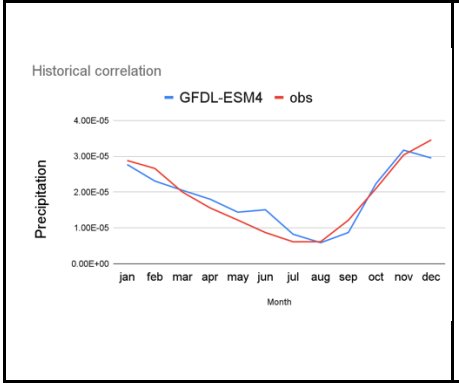
Historical correlation
GFDL-ESM4
obs
Precipitation
4.00E-05
3.00E-05
2.00E-05
1.00E-05
0.00E+00
jan feb mar apr may jun jul aug sep oct nov dec
Month

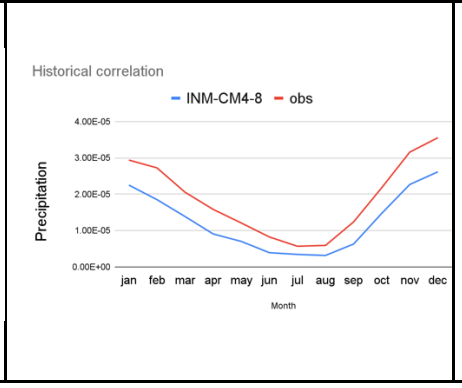
Historical correlation
INM-CM4-8
obs
Precipitation
4.00E-05
3.00E-05
2.00E-05
1.00E-05
0.00E+00
jan feb mar apr may jun jul aug sep oct nov dec
Month

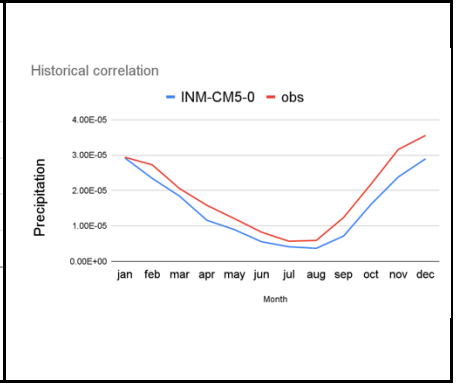
Historical correlation
INM-CM5-0
obs
Precipitation
4.00E-05
3.00E-05
2.00E-05
1.00E-05
0.00E+00
jan feb mar apr may jun jul aug sep oct nov dec
Month

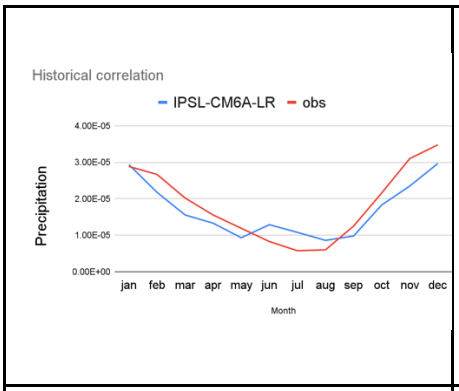
Historical correlation
IPSL-CM6A-LR
obs
Precipitation
4.00E-05
3.00E-05
2.00E-05
1.00E-05
0.00E+00
jan feb mar apr may jun jul aug sep oct nov dec
Month

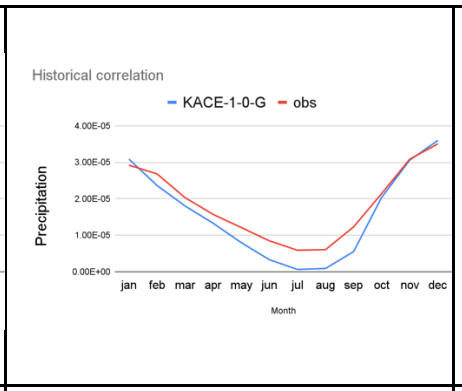
Historical correlation
KACE-1-0-G
obs
Precipitation
4.00E-05
3.00E-05
2.00E-05
1.00E-05
0.00E+00
jan feb mar apr may jun jul aug sep oct nov dec
Month

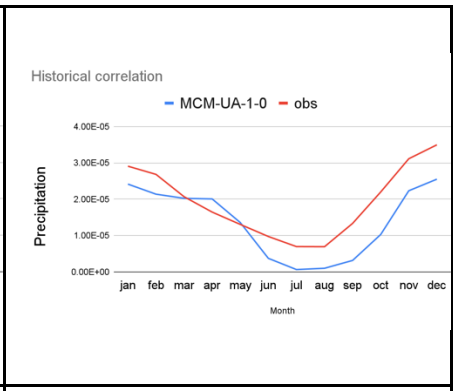
Historical correlation
MCM-UA-1-0
obs
Precipitation
4.00E-05
3.00E-05
2.00E-05
1.00E-05
0.00E+00
jan feb mar apr may jun jul aug sep oct nov dec
Month

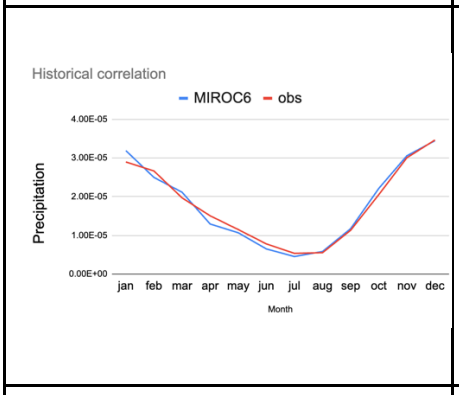
Historical correlation
MIROC6
obs
Precipitation
4.00E-05
3.00E-05
2.00E-05
1.00E-05
0.00E+00
jan feb mar apr may jun jul aug sep oct nov dec
Month

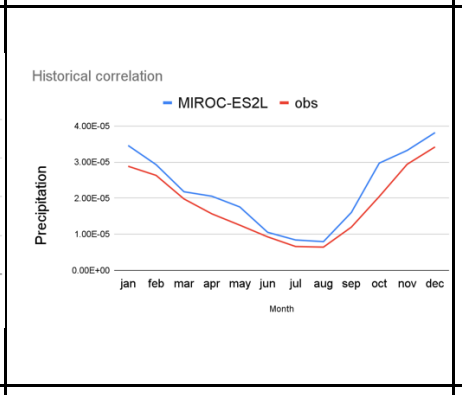
Historical correlation
MIROC-ES2L
obs
Precipitation
4.00E-05
3.00E-05
2.00E-05
1.00E-05
0.00E+00
jan feb mar apr may jun jul aug sep oct nov dec
Month

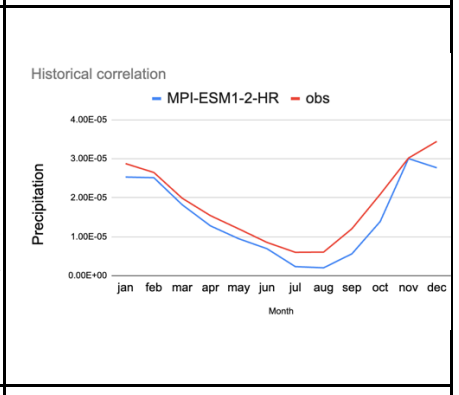
Historical correlation
MPI-ESM1-2-HR
obs
Precipitation
4.00E-05
3.00E-05
2.00E-05
1.00E-05
0.00E+00
jan feb mar apr may jun jul aug sep oct nov dec
Month

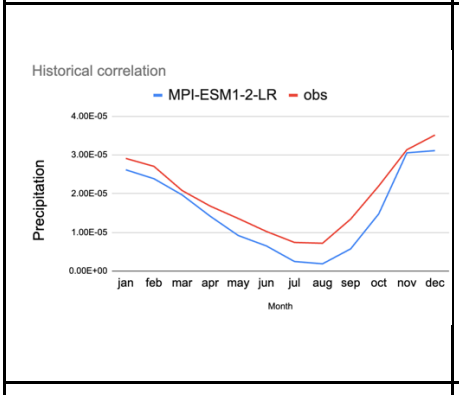
Historical correlation
MPI-ESM1-2-LR
obs
Precipitation
4.00E-05
3.00E-05
2.00E-05
1.00E-05
0.00E+00
jan feb mar apr may jun jul aug sep oct nov dec
Month

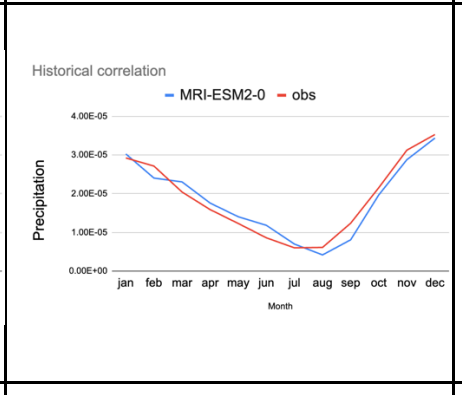
Historical correlation
MRI-ESM2-0
obs
Precipitation
4.00E-05
3.00E-05
2.00E-05
1.00E-05
0.00E+00
jan feb mar apr may jun jul aug sep oct nov dec
Month

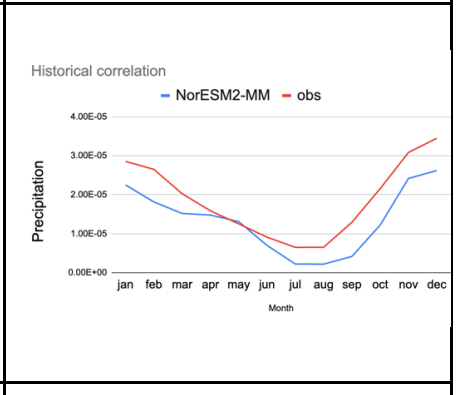
Historical correlation
NorESM2-MM
obs
Precipitation
4.00E-05
3.00E-05
2.00E-05
1.00E-05
0.00E+00
jan feb mar apr may jun jul aug sep oct nov dec
Month

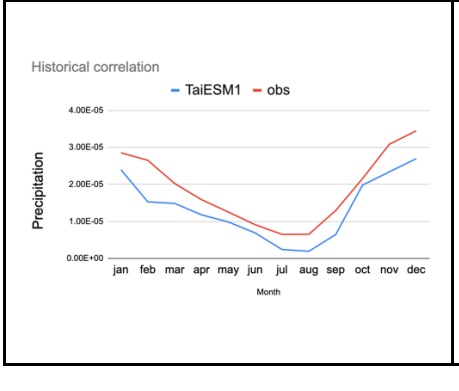
Historical correlation
TaiESM1
obs
Precipitation
4.00E-05
3.00E-05
2.00E-05
1.00E-05
0.00E+00
jan feb mar apr may jun jul aug sep oct nov dec
Month

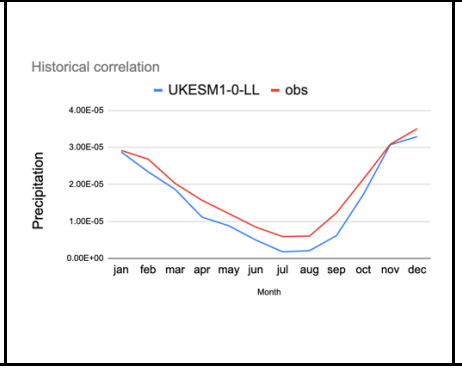
Historical correlation
UKESM1-0-LL
obs
Precipitation
4.00E-05
3.00E-05
2.00E-05
1.00E-05
0.00E+00
jan feb mar apr may jun jul aug sep oct nov dec
Month

Evaluation Metrics

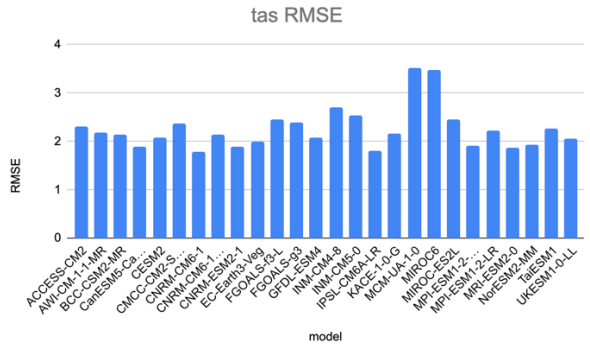

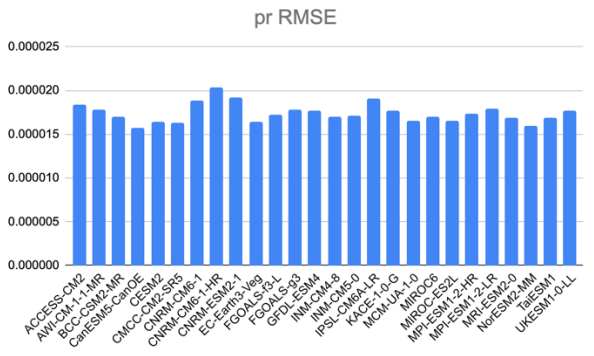

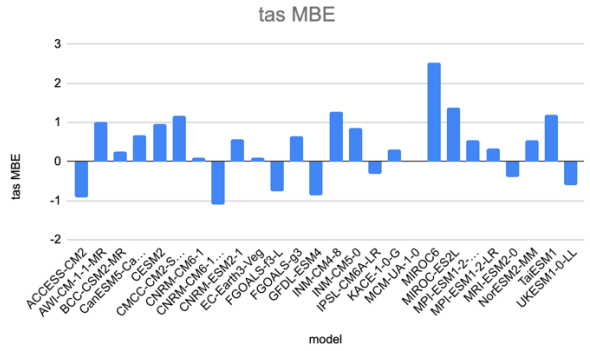

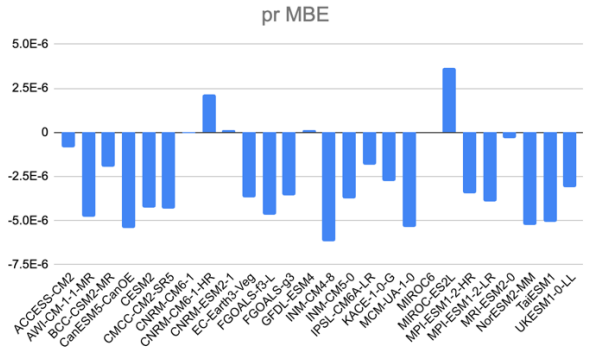

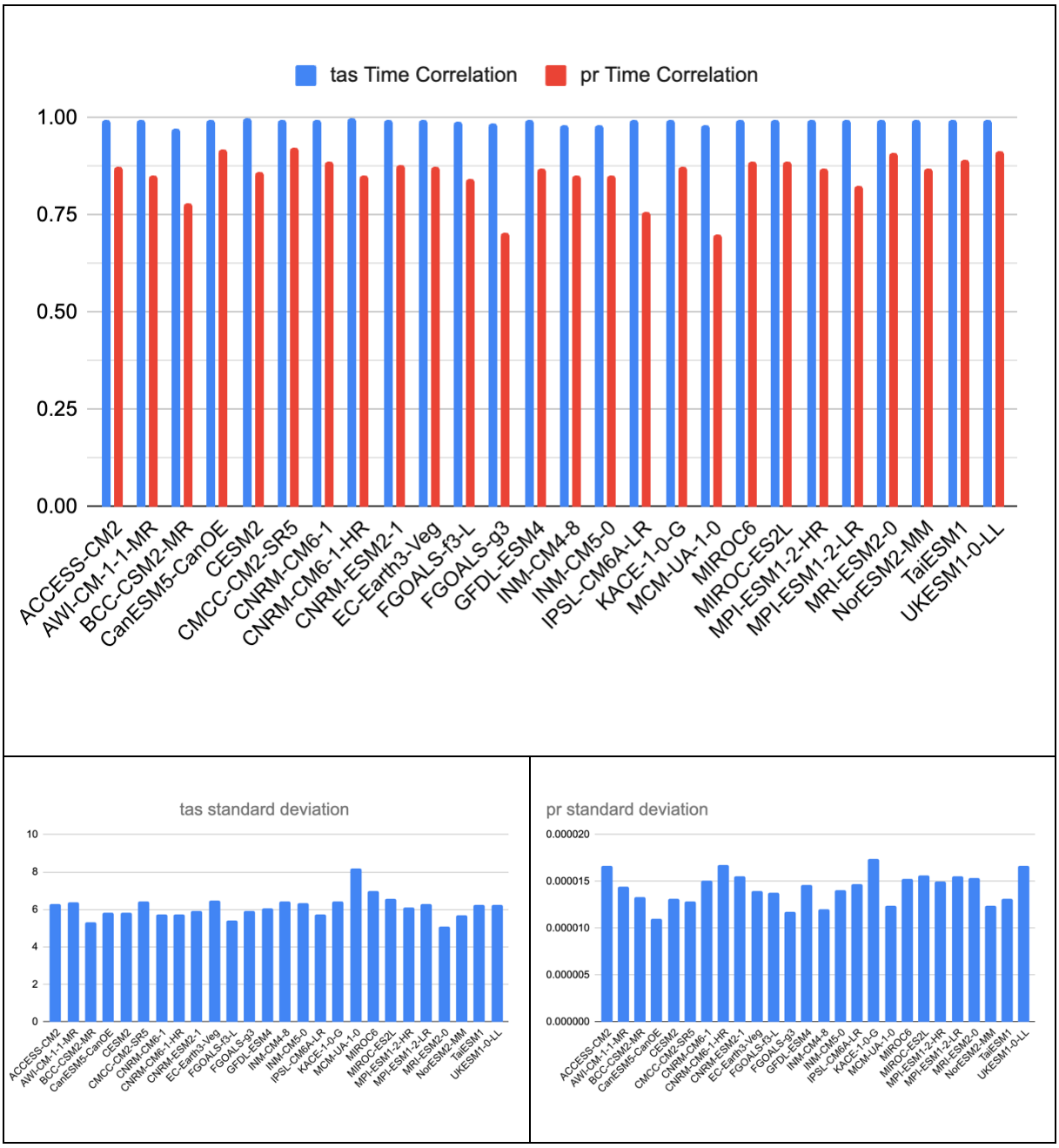
tas Time Correlation
pr Time Correlation
1.00
0.75
0.50
0.25
0.00
ACCESS-CM2
AWI-CM-1-1-MR
BCC-CSM2-MR
CanESM5-CanOE
CESM2
CMCC-CM2-SR5
CNRM-CM6-1
CNRM-CM6-1-HR
CNRM-ESM2-1
EC-Earth3-Veg
FGOALS-f3-L
FGOALS-g3
GFDL-ESM4
INM-CM4-8
INM-CM5-0
IPSL-CM6A-LR
KACE-1-0-G
MCM-UA-1-0
MIROC6
MIROC-ES2L
MPI-ESM1-2-HR
MPI-ESM1-2-LR
MRI-ESM2-0
NorESM2-MM
TaiESM1
UKESM1-0-LL

tas standard deviation
10
8
6
4
2
0

pr standard deviation
0.000020
0.000015
0.000010
0.000005
0.000000

Temperature & Precipitation. SSP scenarios

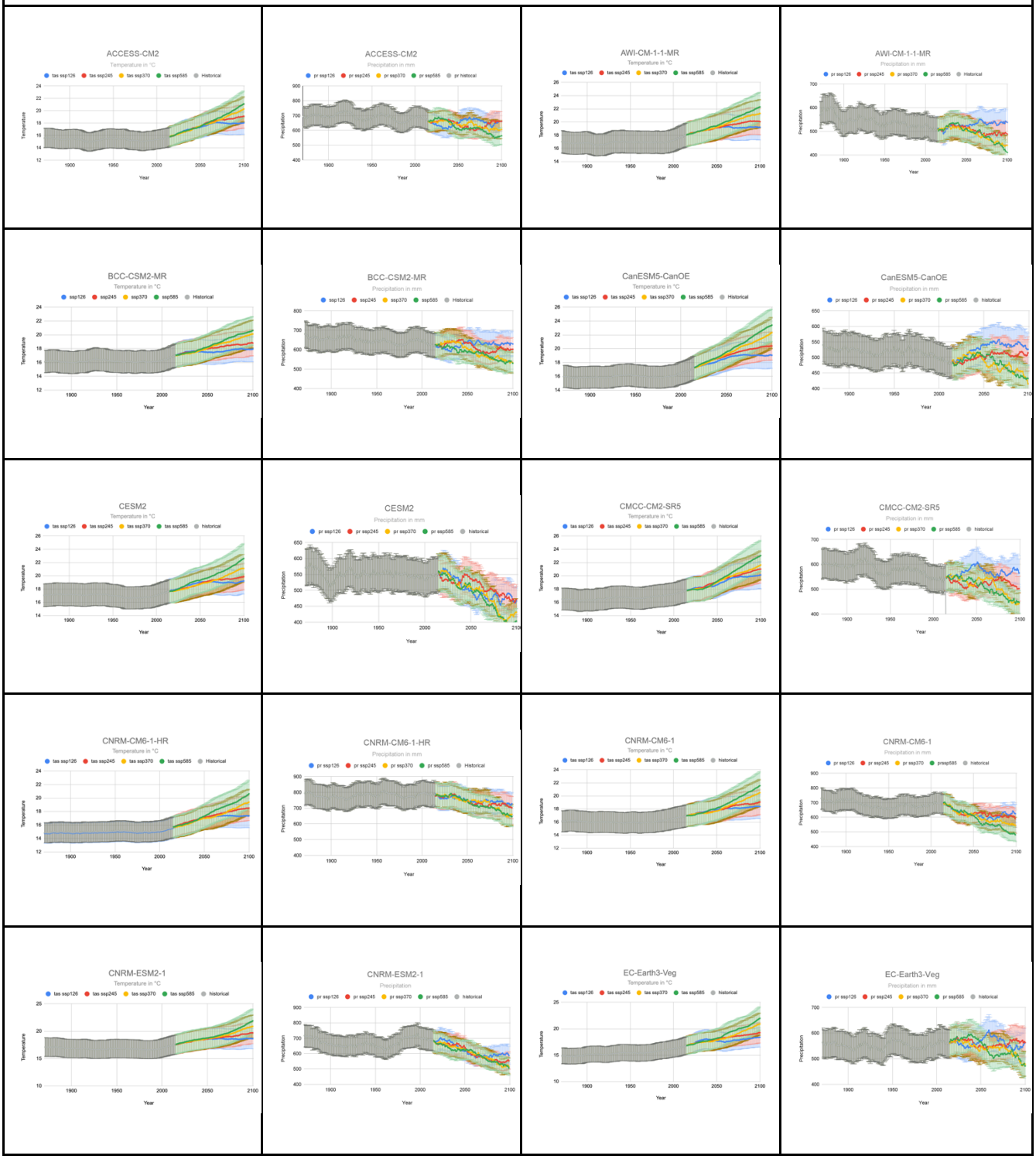

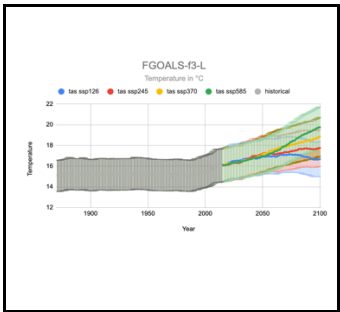
FGOALS-f3-L
Temperature in °C
tas ssp126 tas ssp245 tas ssp370 tas ssp585 historical
Temperature
Year

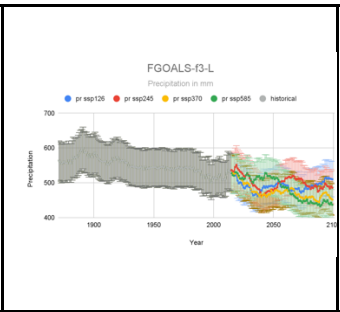
FGOALS-f3-L
Precipitation in mm
pr ssp126 pr ssp245 pr ssp370 pr ssp585 historical
Precipitation
Year

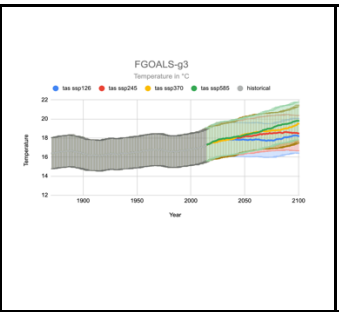
FGOALS-g3
Temperature in °C
tas ssp126 tas ssp245 tas ssp370 tas ssp585 historical
Temperature
Year

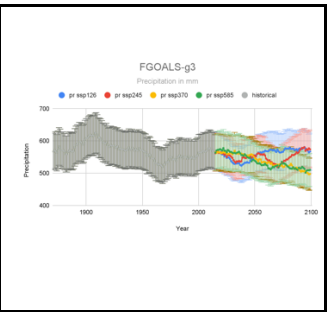
FGOALS-g3
Precipitation in mm
pr ssp126 pr ssp245 pr ssp370 pr ssp585 historical
Precipitation
Year

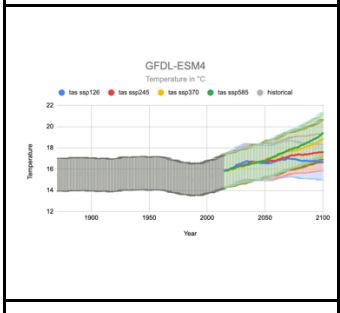
GFDL-ESM4
Temperature in °C
tas ssp126 tas ssp245 tas ssp370 tas ssp585 historical
Temperature
Year

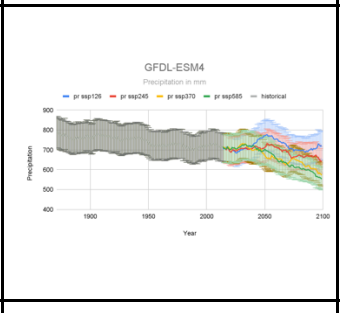
GFDL-ESM4
Precipitation in mm
pr ssp126 pr ssp245 pr ssp370 pr ssp585 historical
Precipitation
Year

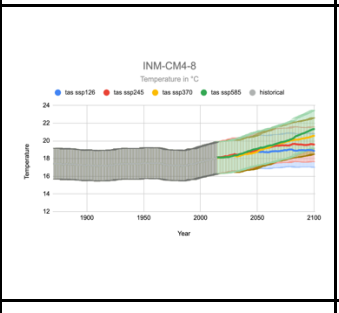
INM-CM4-8
Temperature in °C
tas ssp126 tas ssp245 tas ssp370 tas ssp585 historical
Temperature
Year

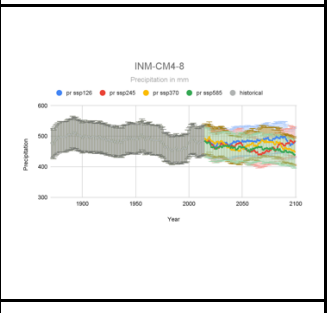
INM-CM4-8
Precipitation in mm
pr ssp126 pr ssp245 pr ssp370 pr ssp585 historical
Precipitation
Year

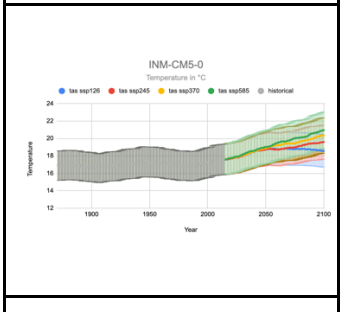
INM-CM5-0
Temperature in °C
tas ssp126 tas ssp245 tas ssp370 tas ssp585 historical
Temperature
Year

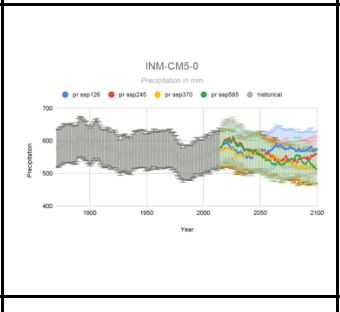
INM-CM5-0
Precipitation in mm
pr ssp126 pr ssp245 pr ssp370 pr ssp585 historical
Precipitation
Year

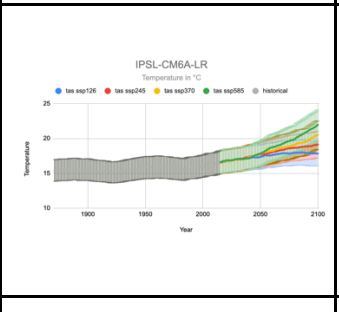
IPSL-CM6A-LR
Temperature in °C
tas ssp126 tas ssp245 tas ssp370 tas ssp585 historical
Temperature
Year

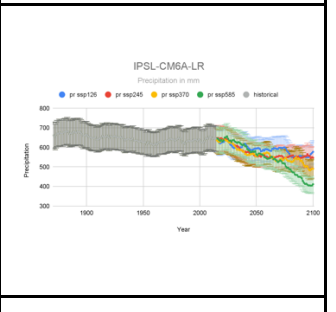
IPSL-CM6A-LR
Precipitation in mm
pr ssp126 pr ssp245 pr ssp370 pr ssp585 historical
Precipitation
Year

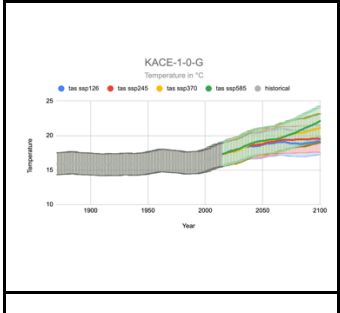
KACE-1-0-G
Temperature in °C
tas ssp126 tas ssp245 tas ssp370 tas ssp585 historical
Temperature
Year

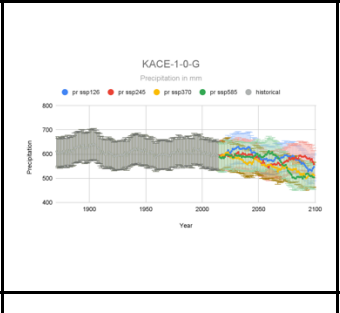
KACE-1-0-G
Precipitation in mm
pr ssp126 pr ssp245 pr ssp370 pr ssp585 historical
Precipitation
Year

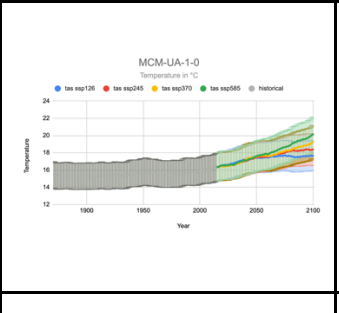
MCM-UA-1-0
Temperature in °C
tas ssp126 tas ssp245 tas ssp370 tas ssp585 historical
Temperature
Year

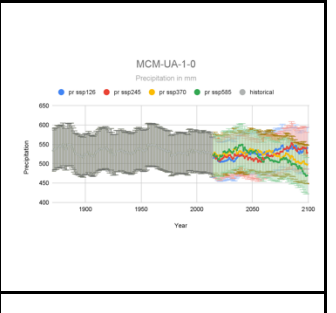
MCM-UA-1-0
Precipitation in mm
pr ssp126 pr ssp245 pr ssp370 pr ssp585 historical
Precipitation
Year

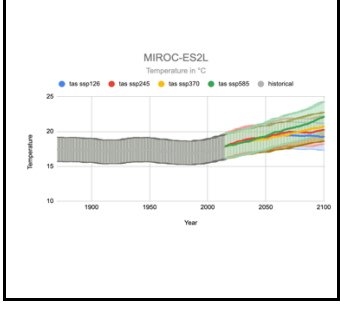
MIROC-ES2L
Temperature in °C
tas ssp126 tas ssp245 tas ssp370 tas ssp585 historical
Temperature
Year

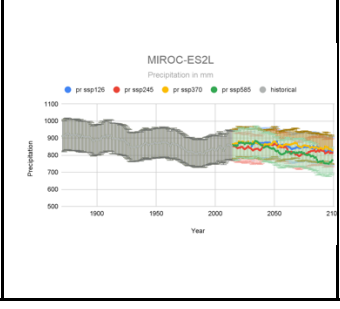
MIROC-ES2L
Precipitation in mm
pr ssp126 pr ssp245 pr ssp370 pr ssp585 historical
Precipitation
Year

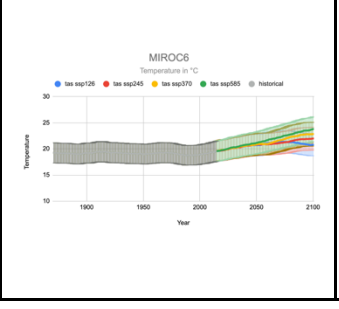
MIROC6
Temperature in °C
tas ssp126 tas ssp245 tas ssp370 tas ssp585 historical
Temperature
Year

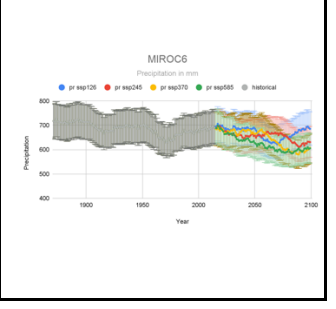
MIROC6
Precipitation in mm
pr ssp126 pr ssp245 pr ssp370 pr ssp585 historical
Precipitation
Year

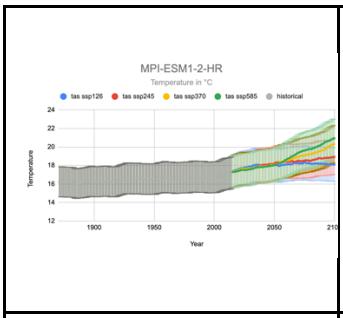
MPI-ESM1-2-HR
Temperature in °C
tas ssp126
tas ssp245
tas ssp370
tas ssp585
historical
Temperature
Year

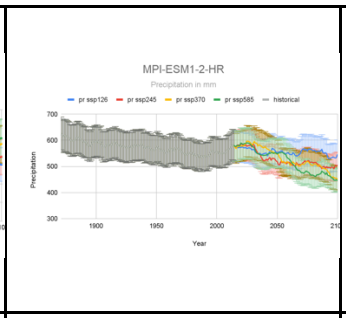
MPI-ESM1-2-HR
Precipitation in mm
pr ssp126
pr ssp245
pr ssp370
pr ssp585
historical
Precipitation
Year

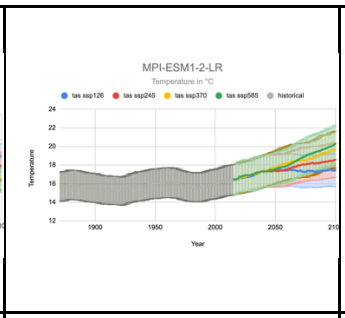
MPI-ESM1-2-LR
Temperature in °C
tas ssp126
tas ssp245
tas ssp370
tas ssp585
historical
Temperature
Year

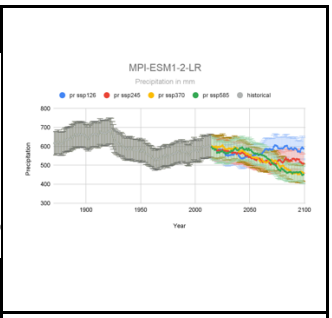
MPI-ESM1-2-LR
Precipitation in mm
pr ssp126
pr ssp245
pr ssp370
pr ssp585
historical
Precipitation
Year

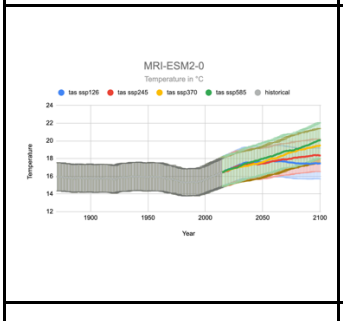
MRI-ESM2-0
Temperature in °C
tas ssp126
tas ssp245
tas ssp370
tas ssp585
historical
Temperature
Year

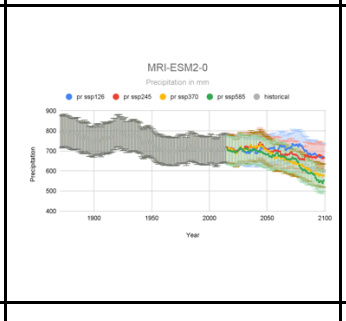
MRI-ESM2-0
Precipitation in mm
pr ssp126
pr ssp245
pr ssp370
pr ssp585
historical
Precipitation
Year

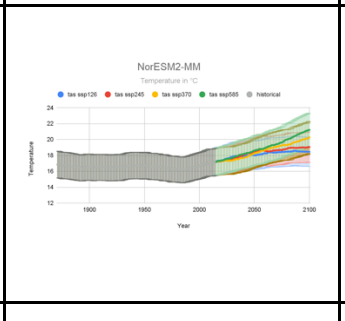
NorESM2-MM
Temperature in °C
tas ssp126
tas ssp245
tas ssp370
tas ssp585
historical
Temperature
Year

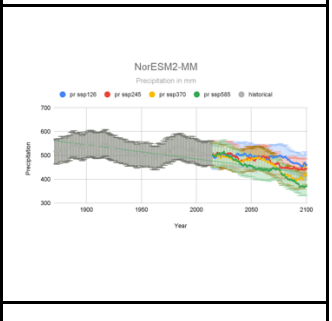
NorESM2-MM
Precipitation in mm
pr ssp126
pr ssp245
pr ssp370
pr ssp585
historical
Precipitation
Year

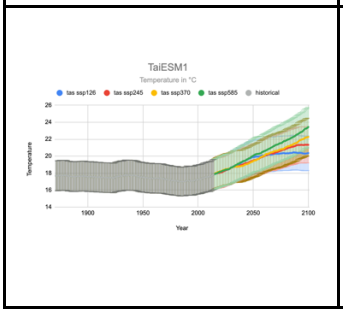
TaiESM1
Temperature in °C
tas ssp126
tas ssp245
tas ssp370
tas ssp585
historical
Temperature
Year

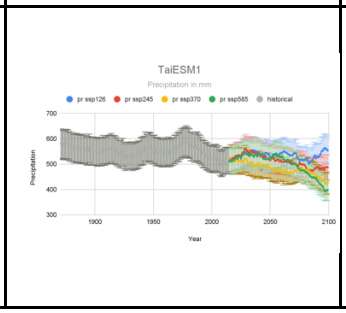
TaiESM1
Precipitation in mm
pr ssp126
pr ssp245
pr ssp370
pr ssp585
historical
Precipitation
Year

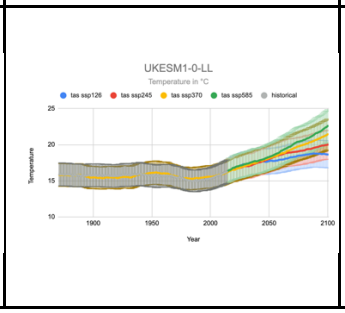
UKESM1-0-LL
Temperature in °C
tas ssp126
tas ssp245
tas ssp370
tas ssp585
historical
Temperature
Year

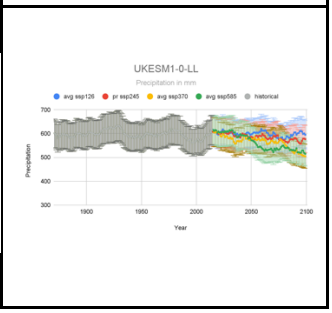
UKESM1-0-LL
Precipitation in mm
avg ssp126
pr ssp245
avg ssp370
avg ssp585
historical
Precipitation
Year

CDO code

```
A.Observation_data_preprocess_(gswp3_w5e5)
#select time period
cdo  seldate,1979-01-01,2014-12-31 infile.nc outfile.nc
#covert daily dataset to monthly
cdo monmean infile outfile
#upscale observational dataset to model's grid
cdo remapcon,model.nc obs.nc upscaled_obs.nc

B.Evaluation_metrics
#Root Mean Square Error(RMSE)
cdo -L sub -sellevidx,1 model.nc upscaled_obs.nc diff.nc
 cdo mul diff.nc diff.nc diff_squared.nc
  cdo timmean diff_squared.nc diff_squared_mean.nc
   cdo sqrt  diff_squared_mean.nc rmse.nc
#Mean Bias Error(MBE)
cdo timmean diff.nc diff_timemean.nc
 cdo fldmean diff_timemean.nc mbe.nc
#Time correlation
cdo ymonmean model.nc model_ymonmean.nc
 cdo ymonmean  upscaled_obs.nc obs_ymonmean.nc
  cdo timcor obs_ymonmean.nc model_ymonmean.nc timcor.nc
#Spatial Mean
 cdo fldmean diff.nc diff_fldmean.nc
#Standart Deviation
 cdo timstd model.nc model_timstd.nc

C.Future_projections
#Mean annual temperature
cdo yearmean model.nc annualmean.nc
#total annual precipetation
cdo yearsum model.nc annualtotal.nc
#change:baseline period(1850-1900) vs far future(2080-2100)
cdo seldate,1850,1900 model.nc baseline.nc
cdo seldate,2080,2100 model.nc farfuture.nc
 cdo timemean ipputfile.nc mean_outfile.nc
  cdo sub farfture_mean.nc baseline_mean.nc change.nc
#Trail Moving Average
cdo timcumsum model.nc
 cdo seldate,1971,2100 model.nc shifted.nc
 cdo seldate,1850,1900 model.nc truncated.nc
  cdo sub shifted.nc truncated diff.nc
   cdo divc,21 diff.n trail_mov_avg.nc
```